University of Stavanger

FACULTY OF SCIENCE AND TECHNOLOGY

MASTER'S THESIS

Study programme/specialisation: Structures and Materials - Civil Engineering	Spring semester, 2021 Open
Author: Petter André Høines	
Programme coordinator: Kjell Tore Fosså Supervisor: Kjell Tore Fosså	
Title of master's thesis: The effect of injecting CO2 in fresh concrete with different content of slag in the binder	
Credits: 30	
Keywords: Concrete Technology, CO2, carbonation, properties in fresh concrete, properties in hardened concrete, Thermogravimetric Analysis, CO2 uptake	Number of pages: 96 + supplemental material/other: 47 Stavanger, 15/06/2021

Abstract

Concrete is one of the most used building material, and cement production alone accounts for 7-8 % of the greenhouse emissions globally. A combination of reducing the amount of cement and injecting CO_2 during mixing might be one method to reduce the greenhouse gas emissions from the concrete industry. In previous research it has been shown that the addition of CO_2 in fresh concrete results in an accelerated degree of hydration and increases mechanical properties. This thesis examines the effect of injecting CO_2 during mixing with different amounts of slag in the binder. The effect this has on the fresh properties (workability, air content, density, temperature), hardened properties (compressive strength, modulus of elasticity, splitting tensile strength) and the chemical properties (pH, TGA) will be examined. Concrete with 0%, 20%, 30% and 70 % slag in the binder are selected, and 0, 1 and 2 wt% (of binder) of CO_2 is used to research the main properties of the concrete.

The results show that the workability is reduced with an increased amount of CO_2 added, which also results in increased air content. It has been observed that the addition of CO_2 results in an immediate reaction resulting in increased initial temperature and a higher maximum temperature. The observed results regarding the fresh properties are independent of the content of slag in the binder, which means it is the addition of CO_2 that is the governing factor. The reference showed only small and insignificant deviations in the compressive strength with increased amount of CO_2 added. Concrete with 20 % slag showed only negative effects regarding the compressive strength. Concrete with 30 % slag showed better improvements at 28 days. Concrete with 70% slag showed significant improvements regarding the compressive strength. It was observed that the increase of slag in the binder has a better reaction with CO_2 injected during mixing, resulting in improvements of the compressive strength. Specimens cured in a CO_2 environment without pressure showed no increased compressive strength because the intrusion was not deep enough. The results show a minor increase in splitting tensile strength with an increased amount of CO_2. The results regarding modulus of elasticity could not be used to conclude on the effect on injecting CO_2. pH-values were not affected by the injecting of CO_2. Regarding the TGA, the reference batch and 70% slag concrete showed the greatest increase in CO_2 uptake. It is observed that concrete with more slag disperses the cement particles and allows more carbonation with less competitive sites.

Preface

This master's thesis was written in the spring of 2021 and will complete my master's degree in structures and material - Civil Engineering at the University of Stavanger.

I would like to thank my supervisor Kjell Tore Fosså for his guidance and support during this research. I would also like to thank Jarle Berge and Samdar Kakay for providing me with materials and equipment in the concrete laboratory. A great gratitude also goes to Stian Penev Ramsnes for his expertise in thermogravimetric analysis.

In the end, I would like to thank Simen Christensen Hjortland for the great cooperation at the lab and during this master's thesis.

Table of Contents

Notations

µm	Micrometer
°C	Celsius
cm	Centimeter
C_2S	Dicalcium silicate
C_3S	Tricalcium silicate
GPa	Gigapascal
C-H	Calcium hydroxide
$CaCO_3$	Calcium carbonate
C-S-H	Calcium silicate hydrate
CO_2	Calcium carbonate
kg	Kilogram
g	Gram
dm^3	Cubic decimeter
cm^2	Square centimeters
m^3	Cubic meter
mm^2	Square millimeters
mg	Milligram
l	Litre
Mpa	Megapascal
ml	Milliliter
mm	Millimeter
N	Newton
nm	Nanometer
s	Second
S-H	Silicate hydrate
TGA	Thermogravimetric analysis
C_4AF	Tetracalcium aluminoferrite
C_3A	Tricalciumaluminate
wt%	Weight percentage
w/c	water-cement ratio

1 Introduction

This chapter will present the background and motivation, objective and scope, and the structure of the thesis.

1.1 Background and Motivation

Global warming is one of the most discussed topics in the world, and is caused by greenhouse gas emissions. Some of the consequences of global warming are increased rainfall, melting of ice in the arctic regions, and rising sea level. A majority of climate scientists have discovered that human emission of greenhouse gases are the main reason for this global warming. There are several greenhouse gases, such as water vapor (H_2O), carbon dioxide (CO_2) and methane (CH_4) [1].

The Paris Agreement is a legally binding international treaty on climate change and was adopted by 196 Parties in Paris in 2015. Its goal is to limit global warming to well below 2, preferably to 1,5 °C, compared to pre-industrial levels. To achieve this long-term temperature goal, countries aim to reach global peaking greenhouse gas emissions as soon as possible to achieve a climate neutral world by mid-century (2050) [2]. Norway is among the 196 countries joining and will by the end of 2030 reduce the emissions by at least 55 % compared to the 1990-levels [3].

To achieve the goals set in the Paris Agreement many industries need to change and develop, such as the concrete industry. Concrete is one of the most used building material, and cement production alone accounts for 7-8 % of the greenhouse emissions globally [4]. There are several reasons for the large emissions connected to the cement. Firstly, it is one of the most used materials and the total cement production was in 2016 approximately 4,2 billion tons. Also the demand is increasing every year. Secondly is the production of cement. Cement is made by burning limestone combined with other materials in a rotating oven (kiln) at 1450 °C, which makes cement clinker. The process is called calcination, and is explained by equation 1.1:

$$CaCO_3\ (s) + \text{Heat} \rightarrow CaO\ (s) + CO_2\ (g) \qquad (1.1)$$

Limestone + Heat → Burnt lime + Carbon dioxide

Most of the greenhouse gas emissions of cement is from calcination. The rest of the emission is due to heating of the kiln and transportation. In the production of 1 ton cement clinker, approximately 1 ton CO_2 is released into the atmosphere [5].

Several methods are discussed to reduce the greenhouse emission from the concrete industry, and there is a broad agreement that it is a change in cement usage and production that needs the biggest change. The following measures is used, or in process of being introduced full scale:

- Use of organic fuel in the kiln.
- Carbon Capture, Utilization and Storage (CCUS) of CO_2 from the calcination process.
- Replace part of cement with pozzolans and hydraulic materials, such as slag and fly ash.

The most important way of reducing the CO_2 emission from the concrete industry is by using less cement. The most common method is to replace the cement with pozzolans and hydraulic materials, such as ground granulated blast furnace slag. In this context slag is considered "climate neutral" since slag is a by-product of the steel production. Slag may replace a large percentage of the cement, up to 90 %, but normal is 30-70 % [6].

Carbon capture, utilization and storage (CCUS) of CO_2 is also considered a great method of reducing the emissions from the concrete industry. The most common method used today is to store the CO_2 permanently in underground geological formations, onshore or offshore [7]. Norcem in Brevik is one of the first cement factories with a full scale carbon capture, and has the goal of being carbon neutral before 2030 [8]. Another method of utilizing the captured CO_2 from the cement production is to induce the captured CO_2 into concrete during mixing or early curing. It is shown that CO_2 will be chemically bound in the concrete and potentially improve several properties of the concrete.

1.2 Objective and Scope

The objective of this thesis is to examine the effect on the properties of concrete when injecting CO_2 during mixing and with different content of slag.

This is an individual thesis written by the author, but the experimental program is conducted in collaboration with Simen Christensen Hjortland. This thesis examines the effect of concrete injected with CO_2 during mixing and with different content of slag. Hjortland is writing about the same subject, but with fly ash instead of slag. Reference batches and several figures are therefore similar in both theses.

The scope of the thesis is limited to the following properties:

- The effect on fresh properties with the addition of CO_2
    - Workability (slump)
    - Density
    - Air content
    - Temperature development
- The effect on mechanical properties with the addition of CO_2
    - Compressive strength
    - Modulus of elasticity
    - Splitting tensile strength
- The effect on chemical changes with the addition of CO_2
    - pH - level
    - Thermogravimetric analysis

1.3 Thesis Structure

An overview of the thesis structure is presented below:

- Chapter 1 - Introduction
- Chapter 2 - Literature Review
- Chapter 3 - Experimental Program
- Chapter 4 - Results and Discussion
- Chapter 5 - Conclusion
- Chapter 6 - Future Work

2 Literature Review

The purpose of this chapter is to provide the relevant theory of injecting CO_2 during mixing of concrete with different content of slag. Subjects that will be discussed are the hydration of cement, effect of slag addition, carbonation and lastly earlier research conducted.

2.1 Cement

Concrete is a mixture of coarse gravel, sand, cement, water, admixtures and additives. Fine and coarse aggregates make up to 70 % of the volume, cement paste makes up to 30 % of the volume. Cement mixed with water is called cement paste and its properties are determined by the mass ratio between water and cement (w/c-ratio). [9]

Cement is made out of finely ground clinker, and the amount of clinker and other additives determines the properties of the cement. The clinker contains four major phases called allite, belite, aluminate and ferrite. Table 2.1 shows the typical composition of clinker, and table 2.2 shows the major phases in typical Portland clinker. [10]

Analyte	**Chemical name**	**Content (wt%)**
CaO	Calcium oxide / lime	60 - 70 %
SiO_2	Silicon dioxide / silica	17 - 24 %
Al_2O_3	Aluminum oxide / alumina	4 - 7 %
Fe_2O_3	Iron oxide	1,5 - 5 %
MgO	Magnesium oxide / magnesia	1 - 5 %
SO_3	Sulfite	0,5 - 3,5 %
$K_2O + Na_2O$	Alkali	0,2 - 1,5 %

Table 2.1: Typical composition of clinker [10]

Major phase	**"Mineralogical" term**	**Shortened cement chemical notation**	**Cement chemical notation**
Tricalciumsilicate	Alite	C_3S	$3CaO \cdot SiO_2$
Dicalciumsilicate	Belite	C_2S	$2CaO \cdot SiO_2$
Tricalciumaluminate	Aluminate	C_3A	$3CaO \cdot Al_2O_3$
Tetracalcium aluminoferrite	Ferrite	C_4AF	$4CaO \cdot Al_2O_3 \cdot Fe_2O_3$

Table 2.2: Major phases in typical Portland cement [10]

The hydration process is setting and hardening of concrete and are the results of chemical reactions between the cement minerals and water. The binder properties of a cement is determined by its composition, i.e. its fineness [11].

Hydration of C_3S and C_2S produces C-S-H (calcium-silicate-hydrates) and C-H (calcium hydroxide). C_3S is the major component in most Portland cements and gives rapid strength development. C_2S contributes to the long term strength development. Both reactions are exothermic, where C_3S have a heat development of 500 kJ/kg at full hydration, whereas C_2S have a heat development of 260 kJ/kg at full hydration. The reactions are shown in equation 2.1 and 2.2 [11].

$$2(3CaO \cdot SiO_2) + 6H_2O \rightarrow 3CaO \cdot 2SiO_2 \cdot 3H_2O + 3Ca(OH)_2 \quad (2.1)$$

Tricalciumsilicate + Water → C-S-H + Calcium hydroxide

$$2(2CaO \cdot SiO_2) + 4H_2O \rightarrow 3CaO \cdot 2SiO_2 \cdot 3H_2O + Ca(OH)_2 \quad (2.2)$$

Dicalciumsilicate + Water → C-S-H + Calcium hydroxide

The hydration of C_3A and C_4AF are in many ways analogous, and therefore the reaction of C_3A will be explained. The reaction between C_3A and water is very rapid and would result in immediate setting (flash set). Due to the fact that gypsum is added to the clinker, this would not occur. C_4AF reacts more slowly and therefore does not give the same setting problems. Both reactions are exothermic, where C_3A has a heat development of 900 kJ/kg at full

hydration, whereas C_4AF has a heat development of 300 kJ/kg at full hydration. The reaction between gypsum and C_3A forms ettringite. Ettringite further reacts with unreacted C_3A and water and forms monosulphate. Equations 2.3 and 2.4 show the reactions [11].

$$3CaO \cdot Al_2O_3 + 3(CaSO_4 \cdot 2H_2O) + 26H_2O \rightarrow 3CaO \cdot Al_2O_3 \cdot 3CaSO_4 \cdot 31H_2O \quad (2.3)$$

Tricalciumaluminate + gypsum + water → Ettringite

$$3CaO \cdot Al_2O_3 + 4H_2O + 3CaO \cdot Al_2O_3 \cdot 3CaSO_4 \cdot 31H_2O \rightarrow 3(3CaO \cdot Al_2O_3 \cdot CaSO_4 \cdot 12H_2O) \quad (2.4)$$

Tricalciumaluminate + water + Ettringite → Monosulphate

2.2 Ground granulated blast furnace slag

Ground granulated blast furnace slag, hereafter referred to as slag, is a by-product of steel production. Slag is a common replacement of cement in the concrete mix. The chemical composition and physical structure depend on the process of production, ore source and cooling procedure.

Analyte	**Chemical name**	**Content (wt%)**
CaO	Calcium oxide / lime	30-50 %
SiO_2	Silicon dioxide / silica	28-38 %
Al_2O_3	Aluminum oxide / alumina	8-24 %
MgO	Magnesium oxide / magnesia	1-18 %
S	Sulfur	1-2,5 %
$MnO + Fe_2O_3$	Manganese (II) oxide + Iron(III) oxide	1-3 %
TiO_2	Titanium dioxide	< 4%
$Na_2O + K_2O$	Alkali	< 2 %

Table 2.3: Typical chemical composition of slag [12]

A typical slag is composed of lime (CaO), silica (SiO_2) and alumina (Al_2O_3), with minor amounts of magnesia, alkali oxides, and iron oxides. Table 2.3 above shows the chemical composition of a typical slag [12].

Achieving quenching of slag is crucial. This quenching leads to the slag precipitates as glass. The precipitates are called granules and have the dimension of 4-5 mm, therefore, it is called granulated blast furnace slag. Slag has a density of 2,9 kg/dm³ and the particles are angular. The slag is ground to desired fineness separately or together with the Portland clinker [12].

Slag is a latent hydraulic material, and by chemical reactions slag does have hydraulic properties and forms C-S-H like cement. Slag does also have a limited element of pozzolan reactivity. When slag is described as latent hydraulic, it means that slag does not react chemically with water but must be activated at high pH to break down the glass phase. Normally slag is mixed with Portland cement, because the alkali hydroxides and calcium hydroxides from the hydration of the cement works as a chemical activator for the slag. The addition of slag usually is between 30 and 70 % (mass of total binder) [6].

Slag is activated chemically by the following ways:

- Alkali activators: NaOH, $Ca(OH)_2$, Na_2CO_3
- Sulfur, for example gypsum or hemihydrate: $CaSO_4 \cdot 2H_2O$, $CaSO_4 \cdot 0{,}5H_2O$

Both these activators may work at the same time, which is the case by using Portland cement as the activator. When water is mixed into the slag-Portland-cement system, a small part of the slag will react immediately and release calcium and aluminum ions. As described above the further reaction needs the pH value to be high enough to break down the glass phase, and this pH-value is about 12. This implies a certain amount of Portland cement has reacted such that the pH level establishes around 12, which happens relatively rapidly when the water has been added. In the Portland cement-slag-water system the slag will react firstly with the alkali hydroxides, then a reaction with C-H [13].

The reaction rate for slag depleted generally with an increase in slag/cement ratio, which is a result of decreasing pH. With an increase in the amount of slag gives a double negative effect. Primarily because there is a lower amount of cement, but also a lower reactivity for the slag part due to low pH. Slag concrete has a considerably increased amount of C-S-H and denser

pore structure in relation to concrete with Portland cement. One of the reasons is the capillary porosity is heavily reduced in slag concrete as C-S-H unfolds in another way than by a hydration of Portland cement. For a normal hydration, C-S-H precipitates on the cement grains surface area, whereas in a slag concrete the C-S-H precipitates in the void between the slag grain and the cement grain. This results in a better distribution of the C-S-H gel [13].

Slag as cement replacement results in a reduced amount of C-H, both as a consequence of reduced cement and because of the use of C-H over time. Slag also reduces the alkalinity of the concrete, due to high concentration of negative sulfur compounds in the pore water. This results in a reduction in OH-, which results in reduced alkalinity in slag concretes [13].

Slag is a widely used cement replacement material. Some of the benefits of using slag are:

- Increased strength and durability, decreased permeability.
- High resistance to chloride penetration, sulphate attack and alkali-silica reaction.
- Very low heat of hydration.
- Suppresses efflorescence.
- Improvement of life cycle costs of concrete structures.

The main issue of concrete containing slag as a cement replacement is that the early strength development over the first few days is slower for concrete with slag than without slag. However, the strength of the concrete with slag can eventually exceed that of the ordinary cement concrete at later ages, typically beyond 28 days [14].

2.3 Carbonation

Carbonation of concrete is where calcium containing hydration products are transformed to $CaCO_3$. There are two distinct types of carbonation concrete may be subjected to, and these are weathering carbonation and early age carbonation [15].

2.3.1 Weathering carbonation

Weathering carbonation concerns mature concrete reacting over an extended period when it is exposed to carbon dioxide in the atmosphere. This is also called atmospheric carbonation and occurs in concrete when calcium compounds react with carbon dioxide (CO_2) from the atmosphere and water in the concrete pores. The first reaction is that CO2 reacts with the water in the pores to form carbonic acid (H_2CO_3). The carbonic acid then reacts with calcium compounds contained within the hydration products, mainly C-H. The reaction between the carbonic acid and C-H forms calcium carbonate ($CaCO_3$) and water. The complete reaction is shown in equation 2.5 and 2.6 [15].

$$CO_2 + H_2O \rightarrow H_2CO_3 \quad (2.5)$$

Carbon dioxide + Water → Carbonic acid

$$Ca(OH)_2 + H_2CO_3 \rightarrow CaCO_3 + 2H_2O \quad (2.6)$$

Calcium hydroxide + Carbonic acid → Calcium carbonate + Water

When the C-H has carbonated and is depleted from the cement paste, the C-S-H gel can be decalcified thereby allowing the liberated CaO to carbonate as shown in equation 2.7 [15].

$$H_2CO_3 + CaO \rightarrow CaCO_3 + H_2O \quad (2.7)$$

Carbonic acid + Calcium oxide → Calcium carbonate + Water

The depletion of C-H will cause the concrete pore solution pH to drop below 13 and may also drop as low as 8 for fully carbonated concrete. Therefore, concrete with ferrous reinforcement requires a high pH to ensure the stability of the protective layer on the surface of the reinforcement. A drop in pH level can therefore cause the passive layer to deteriorate and cause harmful corrosion. Due to the corrosion product occupying a greater volume than

the original reinforcement, internal stresses can cause cracking of the concrete cover. Figure 2.1 illustrates the weathering carbonation process [15].

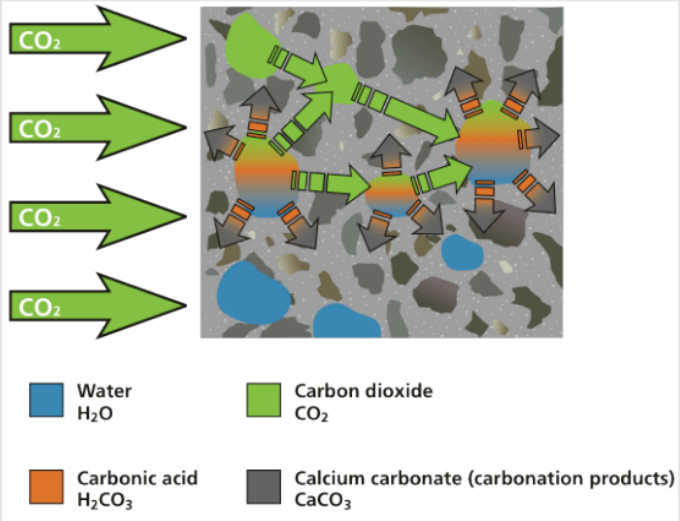

Figure 2.1: Weathering carbonation [15]

2.3.2 Early age carbonation

Early age carbonation occurs when the carbonation reactions occur alongside the early hydration of the cement through a deliberate exposure of fresh concrete to carbon dioxide (CO_2). The carbonation can take place as early as the concrete mixing stage and can end prior to the conclusion of accelerated curing, as much as 48 hours later. The carbonation occurs rapidly and can contribute to a denser and stronger concrete, as the carbonate product formation contributes to strength development. CO_2 gas is injected during mixing and reacts with C_3S and C_2S in the cement. The chemical reaction is shown in equation 2.8 and 2.9 [15].

$$3CaO{\cdot}SiO_2 + (3\text{-}x)\ CO_2 + y\ H_2O \rightarrow x\ CaO{\cdot}SiO_3{\cdot}y\ H_2O + (3\text{-}x)\ CaCO_3 \qquad (2.8)$$

Tricalciumsilicate + Carbon dioxide + water → Calcium silicate hydrate + Calcium carbonate

$$2CaO{\cdot}SiO_2 + (2\text{-}x)\ CO_2 + y\ H_2O \rightarrow x\ CaO{\cdot}SiO_3{\cdot}y\ H_2O + (2\text{-}x)\ CaCO_3 \qquad (2.9)$$

Dicalciumsilicate + Carbon dioxide + water → Calcium silicate hydrate + Calcium carbonate

Both reactions are spontaneous and exothermic, and the nine following steps is a summation of the various reactions for the early age carbonation:

1. CO_2 gas diffuses through the air to reach the concrete.
2. The CO_2 permeates through the air-filled porosity of the concrete mass.
3. Solvation of CO_2 (g) to CO_2 (aq) in the liquid phase of the fresh concrete.
4. Hydration of CO_2 (aq) to H_2CO_3.
5. Ionization of H_2CO_3 to H^+, HCO_3^- and CO_3^{2-}. The presence of H^+ ions causes the pH of the developing cementitious system to drop. The pH can recover as the microstructure matures.
6. Dissolution of C_3S and C_2S, which occurs rapidly, cyclically and exothermically. Cement grains are covered by a loose layer of C-S-H gel that dissolves to release Ca^{2+} and SiO_4^{4-} ions.
7. Nucleation of thermodynamically stable $CaCO_3$ and conventional formation of C-S-H gel.
8. The $CaCO_3$ precipitates as a solid phase. Calcite is the preferred polymorph.
9. Secondary carbonation also occurs; sustained reaction of CO_2 and the cement paste can see C-S-H gel formed through the parallel early hydration decalcified and producing a calcium-depleted silicate hydration and $CaCO_3$.

Figure 2.2 illustrates the nine steps described above [15].

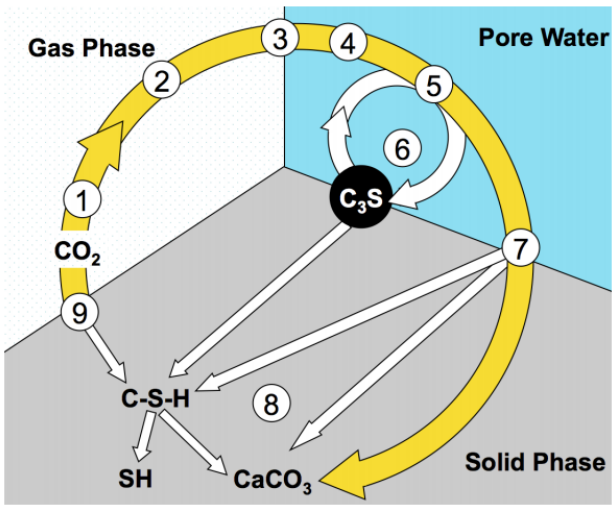

Figure 2.2: Early carbonation of fresh concrete [15]

Larger amounts of CO_2 injected to the concrete may according to equation 2.8 and 2.9 prevent formation of C-S-H and instead form S-H (silicate hydrate) and $CaCO_3$, as shown in equation 2.10 og 2.11 [16].

$$CaO{\cdot}SiO_2 + 3CO_2 + y\ H_2O \rightarrow SiO_2{\cdot}yH_2O + 3\ CaCO_3 \qquad (2.10)$$

Tricalciumsilicate + Carbon dioxide + water → Silicate hydrate + Calcium carbonate

$$2CaO{\cdot}SiO_2 + 2CO_2 + y\ H_2O \rightarrow SiO_2{\cdot}yH_2O + 2\ CaCO_3 \qquad (2.11)$$

Dicalciumsilicate + Carbon dioxide + Water → Silicate hydrate + Calcium carbonate

Reactions in the early ages carbonation can involve calcium that would otherwise have hydrated to form C-H and contribute to high pH. However, the early age carbonation does not hinder the long-term development of the concrete microstructure as the concrete matures. This means that C-H will form during the later hydration and the pore solution pH development continues as normal once the carbonation application ends [15].

During early carbonation, only an infinitesimal amount (<< 1 %) of calcium-silicate phases are carbonated and the subsequent hydration of the phases is not impacted beyond an acceleration in the rate of hydration at early ages. The nature and quantity of the hydrates that form and pH of the concrete remains unchanged. The CO_2 uptake during early carbonation is typically less than 0,2 % by mass of the cement in the mixture, and more than 99 % of the calcium silicates remain to undergo the normal hydration. There has also not been found that early carbonation has any measurable impact on subsequent hydration or alkalinity (pH). Also, no negative impact on subsequent rate of atmospheric carbonation, chloride ingress and does not increase the risk of steel corrosion in reinforced concrete [17].

Another way of carbonation is the reaction between C-H and CO_2, as shown in equation 2.12.

$$Ca(OH)_2 + CO_2 + H_2O \rightarrow CaCO_3 + 2H_2O \qquad (2.12)$$

Calcium hydroxide + Carbon dioxide + Water → Calcium carbonate + Water

In freshly prepared concrete there is negligible calcium hydroxide present, and C_3S and C_2S are the primary reactants for carbonation [18, 20].

There are several methods of injecting CO_2 into the mixing, and the most common method is as gaseous CO_2. Several other methods have also been tested, such as carbonated water and dry ice (solid CO_2) [20].

2.3.3 Carbonation of slag

It is not only the cement that carbonates but also other calcium-carrying materials. Normal additives used in concrete are fly ash and slag. The carbonation of these additives forms thermodynamically stable $CaCO_3$, such as carbonation of cement does.

Weathering carbonation is, as mentioned above, a slow reaction between calcium compounds and carbon dioxide in the air. Blended slag-cement concretes exposed to this type of carbonation have been associated with higher carbonation rates which can lead to lower compressive strengths and increase the risk of steel corrosion in concrete due to the reduction in pH-values [21].

Regarding early carbonation, slag is much less reactive to carbon dioxide because of its glassy nature. Cement is more reactive than the slag, and therefore in a slag cement it is the cement that will be carbonated. The dispersed cement particles carbonate more when the less reactive slag is present. Figure 2.3a shows an ordinary Portland cement. The white circles are the cement with carbonated products surrounding them. Figure 2.3b shows a 50/50 blend of slag and cement, where the white circles are cement and the grey circles are slag. There are more carbonated products on the cement particles when slag is present because the cement is dispersed and more reactive [21].

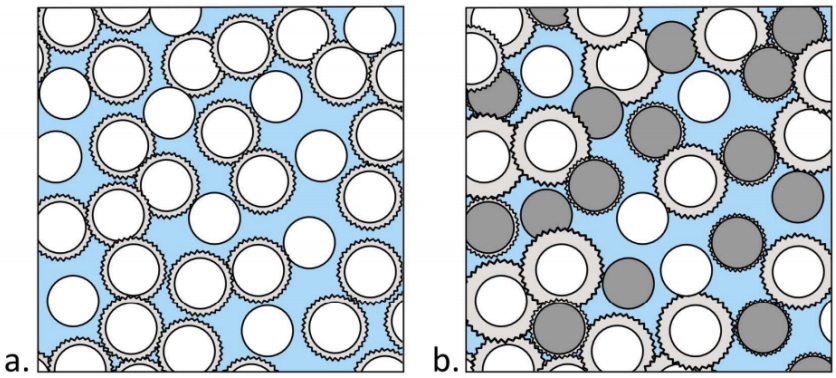

Figure 2.3a: Carbonation of OPC [21]

Figure 2.3b: Carbonation of a slag cement [21]

The slag allowed the vigorous carbonation of cement to take place with fewer competitive sites in which a cement particle was adjacent to another cement particle or CO_2 penetrated deeper into the concrete before ingress was slowed by buildup of carbonation products [21].

2.3.4 Calcium carbonate - $CaCO_3$

The reaction product from both weathering carbonation and early carbonation is calcium carbonate ($CaCO_3$). The formation of $CaCO_3$ in weathering carbonation is not desirable, because of the sour environment created when C-H reacts with CO_2. The case is different in early carbonation, where formation of $CaCO_3$ not only sequesters CO_2, but also may have several other desirable properties.

The reaction between C_3S, C_2S and CO_2 forms $CaCO_3$ and C-S-H. Using $CaCO_3$ as a direct addition is also a normal procedure. The normal particle size of these is 0-100 µm, and therefore classifies as a nanoparticle. In recent years it has been found that adding nanoparticles has many advantages considering the properties of the concrete. The chemical and physical properties of nanomaterials enable several applications ranging from structural reinforcement to environmental pollution reduction. Adding $CaCO_3$ to the concrete mix has shown effects on the hydration and strength development. Hydration has been highly focused, as it is found that $CaCO_3$ acts as a nucleation site which cement hydration products form (C-S-H). The $CaCO_3$ has a larger surface area, which promotes hydration reactions with relatively reasonable cost. Studies also show comparable or better early-age compressive strength results, except with a high dosage. The influence of $CaCO_3$ on the hydration of ordinary Portland cement (OPC) with supplementary cementitious materials, such as slag, accelerated the hydration. The greater the amount of the addition of $CaCO_3$, the greater was the accelerating effect. Effects were also shown at the microhardness and modulus of elasticity at the early stage of the hydration, which increased significantly [22].

$CaCO_3$ has been shown to increase the early hydration, microhardness, and modulus of elasticity when added at 10 % by weight of cement to an ordinary Portland cement (OPC) paste. These improvements are due to the $CaCO_3$ providing nucleation sites for C-S-H development. It has been observed that just a little as 1 % addition of $CaCO_3$ by weight of cement has decreased the setting time, decreased early age shrinkage, improved flexural

strength, and increased its compressive strength. The same beneficial impacts to concrete will occur as $CaCO_3$ is developed through CO_2 injection during mixing. One of the benefits of forming $CaCO_3$ from CO_2 injection is the anticipated efficiency of distributing reactants in gas or liquid form rather than nano-scale particulate materials [23].

The accelerating effect of adding nano-$CaCO_3$ is shown in figure 2.4 [24].

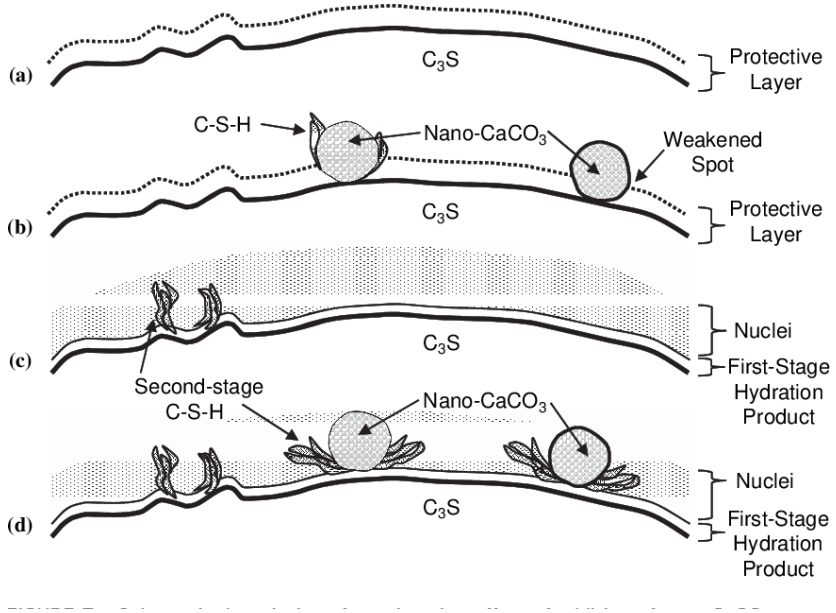

Figure 2.4: Accelerating effect of adding nano-$CaCO_3$ [24]

$CaCO_3$ also has a filler effect and enhanced dilution in the concrete. This will contribute to increasing the density of the concrete [25]. Also a decrease in workability is observed with increasing amounts of $CaCO_3$, due to larger specific surface area and therefore more water absorption [26].

2.4 Previous research

The following chapter will present the previous research done on injecting CO_2 during mixing, also called early age carbonation. The selected previous research is designated in terms of the experimental program that will be conducted in this thesis. Previous research mainly focuses on two different areas; the effect CO_2 has on the fresh and hardened properties, or the effect CO_2 has on microstructure and chemical composition of the concrete. Injecting CO_2 into concrete has been researched from the early 1970s and is still studied in several countries. The procedure is in use in some countries, such as the USA, Singapore, and Canada. The presented results are based on a literature study done during the spring of 2021.

The chapter is divided into fresh properties, hardened properties, and chemical composition.

2.4.1 Fresh properties

2.4.1.1 Workability

In previous studies there has been a reduction in workability, when injecting CO_2 into the concrete during mixing. A reduction in workability is a disadvantage when placing and when compacting the concrete. This is therefore not a desired effect of injecting CO_2 into the fresh concrete.

Kjos [27] observed the reduction in the slump as the dosage of CO_2 increased. The mix with the highest dosage had a reduction of 88 % from the reference, which is a significant reduction. Figure 2.5 shows the reduction of the slump. Kjos assumes that the reduction in slump is because of the formation of $CaCO_3$. As mentioned in 2.3.4, the $CaCO_3$ has a large specific surface area and will absorb free water in the concrete.

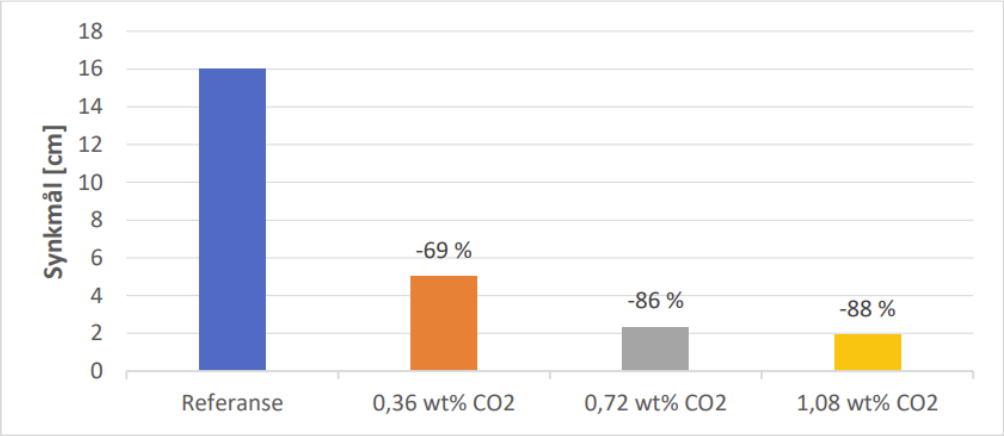

Figure 2.5: Reduction in slump [27]

Monkman, MacDonald and Hooton [28] observed this effect in their experiment. Table 2.4 shows the different mixtures, level of CO_2 dosage and the slump. The slump is a very common way of measuring the workability, and the slump decreases as the dosage of CO_2 increases. This experiment also had a difference in when the injection of CO_2 was performed. Monkman, MacDonald and Hooton do not comment if it is the increase in dosage of CO_2, if it is the age at injection that is the main reason for the reduction in slump or any other reasons for this.

Sample Code	Condition	Age at injection (min)	CO_2 Dose (%bwc)	Slump (inches)	Mix Temperature (°C)
1401	Control	-	-	3.5	23.9
1402	CO_2	42	0.10	3.0	-
1403	CO_2	56	0.30	3.0	25.6
1404	CO_2	71	0.60	2.0	26.5

Table 2.4: Fresh properties of the concrete with CO_2 added [28]

Liu, Chen, Liu and Wang [29] studied the effect of adding nano-$CaCO_3$ directly. Table 2.5 shows the reduction in flowability (slump). The reduction in the workability is explained as the surface area of the $CaCO_3$ needs to be covered with free water.

Specimens	NC (%)	Water requirement of normal consistency (ml)	Setting time		Flowability (mm)
			Initial Setting time (min)	Final setting time (min)	
C0	0	132	200	260	163
NC1	1	132	187	232	137
NC2	2	132	139	221	130
NC3	3	132	131	207	120

Table 2.5: Fresh properties of concrete with direct adding of nano-$CaCO_3$ [29]

2.4.1.2 Air content

The air content influences the compressive strength of the concrete. A rule of thumb states that the compressive strength is reduced by 5 % for each 1 % air [30]. Therefore, an increase in air content is not a desired effect.

Kjos [27] shows a connection between increase in air content and a higher dosage of CO_2. The correlation is shown in figure 2.6. The highest dosage of CO_2 shows an increase in the air content. Kjos assumes that this has a connection with the reduction in slump. The reduction in slump would reduce the compaction ability which results in higher air content in the concrete. A reduction in free water would result in a reduction of the air content of the concrete. Due to the increase of air content, Kjos assumes that it is the reduction in workability that is the main reason for increased air content.

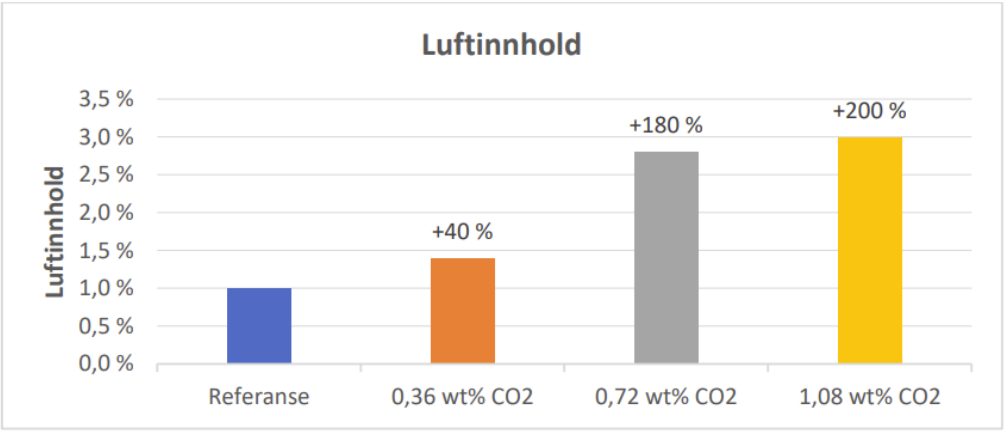

Figure 2.6: Air content in concrete with CO_2 injected [27]

Monkman, MacDonald and Hooton [28] did not report any results regarding the air content in their research. In the research with regards to nano-$CaCO_3$ conducted by Liu, Chen, Liu and Wang [29], no results regarding the air content were reported.

2.4.1.3 Density

Kjos [27] only found a small change in the density when increasing the dosage of CO_2. Figure 2.7 shows the result. The difference in density from the reference mix to the mix with the highest content of CO_2 was only a 0,6 % decrease. It is assumed that the decrease in the fresh density is a result of the reduction in slump because of the reduced compactability. Furthermore it is assumed that this small decrease in density will not have a big consequence of the mechanical properties of the concrete.

As described in section 2.3.4, $CaCO_3$ has a filler effect in the concrete, and would in this case result with an increase in the density. Since Kjos did not observe an increase in the research it was concluded that the main reason for the reduction in density was because of the loss in compactability.

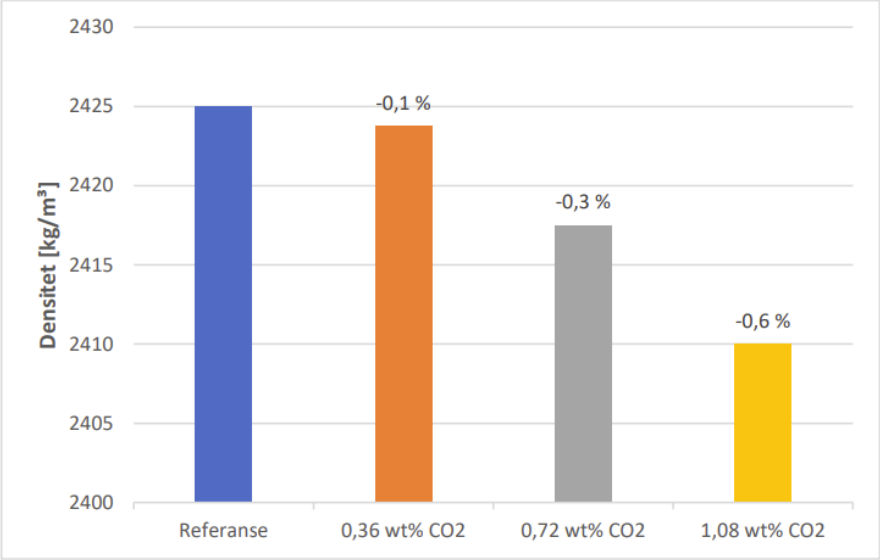

Figure 2.7: Density of concrete with CO_2 injected [27]

Monkman, MacDonald and Hooton [28] did not report any results regarding the density in their research, neither did Liu, Chen, Liu and Wang [29].

2.4.1.4 Temperature development

Temperature development is used as a measure of the development of mechanical properties.

Kjos [27] observed the temperature development presented in figure 2.8. There is no large deviation between the maximum temperatures of concrete with CO_2 addition and without. The starting temperature on the other hand showed a correlation between increasing temperature and increasing CO_2 addition. This is explained as the spontaneous and exothermic reaction between C_3S, C_2S and CO_2. The small deviations in maximum temperature and the lower temperature further in the hydration for batches with 0,72 wt% and 1,08 wt%, is explained as the $CaCO_3$ does not finely disperse in the cement paste. This results in clustering of the $CaCO_3$ particles and reduces the specific surface area which reduces the number of sites where the C-S-H may form. This is the reason for the decrease in heat development.

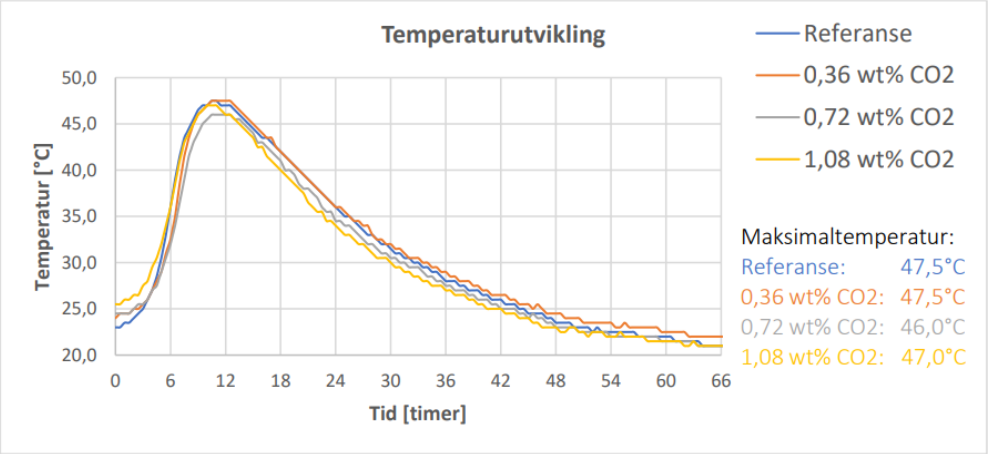

Figure 2.8: Temperature development, Kjos [27]

In the second trial of Monkman, MacDonald and Hooton [28] test there was found similar readings. The batch 805 was mixed with 0,3 wt % CO_2 during mixing, and the heat development is shown in figure 2.9. At 11 hours there was a reduction of 17 %, however the hydration thereafter accelerated to reach 7 % more at 20 hours. The cause of the initial hydration deceleration is due to the hydration being thought to slow due to early hydration products coating the silicates and retarding dissolution or change in the dissolution mechanism. Once the initial product coating on the silicates has been overcome the hydration accelerates due to increased product surface area providing nucleation sites.

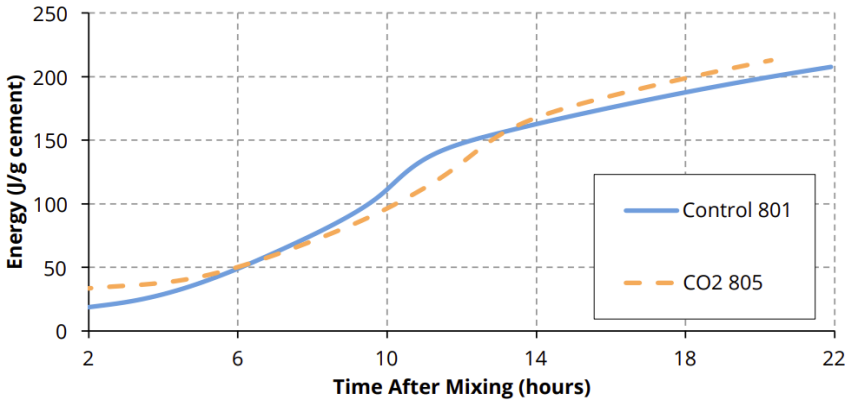

Figure 2.9: Heat development with CO_2 addition in the mixer [28]

Liu, Chen, Liu, and Wang [29] found that both initial and final setting time was reduced with the increase of nano-$CaCO_3$. Table 2.5 shows the results. It is concluded that the acceleration in the hydration is due to the nucleation sites to facilitate the formation of hydration products.

2.4.2 Hardened properties

2.4.2.1 Compressive strength

The compressive strength is one of the most important properties of concrete. Both increase and decrease in compressive strength is observed in earlier research. The main reason for the increase in compressive strength is that $CaCO_3$ acts as a nucleation site which cement hydration products form (C-S-H), i.e. an accelerated formation of the C-S-H gel. A drop in the compressive strength may be explained as a larger dosage of $CaCO_3$ no longer finely divided in the cement paste, but clustered together. This is a reduction in the specific area and therefore reduces the new growth areas for the formation of C-S-H. Too high dosage of CO_2 also may reduce the formation of C-S-H according to equation 2.10 and 2.11.

Kjos [27] performed a compressive strength test at 1, 3, 7 and 28 days after casting. Figure 2.10 shows the mean compressive strength of three specimens. All the mixtures with addition of CO_2 showed a decrease after 1 day, but an increase after 3 and 7 days. After 28 days there was no significant increase or decrease. It is therefore assumed that there is no clear correlation between the amount of CO_2 added and the compressive strength.

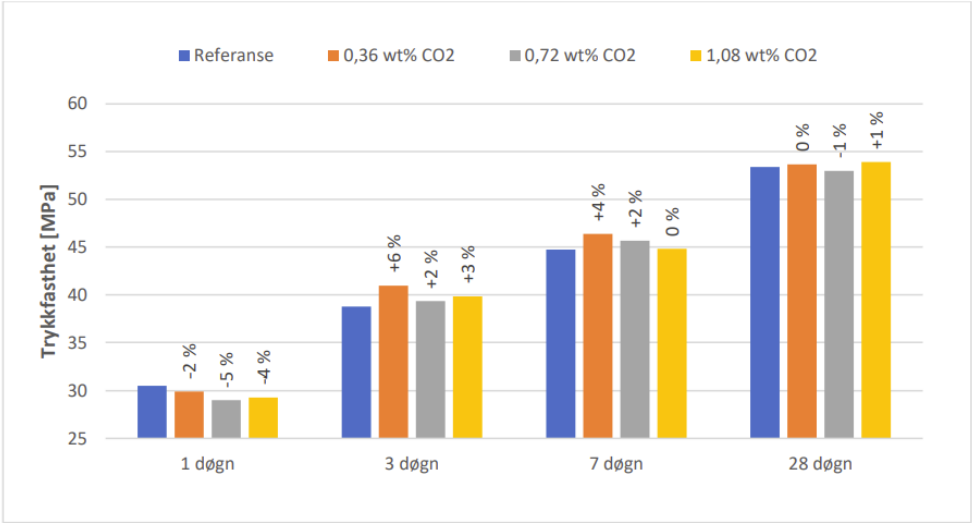

Figure 2.10: Compressive strength of concrete with CO_2, Kjos [27]

Monkman, MacDonald and Hooton [28] observed an increase in compressive strength with increasing dosage of CO_2. Figure 2.11 shows the different mixtures, with 0,10, 0,30 and 0,60 wt% dosage of CO_2. There was no significant increase in the mix with 0,10 wt%, but significant results for the two others. This is concluded to be correct according to the improvement observed through the calorimetry. The compressive strength increased the most in the last mixture, the greatest result of 26 % increase at 58 days.

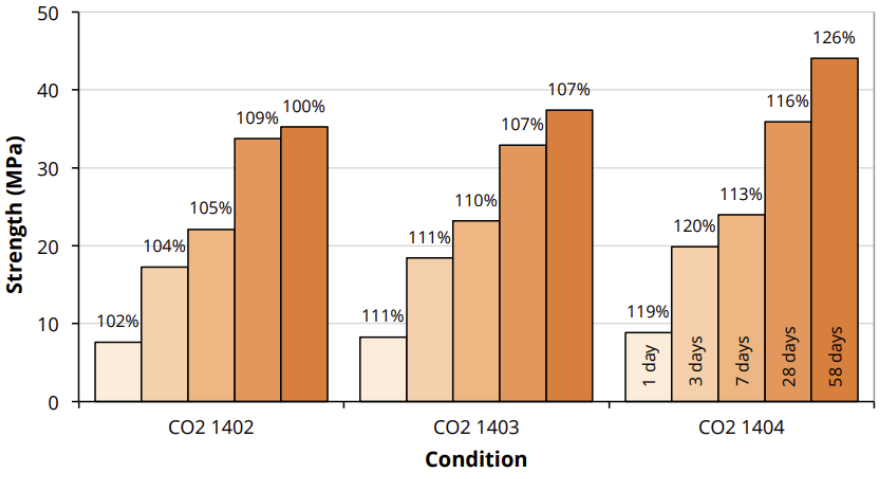

Figure 2.11: Compressive strength with CO_2 added [28]

During the second trial of Monkman, MacDonald and Hooton's research a third batch was done, where the injection of CO_2 was done during the batching stage (batch 805). The dosage for this batch was 0,30 wt%. Table 2.6 shows the compressive strength of the second trail. As

the first trial, an increase in compression strength was presented. The results of batch 805 showed a strength benefit exceeding 14 % at all ages including 26 % benefit at 3 days and 15 % at 91 days. It is also concluded that to induce during mixing is favorable.

Sample Code	Condition	Test age					
		1 day	3 day	7 day	28 day	56 day	91 day
0801	Control	8.0	14.8	19.2	30.8	32.8	36.8
0802	CO_2	8.0	15.8	20.4	32.0	27.9	37.8
0803	CO_2	8.6	16.6	21.4	33.9	37.9	38.9
0804	CO_2	8.7	16.1	22.1	32.8	36.4	39.6
0805	CO_2	9.2	18.6	23.2	35.5	38.7	42.4
0801	Control	100%	100%	100%	100%	100%	100%
0802	CO_2	99%	107%	106%	104%	85%	103%
0803	CO_2	106%	112%	111%	110%	116%	106%
0804	CO_2	108%	109%	115%	107%	111%	107%
0805	CO_2	114%	126%	121%	115%	118%	115%

Table 2.6: Compressive strength of second trail [28]

Liu, Chen, Liu, and Wang [29] observed an increase in compressive strength by adding nano-$CaCO_3$ directly during mixing. Figure 2.12 shows an increase in compressive strength up to 2 wt% addition of nano-$CaCO_3$. After 7 days the increase was 11,2 % and after 28 days it was 8,6 %.

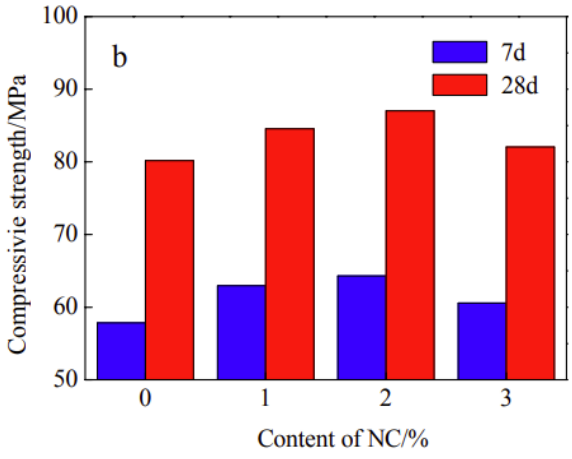

Figure 2.12: Compressive strength with addition of nano-$CaCO_3$ [29]

2.4.2.2 Modulus of elasticity

The Modulus of elasticity of the concrete depends on the modulus of elasticity of the aggregates and the compressive strength of the concrete [31].

Kjos [27] observed an increase in the modulus of elasticity in the batches with 0,36 wt% and 1,08 wt% CO_2, but a reduction at the batch with 0,72 wt% CO_2. Figure 2.13 shows the modulus of elasticity (GPa) and the dots illustrate the compressive strength (MPa) of the different batches. Kjos assumes that there is in fact a correlation between the modulus of elasticity and compressive strength and modulus of elasticity of the aggregates. Kjos also states that it needs more research on the modulus of elasticity, because only one cylinder was tested at each batch.

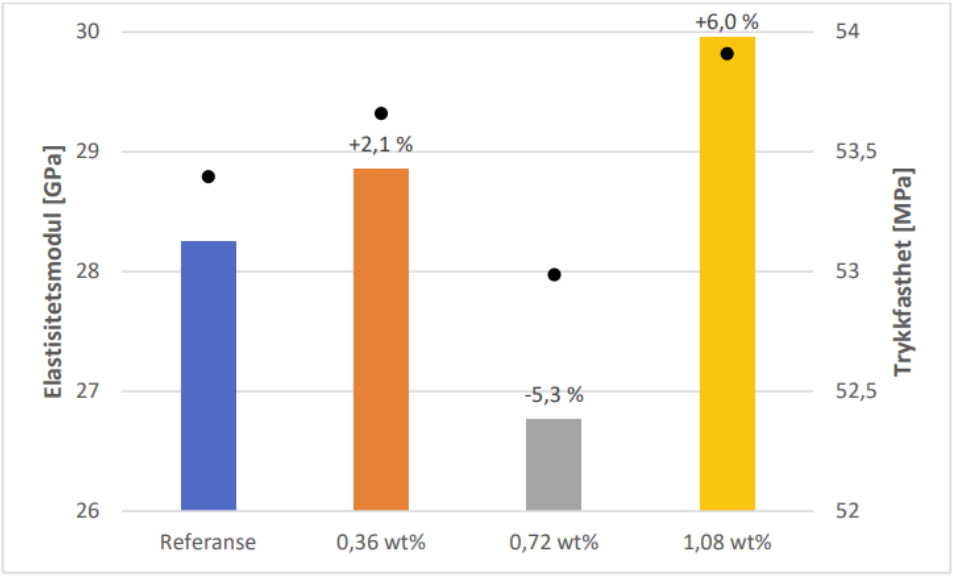

Figure 2.13: Modulus of elasticity of concrete with CO_2, Kjos [27]

Monkman, MacDonald and Hooton [28] did not report any results regarding the modulus of elasticity in their research, neither did Liu, Chen, Liu, and Wang [29].

2.4.2.3 Splitting tension strength

Splitting tension strength is approximately 4-12 % of the concrete's compressive strength and should show some deviations due to the addition of CO_2 [32].

Kjos [27] observes a correlation between dosage of CO_2 and increase of splitting tension strength. All the batches with CO_2 had an increase, where the batch with 1,08 wt% had the greatest increase of 7,2 %. Figure 2.14 shows the splitting tension strength (MPa) and the dots represent the compressive strength (MPa). Kjos only conducted one test for each batch and does not conclude that there is in fact any correlations.

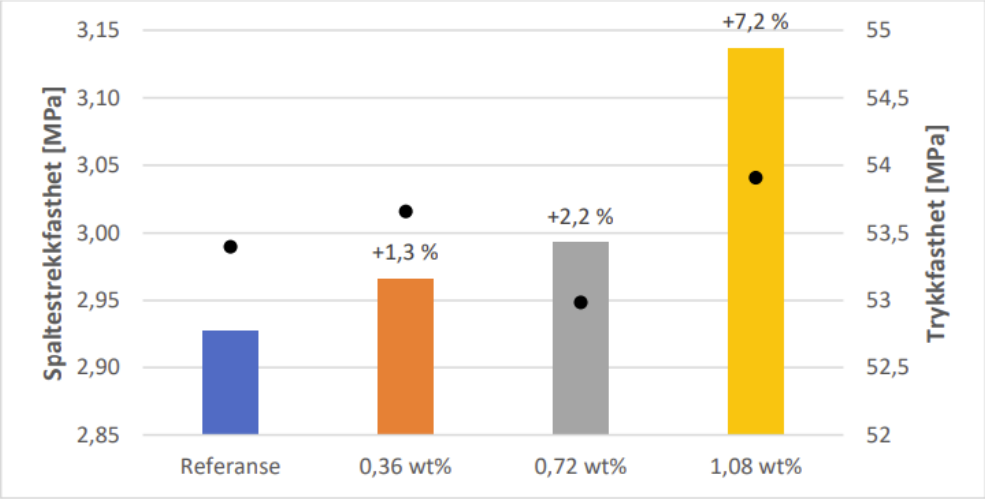

Figure 2.14: Split tension strength of concrete with CO_2 added [27]

Monkman, MacDonald and Hooton [28] did not report any results regarding the split tension strength in their research, nor did Liu, Chen, Liu, and Wang [29].

2.4.3 Chemical composition

2.4.3.1 pH-measurements

Weather carbonation is explained in 2.3.1, and is a result of CO_2 reacting with C-H to make a sour environment and may result in corrosion of steel reinforcement. Early age carbonation is injection of CO_2 during mixing, and research shows that this does not affect the pH-value of the concrete. CO_2 reacts with C_3S and C_2S and therefore it is not any CO_2 left to carbonate later.

Kjos [27] shows the pH-value after 28 days of hardening in figure 2.15. The pH value is steady around 12,3 and it is concluded that the pH-value is not affected by the inducing of CO_2.

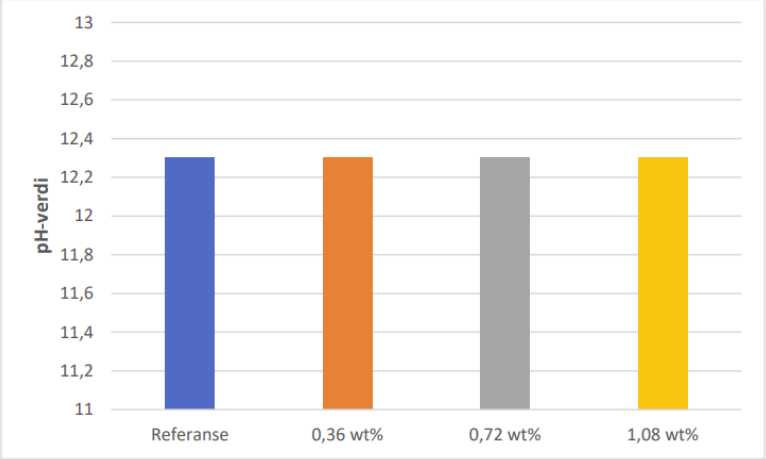

Figure 2.15: pH-values of concrete with CO_2 added, Kjos [27]

Monkman and Thomas [33] tested the pH-value of the pore solution and found that the pH value of 5 carbonated samples range from 13,74 to 13,81. It is concluded that the carbonation treatment does not increase the risk of ferrous reinforcement depassivation due to reduced pore solution alkalinity.

2.4.3.2 Thermogravimetric Analysis

Thermogravimetric Analysis (TGA) is one of several methods to quantify the chemical composition in concrete.

Kjos [27] performed TGA after 28 days from the different concrete batches. Figure 2.16 shows the loss in mass (%) as y-axis and the temperature (°C) as the x-axis. Free water is dissolved in the concrete approximately at 180 °C, in the area of 400-600 °C C-H dehydrates, and $CaCO_3$ decarbonates in the area of 600-900 °C. Batches with CO_2 added show a greater loss in mass around 700 °C, which is due to $CaCO_3$ being created due to the early carbonation. Figure 2.17 shows mass loss at the intervals of 180-400 °C, 400-600 °C and 600-900 °C. The majority of C-S-H is dissolved around 180-400 °C, and the batch with 0,36 wt % CO_2 shows that there is produced more C-S-H in this batch. Kjos refers to the nucleation site the $CaCO_3$ crates. The reduction of C-S-H in the batches with 0,72 and 1,08 wt % CO_2 is explained as the $CaCO_3$ clustering and reduced the specific surface area and therefore reducing the nucleation sites for C-S-H production. In the interval of 600-900 °C, $CaCO_3$ decarbonates. An increasing dosage shows an increase in $CaCO_3$, which is expected as C_3S and C_2S forms $CaCO_3$ in a reaction with CO_2. Also the reference has a mass loss in this interval, but this is explained as C-S-H does not completely dissolve in the 180-400 °C interval, but some may also be dissolved in the interval of 105-1000 °C.

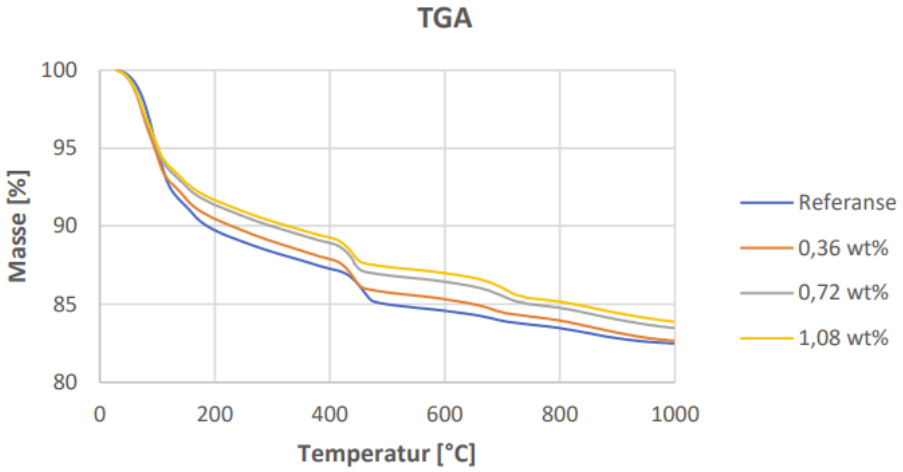

Figure 2.16: TGA [27]

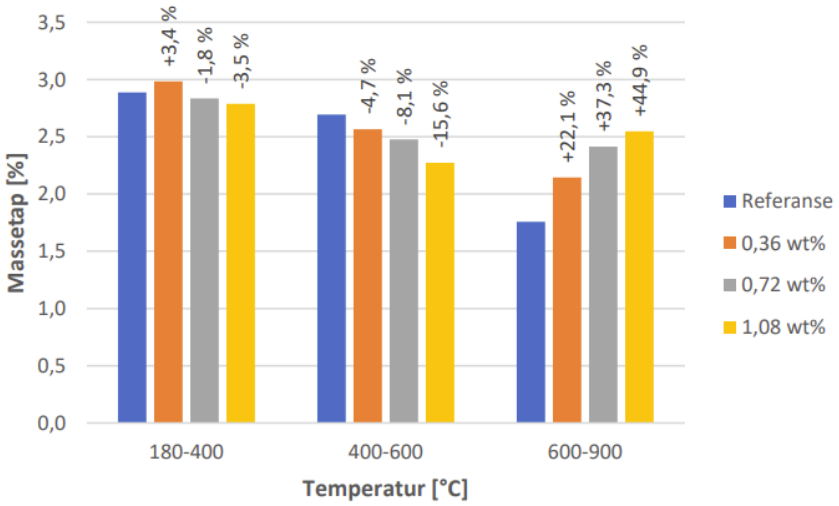

Figure 2.17: Mass loss in three intervals [27]

Figure 2.18 shows the amount of CO_2 and the amount of $CaCO_3$ in the different concrete batches. The increase in CO_2 dosage is an increase in both CO_2 content and $CaCO_3$. In the batch with 0,36 wt % CO_2, the figure shows more CO_2 than that was added. This is explained as there have been more C-S-H created, which in a later state dissolved in the interval of 600-900 °C. Also, the amount of reactive CO_2 is reduced with the increasing amount of CO_2 added to the mix. This may imply that there is a limit of how much CO_2 that may be sequestrated in the concrete.

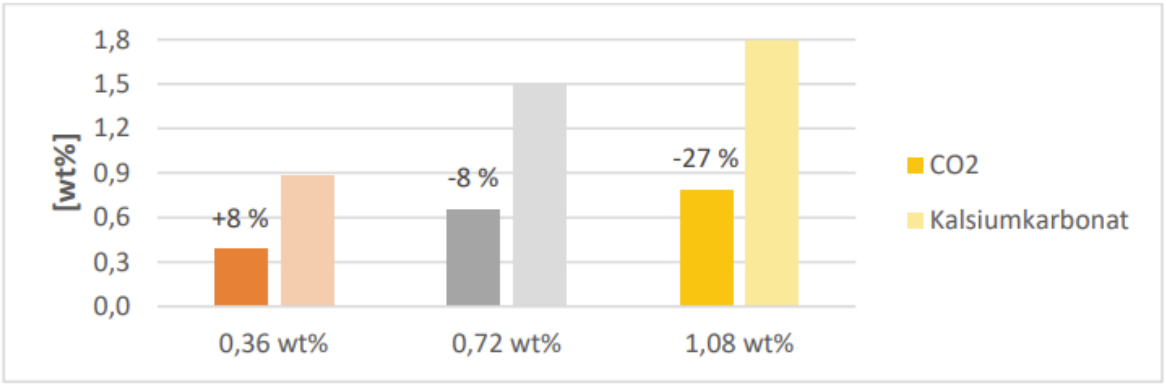

Figure 2.18: Amount of CO_2/$CaCO_3$ in the concrete batches [27]

3 Experimental Program and Method

This chapter explains the different experiments and procedures conducted in the thesis. This chapter is divided into five sections:

3.1 - Experimental Work Plan

3.2 - Materials

3.3 - Preparations of Specimen

3.5 - Concrete Curing

3.4 - Test Procedure

The purpose of the experimental program is to examine how concrete with different amounts of slag behaves with injection of CO_2 during mixing. Different curing methods will also be tested. Several different tests will be carried out to investigate effect of these various parameters, both in fresh and hardened state. The plan for the experimental program is illustrated in figure 3.1 below.

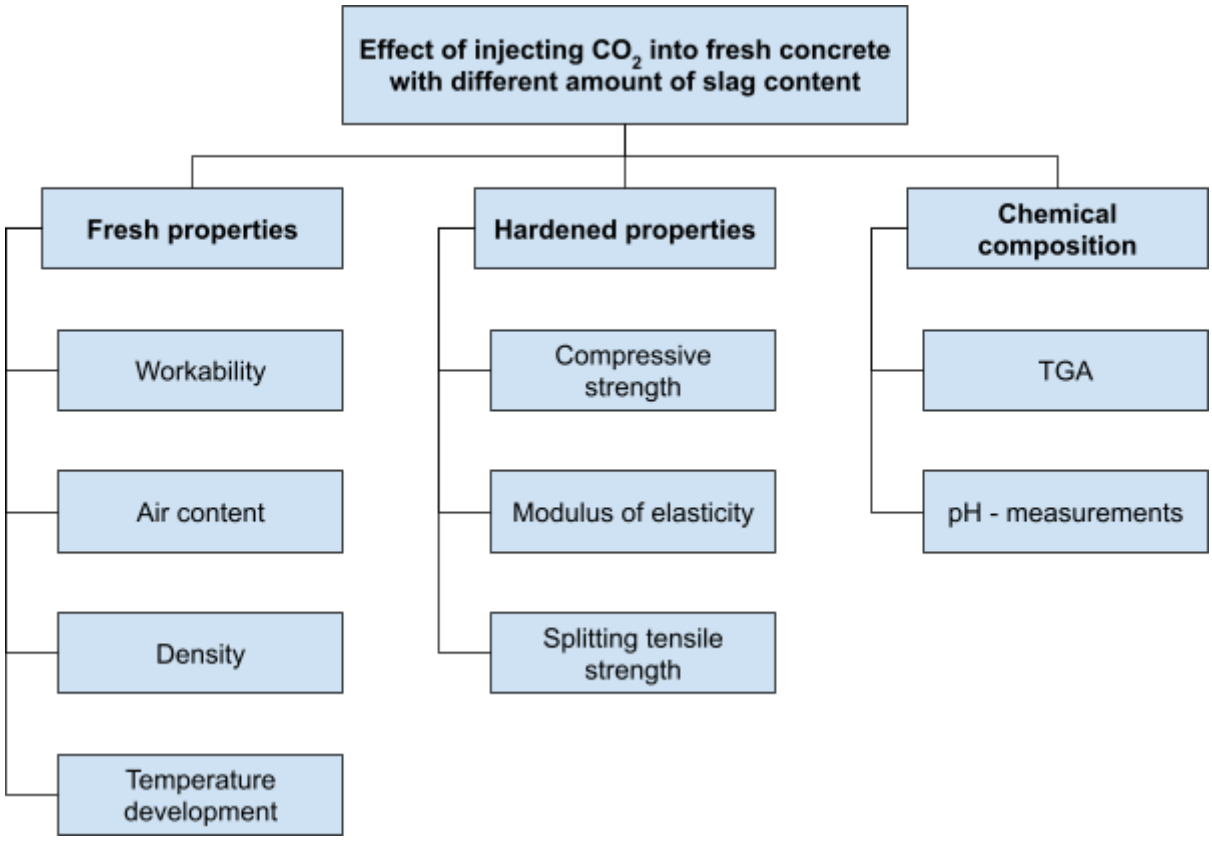

Figure 3.1: Plan for the experimental program

3.1 Experimental Work Plan

The experimental program is conducted with 12 different mix designs. Each of the concrete mixtures has different content of slag and dosage of CO_2. The amount of CO_2 is measured as the weight percentage of the binder. Table 3.1 shows the dosage of CO_2 and percentage of slag in the binder.

	0% Slag	**20% Slag**	**30% Slag**	**70% Slag**
0 wt% CO_2	BA-0-0	SL-20-0	SL-30-0	SL-70-0
1 wt% CO_2	BA-0-1	SL-20-1	SL-30-1	SL-70-1
2 wt% CO_2	BA-0-2	SL-20-2	SL-30-2	SL-70-2

Table 3.1: Overview of the mix designs, dosage of CO_2 and slag content.

Different naming is used to differentiate the batches and the different curing methods. The letters (BA or SL) indicate whether it is base mixture (reference) or a slag cement. The first number indicates the content of slag in the binder, and the second number indicates the wt% CO_2 injected to the concrete. Section 3.4 explains the different curing methods used, therefore the last letter indicates which curing is used. W indicates water curing, C indicates CO_2 curing, and A indicates air curing. For example a batch with 30 % slag in binder and 1 wt% CO_2 induced during mixing and cured in a CO2 rich environment will have the following name: SL-30-1-C.

The experiment consists of two parts. Part one is the mix designs without CO_2, i.e. four batches. These concrete mixtures are smaller batches of around 65 liters, due to these only being cured in water. Table 3.2 lists the number of specimens and time of testing for part one. Part two is all the mixtures with CO_2, i.e. eight batches. These will undergo three different types of curing; in water, in air and in CO_2 filled atmosphere. Table 3.3 lists the number of specimens and time of testing for part two.

The order of the execution of the experimental program is dependent on the amount of CO_2. Firstly all batches without any addition of CO_2 is conducted, from 0 % slag to 70 % slag.

Secondly the batches with 1 wt% CO_2 is done, starting from 0 % slag to 70 % slag. Lastly the batches with 2 wt% CO_2 is done, with the same order as above.

Test	**Test time**	**No. of specimen**
Compressive strength	1 day	3 cubes
Compressive strength	3 days	3 cubes
Compressive strength	7 days	3 cubes
Compressive strength	28 days	3 cubes
Modulus of elasticity	28 days	1 cylinder
Splitting tensile strength	28 days	1 cylinder
pH	28 days	Crushed samples
TGA	28 days	Crushed samples

Table 3.2: Overview of number of specimens and time of testing, without CO_2 addition

Test	**Test time**	**No. of specimen**
Compressive strength	1 day	3 cubes
Compressive strength	3 days	9 cubes
Compressive strength	7 days	9 cubes
Compressive strength	28 days	9 cubes
Modulus of elasticity	28 days	3 cylinders
Splitting tensile strength	28 days	3 cylinders
pH	28 days	Crushed samples
TGA	28 days	Crushed samples

Table 3.3: Overview of number of specimens and time of testing, with CO_2 addition

Figure 3.2 shows a schematic overview of part two of the experiment plan. Part one only deviates from the schematic that they do not contain CO_2 and all the specimens are cured in water.

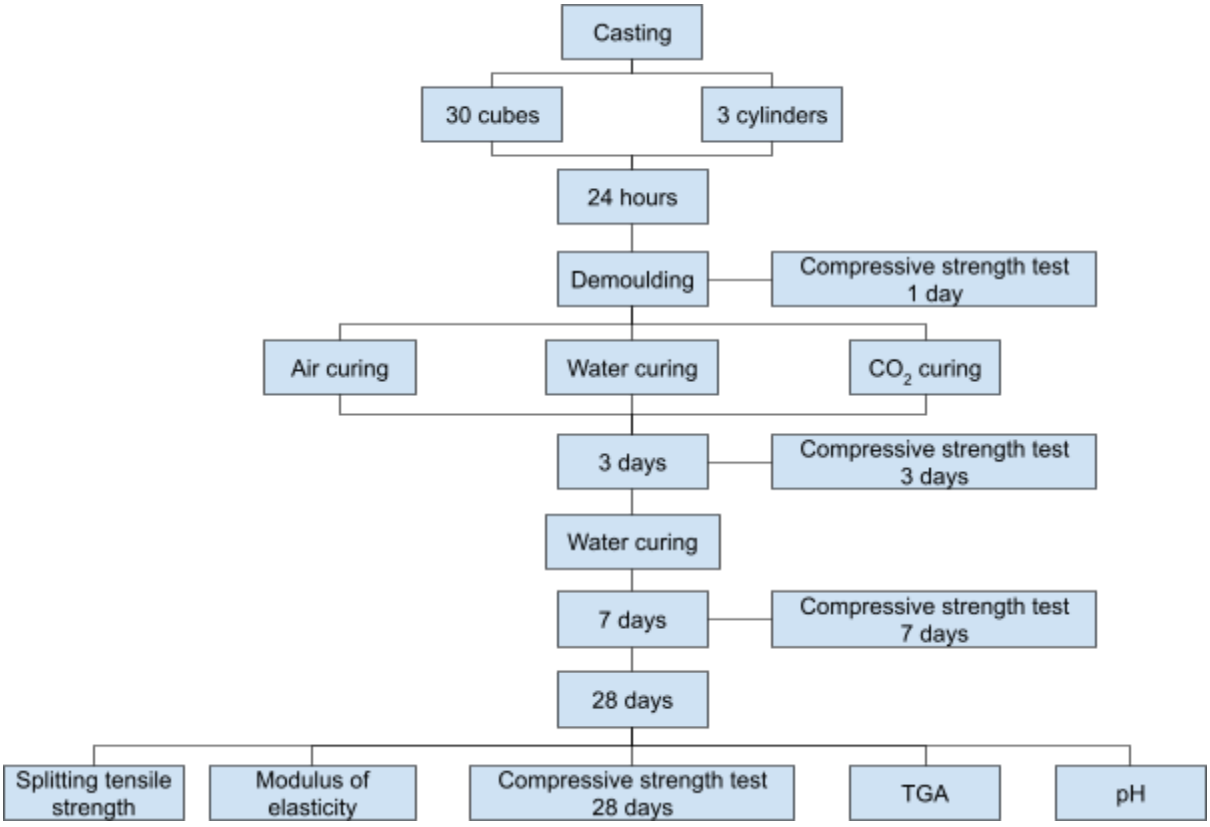

Figure 3.2: Overview of part two of the experiment plan

3.1.1 Standards

NS-EN 12350 is the standard used as a requirement and guideline for testing of the fresh properties of the concrete batches. NS-EN 12390 is the standard used as a requirement and guideline for testing of the hardened properties of the concrete batches. These standards are used as a framework, as there are some necessary modifications carried out to implement some of the tests. These modifications are clearly described where the method deviates from the standards.

3.2 Materials

This section will describe all the materials and the essential properties of these materials.

3.2.1 Cement

Cement used in the experiment is “Anleggsement” (construction cement) provided by Norcem AS. The cement satisfies the requirements according to “NS-EN 197-1:2011 til Portlandcement CEM I 52,5 N”. Table 3.4 shows the chemical and physical properties of the cement.

Property	**Value**
Fineness (Blaine)	415 m^2/kg
Specific weight	3,14 kg/dm^3
Expansion	1 mm
Beginning Solidification	120 min
Compressive strength - 1 day	21 MPa
Compressive strength - 2 day	33 MPA
Compressive strength - 7 day	49 MPa
Compressive strength - 28 day	63 MPa
Sulfate content (SO_3)	$\leq$ 4,0 %
Chloride content (Cl^-)	0,07 %
Water-soluble chromium (Cr^{6+})	2 ppm
Alkali (Na_2O_{ekv})	0,6 %
Clinker	96 %
Secondary constituents	4 %

Table 3.4: Chemical and physical properties of CEM I 52,5 N

3.2.2 Ground granulated blast furnace slag

Ground granulated blast furnace slag (slag) used in the experiment is provided by SSAB Merox AB. The slag used in the experiments satisfies the requirements given in NS-EN 15167. Table 3.5 shows the chemical and physical properties of the slag.

Property	**Value**
Physical state	Solid - amorphous powder
Granulometry	D10 ~ 2,4 µm D50 ~ 12 µm D90 ~ 45 µm
Color	White
pH	11,2
Density	2920 kg/m^3
Bulk density	Ca 600 - 1400 kg/m^3
Glass content	99 %
Specific surface	4600 - 5400 cm^2/g (Blaine)

Table 3.5: Chemical and physical properties of slag

3.2.3 Aggregates

Aggregates used in the experiment are provided by Norstone Årdal. Fractions used in the mix design are 0/8 mm and 8/16 mm. Both fractions are tested and approved according to the requirements in "NS-EN 12620:2002+A1:2008+NA:2016 - Tilslag for betong". Essential properties of the fractions are presented in table 3.6, and sieve curves for the fractions are presented in figures 3.3 and 3.4.

Norstone Årdal 0/8 mm			
Grain density	Water absorption	Fineness content	Alkali
2,68 Mg/m^3	0,3 %	3 %	0,9 %
Norstone Årdal 8/16 mm			
Grain density	Water absorption	Fineness content	Alkali
2,69 Mg/m^3	0,4 %	0,4 %	0,8 %

Table 3.6: Properties of Årdal 0/8 and 8/16 mm

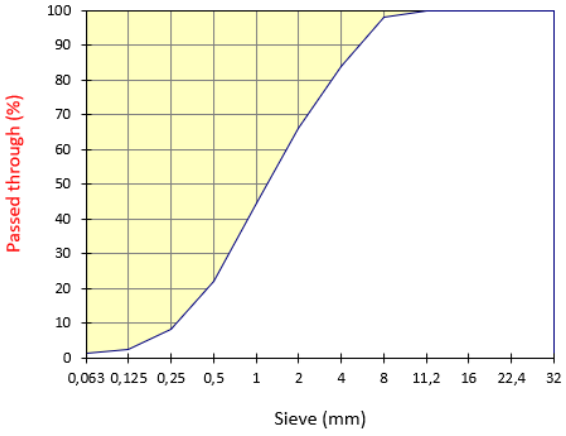

Figure 3.3: Sieve curve Årdal 0/8 mm

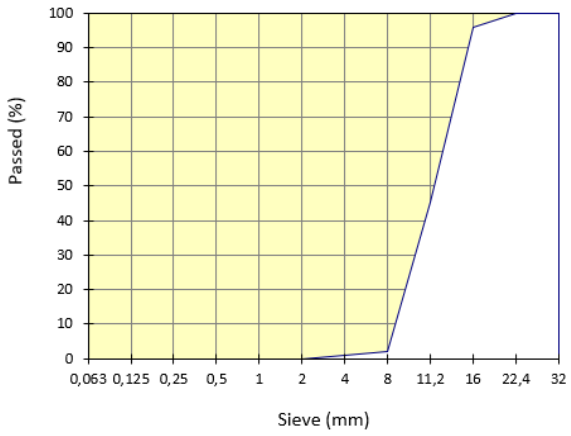

Figure 3.4: Sieve curve Årdal 8/16 mm

3.2.3.1 Moisture in aggregates

Sand (0/8 mm) contains moisture, which needs to be determined to ensure the correct amount of water to be added to the concrete mixture. To determine the moisture in the sand, a sample of about 1000 g is heated in an oven at 105 ^{0}C. After approximately 24 hours, the sample is weighed again and the weight loss in percentage is then the moisture in the sand. Another widely used method to determine the moisture content of the sand is “Speedy moisture test”.

3.2.4 Superplasticizer

Dynamon SX-N is the superplasticizer used in this experimental program, and is delivered by Mapei AS. It is a very efficient superplasticizer based on modified acrylic polymers. These acrylic polymers effectively disperse cement clusters. This effect gives a number of advantages, such as the workability and fluidity of the concrete can be substantially increased without affecting the strength. Superplasticizer also reduces the amount of water needed and retains the same workability of the concrete. Recommended dosage is between 0,4 - 2,0 % of the amount of cement + slag. Table 3.7 shows the technical data of Dynamon SX-N.

Property	**Value**
Appearance	Liquid
Color	Yellow-brown
Viscosity	Easy flowing; < 30 mPa*s
Dried solid content (%)	18,5 ± 1,0
Density	1,06 ± 0,02 g/cm^3
pH	6,5 ± 1
Chloride content	0,05 %
Alkali content (Na_2O-equivalents)	< 2,0 %

Table 3.7: Technical data of Dynamon SX-N

3.2.5 Water

Normal tap water is used in the experiments and is considered to be acceptable. The water was tapped directly from the tap, and had a temperature of as 4 °C. The same method will be used in each concrete mixture.

3.2.6 Carbon dioxide (CO_2)

The high-pressure CO_2 tank is provided from Nippon Gases Norge AS. The CO_2 tank contains a liquid state of the carbon dioxide at 50 bar. The purity of the gas is 99,7 %. To induce the gas in the concrete mix, a regulator and hose is used. Table 3.8 shows an overview of the chemical and physical properties of CO_2.

Property	**Value**
Physical state at 20 °C / 101,3 kPa	Gas
Color	Colorless
Odor	Odorless
pH	Not relevant for gases
Melting point / Freezing point	-56,6 °C
Boiling point	-78,5 °C at atmospheric pressure
Flammability	Non-flammable
Vapor pressure [20 °C]	57,3 bar
Relative density, gas (air = 1)	1,52
Water solubility	2000 mg/l
Molar mass	44 g/mol
Critical temperature	31 °C

Table 3.8: Chemical and physical properties of CO_2

3.3 Preparations of specimens

In the following section, the preparation of the concrete mix design is described. As mentioned in 3.1 there are two parts of the program. All the concrete mixes have a water-cement ratio of 0,40 (w/c=0,40)

3.3.1 Mix design

The mix design is based on the excel sheet "Proporsjonering av betong", developed by Sverre Smedplass from Skanska. Matrix volume, w/c-ratio, moisture in aggregate and volume of the batch is plotted into the mixing form, and the program calculates the amounts of aggregates, cement, slag, and water. Matrix volume of 340 l/m³ is chosen. Superplasticizer is added to obtain a slump of 230 mm, and different amounts of CO_2 is added depending on table 3.1. The dosage of CO_2 is 1 wt % and 2 wt % of the total binder content. Table 3.9 presents the concrete mixes for part one and two, where the only difference is the addition of CO_2.

	Reference	**20 % slag**	**30 % slag**	**70 % slag**
Material	**Amount**			
Cement - CEM I 52,5 N [kg/m³]	461,5	369,2	323,0	138,4
Slag [kg/m³]	0	92,3	138,4	323,0
Aggregate - 0/8 mm [kg/m³]	864,7	864,7	864,7	864,7
Aggregate - 8/16 mm [kg/m³]	869,1	869,1	869,1	869,1
Water [kg/m³]	184,6	184,6	184,6	184,6
Superplasticizer - Dynamon SX-N	0,4-2 wt% of binder	0,4-2 wt% of binder	0,4-2 wt% of binder	0,4-2 wt% of binder
CO_2 - gas	[1, 2] wt% of binder	[1, 2] wt% of binder	[1, 2] wt% of binder	[1, 2] wt% of binder

Table 3.9: Mix design for the experimental program

3.3.2 Molds

3.3.2.1 Cubes

Concrete cubes are cast in a metal cube mold with dimensions 100 mm x 100 mm x 100 mm, according to NS-EN 12390-1, illustrated in figure 3.5. These cubes are used to determine the compressive strength, and crushed sample is retrieved for pH-measurements and TGA after the 28-day compressive strength test.

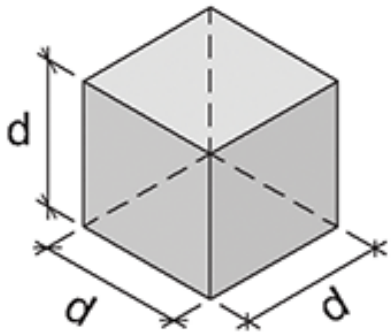

Figure 3.5: Concrete cube

Figure 3.6: Cube mold

3.3.2.2 Cylinder

Concrete cylinders are cast in a mold with dimensions 150 mm x 300 mm, according to NS-EN 12390-1, illustrated in figure 3.7. These cylinders will be used to determine modulus of elasticity and splitting tensile strength.

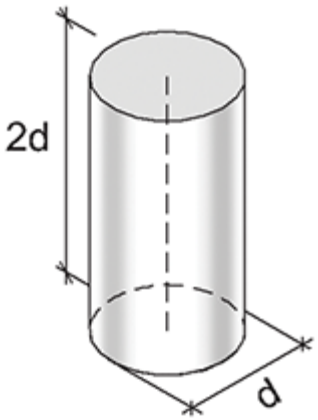

Figure 3.7: Concrete cylinder

Figure 3.8: Cylinder mold

3.3.3 Mixing of fresh concrete

3.3.3.1 Setup of concrete mixer

The concrete mixer used is a Eirich R09T 150 L/240 kg forced action mixer. All the air vents are sealed, and a CO_2 intake is mounted in the lid of the mixer. It is very challenging to get a 100 % airtight environment, and there will be leaks. The atmospheric pressure inside the concrete mixer is 1 atmosphere. From the CO_2 tank a regulator is connected, which regulates the amount of CO_2 induced into the concrete. Attached to the regulator is a hose which releases the gas into the mixer. CO_2 gas has a greater density than air, and therefore will displace the air and excess CO_2 gas in the mixer. Figure 3.9 shows the setup of the concrete mixer.

Figure 3.9: Setup of the concrete mixer.

3.3.3.2 Procedure of concrete mixing

The mixing procedure is based on the procedure used by Monkman, MacDonald and Hooton [28]. Part one and two of the experimental program is done with the same procedure, with exception of part one where the CO_2 is not added. Table 3.10 shows the steps of the mixing procedure.

Step	Time	Procedure
1	0 Sec	Adding aggregates, cement, and slag
2	60 Sec	Adding half of the water
3	120 Sec	Adding CO_2 -gas
4	240 Sec	Adding rest of the water and superplasticizer
5	360 Sec	Stop mixer and remove mortar adhering to wall
6	420 - 480 Sec	Finish mixing if the concrete has satisfactory workability

Table 3.10: Procedure of mixing concrete

3.3.3.3 Procedure for dosing CO_2

To get approximately right dosage of CO_2 into the concrete, the CO_2 tank was weighted. Afterwards the regulator (figure 3.10) was opened at a release of 5 bars for 30 seconds. Then the CO_2 container was again weighted. The weight loss was then calculated and the approximated dosage of CO_2 for each concrete mix was calculated.

Figure 3.10: CO_2 regulator

3.3.3.4 Casting of concrete

The molds used in the experimental program were lubricated with formwork oil so the concrete would not stick to the mold. The molds are filled layer by layer with concrete and compacted using a rod. The specimens will then cure for 24 hours underneath plastic to contain the specimen as moist as possible. After 24 hours the specimens are demoulded. The casting, filling of the molds, and compacting is done according to NS-EN 12390-3.

3.4 Concrete curing

The experimental program is divided into two parts, as mentioned in 3.3. Both part one and two are very similar, except the addition of CO_2 and curing methods. The specimens are demoulded after 24 hours of curing, and 1-day compressive strength are conducted for part one and two.

Part one of the experimental program, the cubes are cured for 3, 7 or 28 days. The cylinder is water cured straight after demoulding and cured for 28 days. The curing process is according to NS-EN 12390-3 (figure 3.11).

Figure 3.11: Water curing

Part two of the experiment program, the specimens are divided into three groups. Group 1 is cured in water (NS-EN 12390-3), group 2 is cured in air (figure 3.12), and group 3 is cured in a CO_2 rich environment (figure 3.13). After 48 hours, group 2 and 3 are moved to water curing. It is shown that curing with CO_2 has little effect after 48 hours, therefore, the specimens are moved to water curing referring to section 2.3.2. The same duration of curing as used in part one is used for part two, i.e. 3, 7 or 28 days.

Figure 3.12: Container used for air curing.

Group 3 is cured in a CO_2 rich environment but with an atmospheric pressure, i.e. not in a pressure vessel. The curing framework is shown in figure 3.13. The plastic box is filled with CO_2 gas from the bottom. The CO_2 is heavier than air, and therefore the air will be pushed out of the holes in the lid of the box. After a constant filling for 30 minutes, the holes are covered, and the inducing of gas shut off. This method is not based on any standards, and how much CO_2 there is inside the box at any given time is uncertain. The reason for conducting such a test is to see if there must be a pressure for the concrete to capture CO_2, or it can be done in a CO_2 rich environment. The reason for group 2 (air curing) is to compare the effect the 48 hours in a CO2 rich environment has on the CO_2 uptake and other hardened properties.

Figure 3.13: CO_2 curing equipment

3.5 Test Procedure

This section will present the procedure of various experiments performed, and the section is divided into fresh properties, hardened properties, and chemical composition.

3.5.1 Fresh Properties

3.5.1.1 Slump

Slump is a common method for measuring the workability and is performed according to NS-EN 12350-2. A cone is placed on a level metal plate. The dimensions of the cone are the following: 200 mm diameter at the bottom, 100 mm diameter at the top, and the height is 300 mm (figure 3.14). The cone is filled in three layers and the concrete is compacted after each layer. When the cone is filled with concrete, it is lifted at a constant movement lasting 2-5 seconds. The difference between the height of the cone and the highest point of the concrete indicates the slump of the concrete. According to NS-EN 12350-2 this method is used when the slump is between 10 and 210 mm, but in practice the method is used for slumps up to 240 mm.

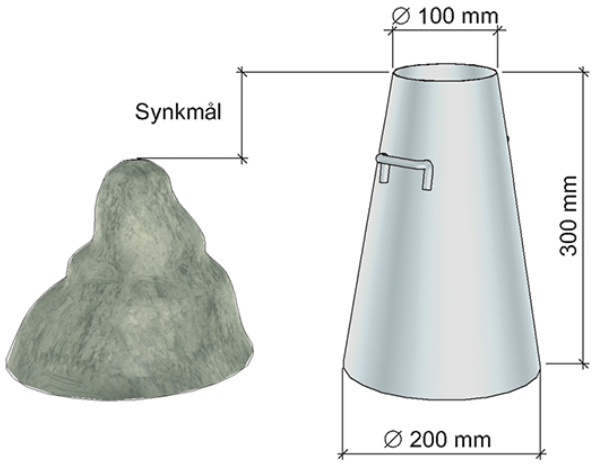

Figure 3.14: Cone for measuring the slump

Figure 3.15: Slump of concrete

3.5.1.2 Density

The fresh density of the concrete is determined according to NS-EN 12350-6. A container with known mass and volume is filled with concrete and compacted. The container is then weighed, and the density can be calculated using the equation 3.1:

$$\rho = \frac{M_2 - M_1}{V} \qquad (3.1)$$

Where ρ = Density of the fresh concrete [kg/m³]

M_2 = Mass of container filled with concrete [kg]

M_1 = Mass of empty container [kg]

V = Volume of the container [m^3]

Density of the concrete is normally measured using the cylindrical container used to measure the air content. This container has a volume of 8 liters and is illustrated in figure 3.16.

Figure 3.16: Density of fresh concrete

3.5.1.3 Air content

The air content of the concrete is measured according to NS-EN 12350-7. The principle of the method is to put fresh concrete under pressure and measure the volume changes in relation to normal air pressure. The concrete needs to be compacted between each layer of concrete to remove air pockets. Figure 3.17 shows the container used.

Figure 3.17: Equipment used to measure air content

3.5.1.4 Temperature development

The fresh concrete is put into a styrofoam box with the dimension of 150 mm x 150 mm x 150 mm, with the wall and lid thickness of 20 mm. A temperature gauge is placed in the center of the box. There are two different systems for measuring the temperature, EL -USB -TC -LCD Thermocouple Data Logger and Hioki LR8431-20 Memory HiLogger.

EL-USB-TC-LCD Thermocouple Data Logger is a simple system that measures the temperature every 15 or 30 minutes. Figure 3.18 presents the equipment used.

Figure 3.18: EL-USB-TC-LCD Thermocouple Data Logger

Hioki is a more advanced system, which can measure several concrete batches at once. It can also be modified to measure the temperature more rapidly, and it can be programmed to stop the measurements at any given time or temperature. It will be set to measure the temperature every 10 minutes. Figure 3.19 presents the Hioki logger.

Figure 3.19: Hioki LR8431-20 Memory HiLogger

The normal procedure is to log the temperature until room temperature is reached. Figure 3.20 presents all the equipment used to measure the temperature development.

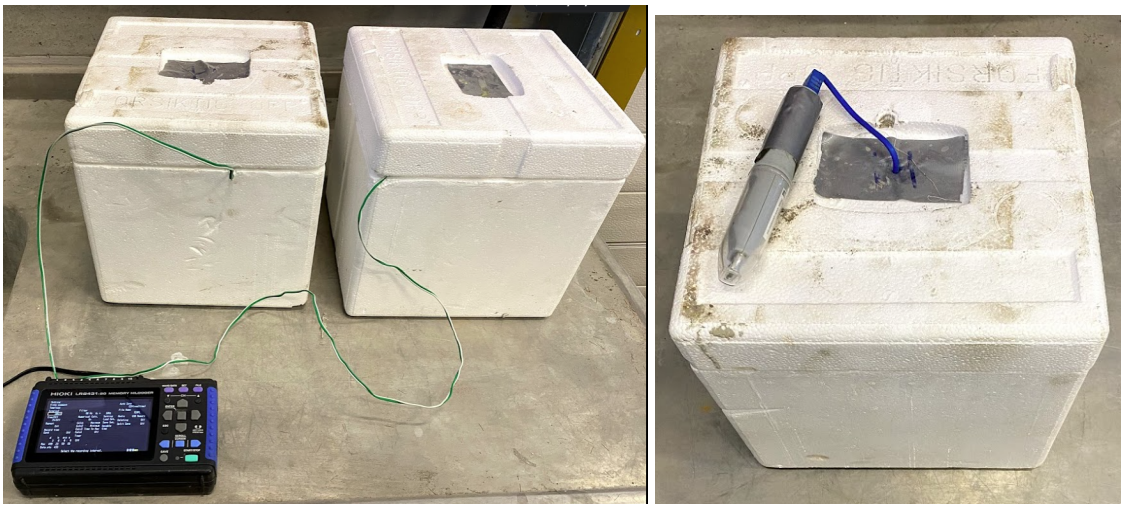

Figure 3.20: Equipment for measuring temperature development

3.5.2 Hardened properties

3.5.2.1 Compressive strength

The compressive strength of the concrete is measured according to NS-EN 12390-3. Cubes with dimensions 100 mm x 100 mm x 100 mm are inserted into a Toni Technik compressive strength machine as illustrated in figure 3.20. The machine will apply an increasing force perpendicular on the cube until fracture occurs, as illustrated in figure 3.21. The maximum force registered at fracture is used to calculate the compressive strength of the concrete cube with equation 3.2:

$$F_c = \frac{P}{A_c} \tag{3.2}$$

Where F_c = Compressive strength [MPa]

P = Maximum force at fracture [N]

A_c = Cross-sectional area of the specimen [mm^2]

Compressive strength is tested at 1, 3, 7 and 28 days. Three concrete cubes are tested for each day. If there is no visible damage on the cubes, or some suspicious compressive strength values, the compressive strength of the batch is the average of the three specimens tested.

Figure 3.20: Compressive strength testing

Figure 3.21: Fracture due to compressive strength testing

3.5.2.2 Modulus of elasticity

The modulus of elasticity of the concrete is measured according to NS-EN 12390-13. Cylinders with dimensions 150mm x 300mm need to be cut to get an even surface, and therefore dimensions are 150mm x 281mm. The cylinder is placed in an upright position inside a Toni Technik compression machine with strain gauges connected, as illustrated in figure 3.22.

Figure 3.22: Test of Modulus of elasticity

The machine applies an axial force through three load cycles, and the limit values of the load cycles are determined by the equations 3.4, 3.5 and 3.6. The limit values depend on the compressive strength of the cylinder, which is determined by the equation 3.3.

$$f_c = F_c * 0{,}8 \tag{3.3}$$

$$\sigma_a = \frac{f_c}{3} \tag{3.4}$$

$$0{,}10 * f_c \leq \sigma_b \leq 0{,}15 * f_c \tag{3.5}$$

$$0{,}5\ MPa \leq \sigma_p \leq \sigma_b \tag{3.6}$$

Where f_c = Compressive strength, cylinder [MPa]

F_c = Compressive strength, cube [MPa]

σ_a = Upper stress [MPa]

σ_b = Lower stress [MPa]

σ_p = Pre-load stress [MPa]

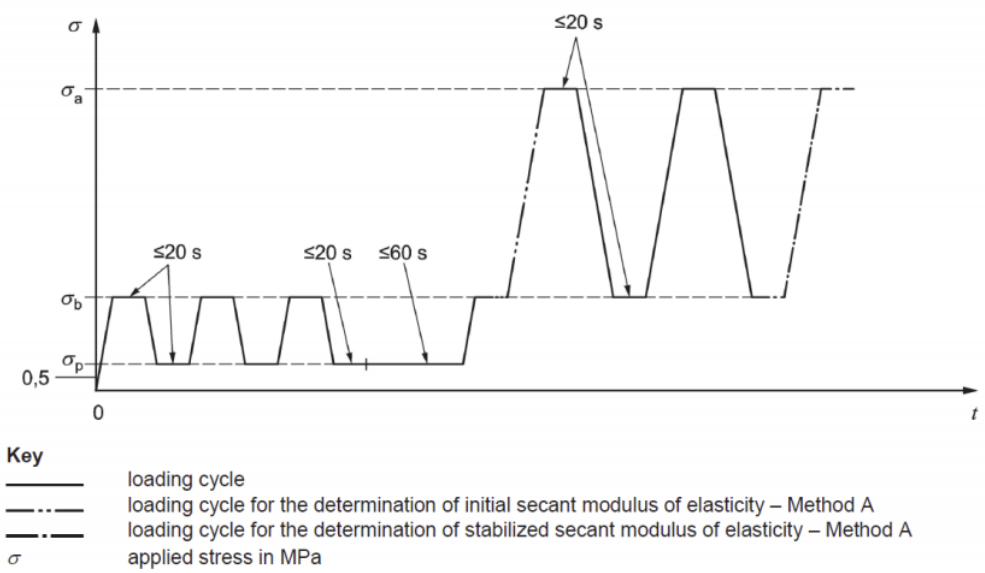

Figure 3.23: Load cycles in determination of Modulus of elasticity

Figure 3.23 illustrates the cyclic load. During the load cycles, the strains and stresses is registered, and the modulus of elasticity is calculated by the equation 3.7:

$$E_{C,S} = \frac{\sigma_a^m - \sigma_b^m}{\varepsilon_{a,3} - \varepsilon_{b,2}} \tag{3.7}$$

Where $E_{C,S}$ = Modulus of elasticity [GPa]

σ_a^m = Upper stress [MPa]

σ_b^m = Lower stress [MPa]

$\varepsilon_{a,3}$ = Average strain at the upper stress at third load cycle [mm/mm]

$\varepsilon_{b,2}$ = Average strain at the lower stress at second load cycle [mm/mm]

3.5.2.3 Splitting tensile strength

The splitting tensile strength of the concrete is measured according to NS-EN 12390-6. The same cylinders used in testing of the modulus of elasticity are used in this test, i.e. the dimensions are 150 mm x 281 mm. The specimen is mounted "lying" in the Toni Technik pressure testing machine and loaded on two opposite sides in the longitudinal direction, see figure 3.24. The compressive forces cause tensile stresses perpendicular to the direction of the force. The maximum force at fracture is registered and is used to calculate the tensile strength with equation 3.8:

$$f_{ct} = \frac{2 * F}{\pi * L * d} \tag{3.8}$$

Where f_{ct} = Splitting tensile strength [MPa]

F = Maximum force at fracture [N]

L = Length of the contact line of the cylinder [mm]

d = Cross sectional diameter [mm]

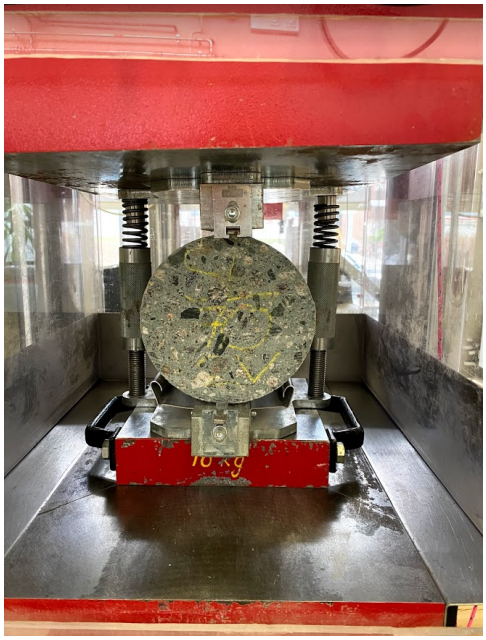

Figure 3.24: Splitting tensile strength

Figure 3.25: Splitting fracture

3.5.3 Chemical composition

3.5.3.1 pH-measurements

Measurements of the pH-values is based on the procedure developed by Grubb, Limaye and Kakade [34]. The pH-value is measured after 28 days of curing. 5 gram of finely crushed sample is extracted from the cubes and mixed with 10ml distilled water. The mixture of crushed sample and distilled water is sieved such that only particles smaller than 8 mm is used. The instrument used to measure the pH is a digital probe meter and named VWR pH110M, which needs to be calibrated beforehand. Three buffer solutions with the pH value of 4, 7 and 10 respectively, are used to calibrate the pH probe meter. Figure 3.26 presents the pH probe meter and the buffer solutions. After calibration the pH probe is inserted into the solution with the crushed sample, illustrated in figure 3.27. After stabilization of the temperature, the pH-value is registered.

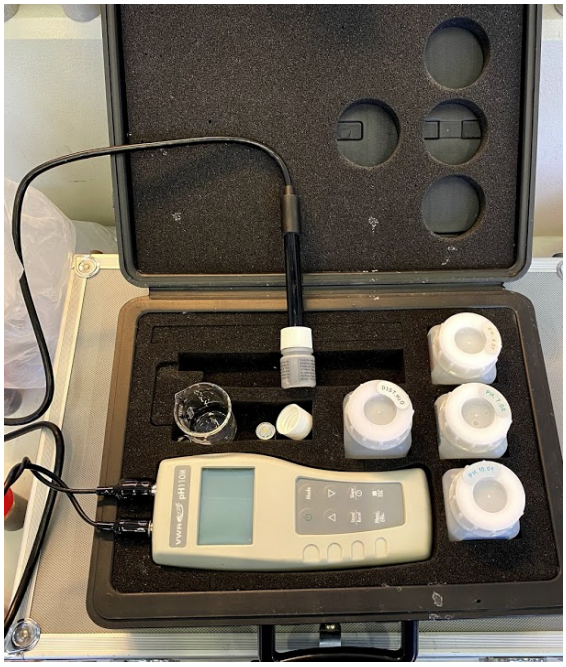

Figure 3.26: pH instrument and buffer solutions

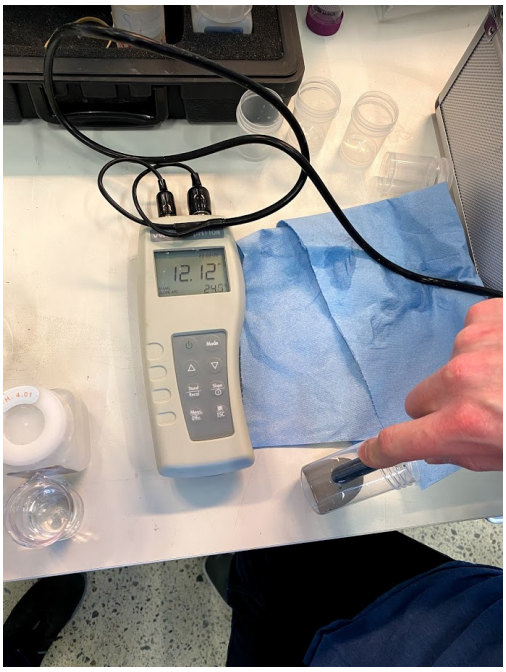

Figure 3.27: pH measurement

3.5.3.2 Thermogravimetric Analysis

The chemical composition and the CO_2 uptake is found with a Thermogravimetric Analysis (TGA). TGA is widely used to determine the mineralogical changes and thermal decomposition in materials, such as concrete. The method is based on monitoring the mass of a sample as a function of temperature, i.e. the mass loss at certain temperatures. The method used in the experimental program is based on Kwasny, Basheer and Russel [19] and Kjos [27].

Procedure of the TGA is as follows; after 28 days curing the crushed sample is retrieved from the cubes subjected to compressive strength test. The crushed sample is then ground to fine powder using mortar and pistil. The finely ground powder is then sieved through a 63 micrometer sized sieve, making sure the powder does not contain coarse aggregates. The finely ground powder is then passed to a crucible (figure 3.28) and the sample is weighted. The weight should be around 40 mg of sample powder. One empty crucible and the crucible with the sample are inserted into the TG machine (figure 3.29). The TG machine used is TGA/DSC 3+ Mettler-Toledo, shown in figure 3.30.

Figure 3.28: Crucible with sample

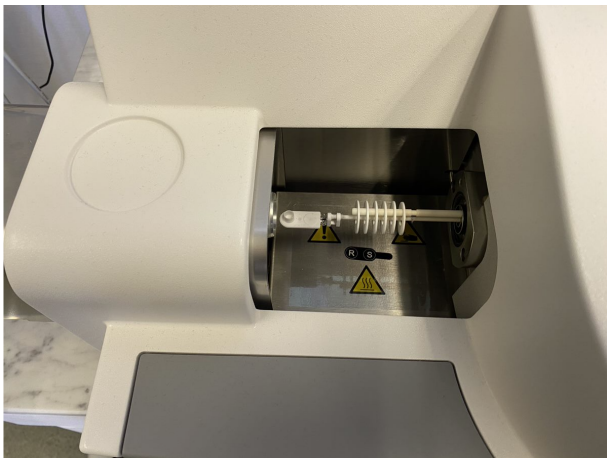

Figure 3.29: Sample inserted into TG machine

The sample is weighted continuously as the temperature increases from 50 -1000 °C, with an increment of 20 °C/min. The temperature increase is carried out under the protection of nitrogen gas. Each phase in the material is characterized by its own temperature range of decomposition and specific mass loss. The tests take approximately 50 minutes, and another 20 minutes of cooling in order to prepare for the next test can be conducted.

Figure 3.30: TG machine - TGA/DSC 3+ Mettler-Toledo

Mass loss at certain temperatures is used to analyze the chemical composition and calculate the CO_2 uptake. From earlier research [35] it is shown that the majority of C-S-H is degraded in the temperature interval 180-400 °C. The dehydration of C-H ($Ca(OH)_2$) is in the interval 400 - 600 °C, and the decarbonization of $CaCO_3$ is in the interval 600 - 900 °C. As described in section 2.3.2, the carbonation of concrete will form $CaCO_3$, which means that the carbonated samples should have a greater mass loss in the interval 600 - 900 °C than batches which are not carbonated. Determination of the CO_2 content is therefore calculated as mass loss in carbonated batch ($C_{600\text{-}900\,°C}$) subtracted of mass loss in reference to batch ($R_{600\text{-}900\,°C}$), as equation 3.9 shows:

$$CO_2\ content = C_{600-900\,°C} - R_{600-900\,°C} \tag{3.9}$$

4 Results & Discussion

This chapter will present and discuss the results and observations from the experimental program. First the properties of the fresh concrete will be presented and discussed, followed by the hardened properties, and finally the chemical properties. A presentative part of the results are given in this chapter, the complete results are given in the appendix The mix design of each batch is presented in appendix A.

4.1 Effect on fresh properties

4.1.1 Slump

Slump measurements are presented in table 4.1. One test of slump measurements was performed for each concrete batch.

Slump measurements of the experimental program			
Concrete batch	**Slump [cm]**	**Concrete batch**	**Slump [cm]**
BA-0-0	23,5	SL-30-0	23,0
BA-0-1	9,5	SL-30-1	5,5
BA-0-2*	15,0	SL-30-2*	25,0
SL-20-0	22,5	SL-70-0	22,0
SL-20-1	9,0	SL-70-1*	24,0
SL-20-2*	23,5	SL-70-2*	25,0

*More superplasticizer added

Table 4.1: Slump measurements of the experimental program

A significant reduction in slump when injecting CO_2 was observed, which made it very challenging to cast good concrete cubes and cylinders. Batch SL-70-1 had to be redone because of the reduction in slump illustrated in the figure 4.1 below. This picture was taken approximately 10-15 minutes after casting, and the molds could be removed because of the fast settling. The slump measurements of this discarded batch was only 4,5 cm, a 79,5% reduction in relation to SL-70-0.

Figure 4.1: Discarded batch SL-70-1

It was therefore decided to increase the amount of superplasticizer to maintain a slump of 23-25 cm. It was in order to reduce the risk of honeycombs and other damages on the casted cubes and cylinders. Therefore, the batches with 2 wt% CO_2 and SL-70-1 were carried out with an increased amount of superplasticizer as seen in table 4.1 marked with *. It was also observed that the workability of the concrete batches with CO_2 injected and increased amount of superplasticizer lost the workability very rapidly in relation to batches without the CO_2. According to section 3.2.4, an increased amount of superplasticizer will substantially increase the workability and fluidity of the concrete without affecting the strength. It is therefore assumed that the increased amount of superplasticizer will not affect the mechanical properties of the concrete.

Figure 4.2 below illustrates the decrease in slump in the BA-0 batches. The reduction is shown in percentage in relation to BA-0-0. BA-0-1 had a 60% reduction in slump because of

the CO_2 addition. Even with an increase in superplasticizer in batch BA-0-2 it is not a desired slump with a reduction of 36 % relative to the reference.

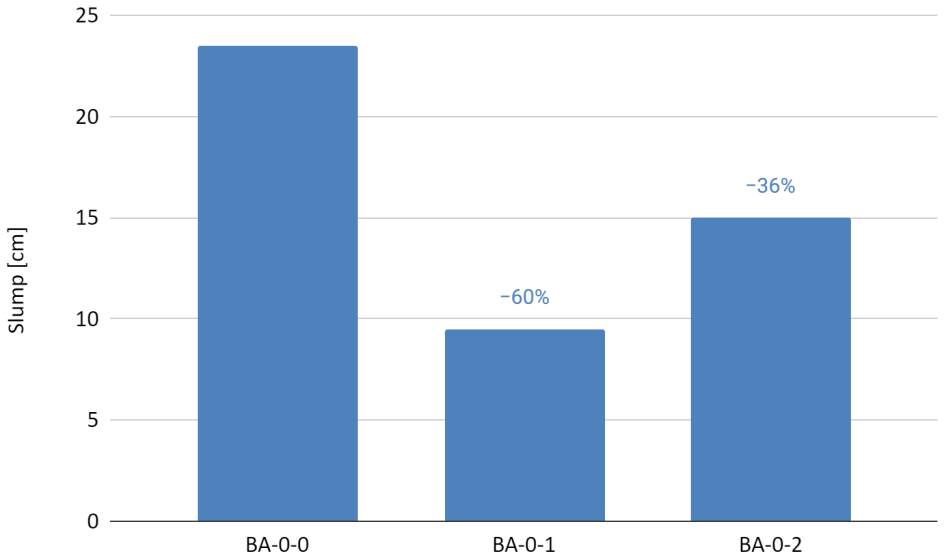

Figure 4.2: Slump measurements in reference batches

The low workability is not a desired property and will affect the compactability which may impact the compressive strength of the concrete. The observed decrease in slump is assumed to be because of the formation of $CaCO_3$ in the concrete, as explained in section 2.3.4. The $CaCO_3$ has a larger specific surface area and therefore more water is absorbed, and this results in lower workability and lower slump.

Previous research presented in section 2.4.1.1, also observed a reduction in the slump measurements. Kjos [27] observed a reduction for every batch with CO_2 added during mixing. The maximum loss in slump was 88 % in the batch with 1,08 wt% CO_2.

4.1.2 Air Content

Air content measurements are presented in table 4.2. One measurement of the air content was performed for each concrete batch.

Air content measurements of the experimental program			
Concrete batch	**Air content [%]**	**Concrete batch**	**Air content [%]**
BA-0-0	1,0	SL-30-0	1,2
BA-0-1	1,9	SL-30-1	2,0
BA-0-2	2,0	SL-30-2	0,9
SL-20-0	1,1	SL-70-0	1,6
SL-20-1	1,8	SL-70-1	1,6
SL-20-2	1,1	SL-70-2	0,9

Table 4.2: Air content measurements of the experimental program

The air content is closely related to the workability of the concrete. Therefore an increase in air content is observed in the batches with increased amounts of CO_2. Despite the low workability, every measurement of the air content is within acceptable range (1-2 %). The largest deviations are observed in the BA-0 batches, where the air content increased 90 % and 100 % with 1 wt% and 2 wt% CO_2 added, respectively.

Figure 4.3 below shows the air content of batches with 20 % slag in binder, SL-20 batches. As explained in section 4.1.1 a significant reduction in slump was an issue, and therefore it is a 63,6 % increase in air content in the SL-20-1 batch. Because of the increased amount of superplasticizer, there was no change in the air content of SL-20-2.

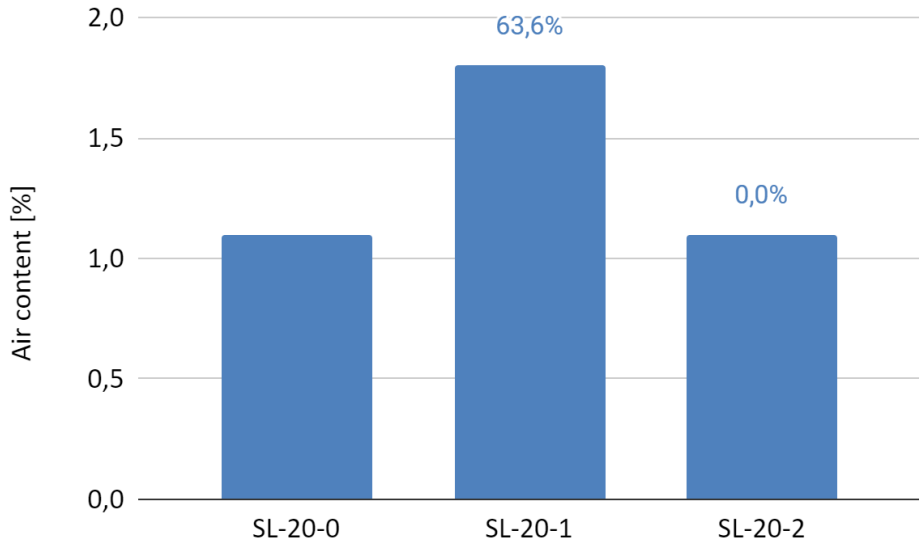

Figure 4.3: Air content of SL-20-0, SL-20-1 and SL-20-2

The increased amount of CO_2 added will affect the air content of the concrete. This is explained as the reason of the low workability due to the larger surface area of the $CaCO_3$, which absorbs more water. An increased amount of superplasticizer will reduce the risk of large amounts of air content in the concrete, as the workability is increased.

Kjos [27] observed an increase in air content and assumed a connection between increased air content and addition of CO_2. This is explained as a reduction in workability due to water absorption of $CaCO_3$.

4.1.3 Density

Density measurements are presented in table 4.3. One measurement of density of the fresh concrete was performed for each batch.

Density measurements of the experimental program			
Concrete batch	**Density [kg/m³]**	**Concrete batch**	**Density [kg/m³]**
BA-0-0	2465	SL-30-0	2445
BA-0-1	2428	SL-30-1	2418
BA-0-2	2433	SL-30-2	2413
SL-20-0	2438	SL-70-0	2420
SL-20-1	2428	SL-70-1	2423
SL-20-2	2440	SL-70-2	2413

Table 4.3: Density measurements of the experimental program

The density of the concrete is closely related to the compactability and workability of the concrete. This indicates a reduction in density with an increase in CO_2 content. Figure 4.4 below shows the SL-20 batches and presents a decrease of 0,4 % in density of the SL-20-1 batch, but an increase of 0,1 % in the SL-20-2 batch. As stated in section 4.1.1, an increase in dosage of superplasticizer was added to make the concrete batches more workable, therefore the increase in density of SL-20-2. It is assumed that the small deviations in density will not have any effect on the mechanical properties of the concrete batches.

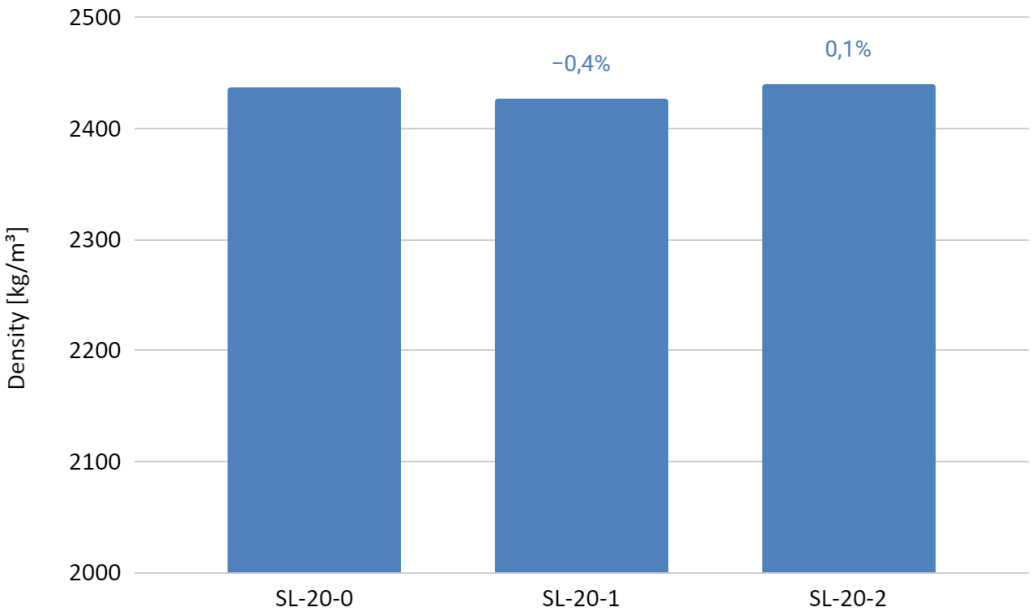

Figure 4.4: Density SL-20-0, SL-20-1 and SL-20-2

According to section 2.4.1.3, did Kjos [27] observe a similar small reduction in density. This was explained as a reduction in the slump of the concrete and assumed that this would not affect the mechanical properties.

4.1.4 Temperature Development

Figure 4.5 presents the temperature development of every concrete batch. The y-axis is the temperature in °C and the x-axis is the time period in hours. The graph illustrates several important parameters. The lower temperature of blended slag cement in relation to ordinary cement is clearly shown, which was discussed in section 2.2. Hydration process of slag cement is slower, resulting in lower early compressive strength. The graph is cut at 72 hours to illustrate the differences in max temperature, and all the results are given in the appendix A.

Because of equipment malfunction the SL-30-0 measurements were cut off uncontrolled and therefore not completed. It was then decided to use the Hioki temperature gauge, which is a more precise and advanced equipment. Table 4.4 below presents the maximum temperature and the amount of hours after casting the maximum temperature is registered.

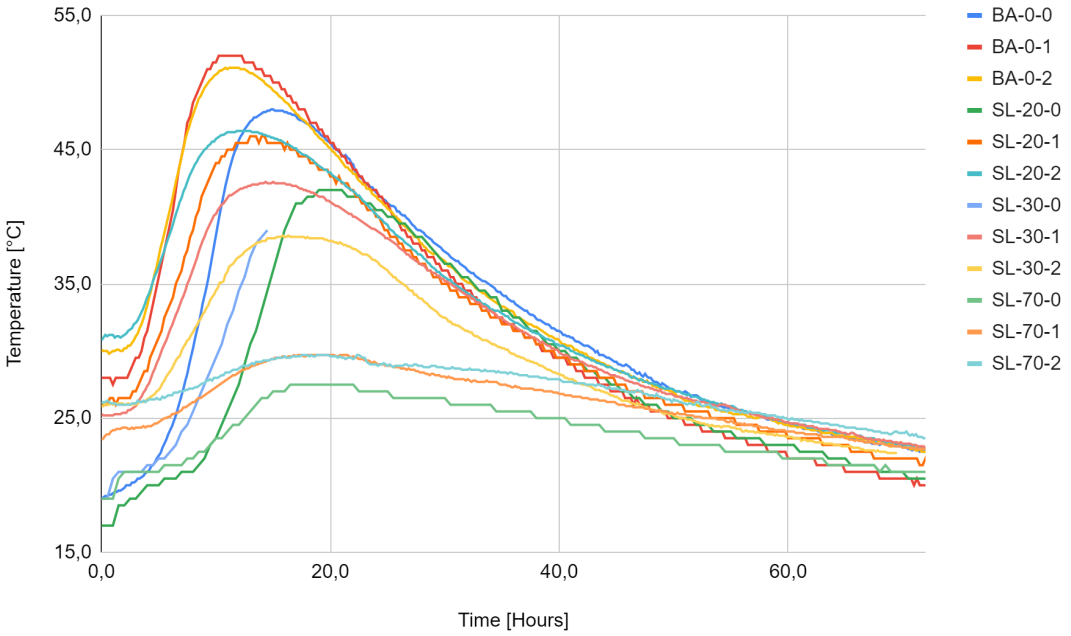

Figure 4.5: Temperature development of all concrete batches

Concrete batch	**Max temperature [°C]**	**Time duration [Hours]**
BA-0-0	48,0	15,0
BA-0-1	52,0	10,0
BA-0-2	51,1	11,0
SL-20-0	42,0	19,0
SL-20-1	46,0	13,0
SL-20-2	46,4	12,0
(SL-30-0)*	(39,0)	(14,5)
SL-30-1	42,6	14,0
SL-30-2	38,6	16,0
SL-70-0	27,5	16,5
SL-70-1	29,7	17,0
SL-70-2	29,7	17,5

*Equipment malfunction and will therefore not be discussed in detail.

Table 4.4: Maximum temperature of the concrete batches

Every batch containing CO_2 has a larger maximum temperature than the batches without CO_2 (not considering SL-30). In BA-0 and SL-20 batches with CO_2 the max temperature also appears earlier than the batches without CO_2. This is not the case for SL-70 batches, where the 0 wt% CO_2 batch is 30 and 60 min earlier than the batches with CO_2. It is not easy to analyze the SL-30 batches, due to the equipment malfunction, but the temperature at 14,5 hours is 39,0 °C for SL-30-0, which is larger than SL-30-1.

The increase in maximum temperature at the earlier time when it appears is assumed to be due to the increased hydration degree because of the higher temperatures. Combined with the formation of C-S-H and $CaCO_3$ which facilitates the formation of C-S-H. It seems that the hydration degree is larger in the batches with CO_2 added.

Figure 4.6 below describes the temperature development for the SL-20 batches. The difference in maximum temperatures and when it appears is shown clearly, as well is the starting temperatures. Equation 2.8 and 2.9 explain the carbonation in fresh concrete, and both these reactions are spontaneous and exothermic. This large starting temperature is therefore explained as the CO_2 reacting with C_3S and C_2S which releases heat. Higher temperature is known to increase the hydration and therefore the earlier setting time. The same relation is present in BA-0. Later in the hydration it seems like the temperature drops faster for the batches with CO_2. This is assumed to be due to the $CaCO_3$ not being finely divided in the concrete and therefore no longer acts as a site for C-S-H to form.

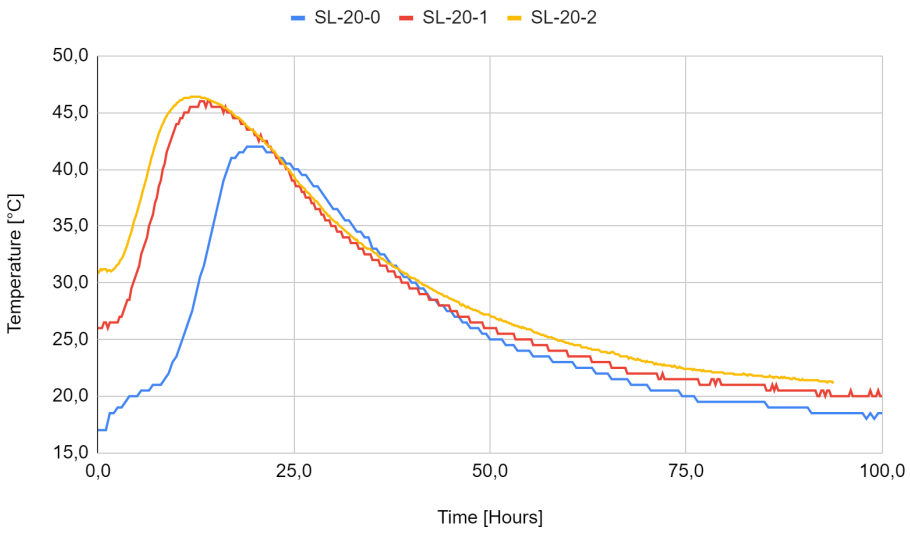

Figure 4.6: Temperature development for SL-20-0, SL-20-1 and SL-20-2

Figure 4.7 below presents the SL-70 batches. The increased starting temperature is due to the exothermic reaction between C_3S, C_2S and CO_2 as explained above. What separates these batches from the others is that the temperature of SL-70-0 is always lower than the batches with CO_2 injected. It is assumed that the $CaCO_3$ formed is finely divided in the concrete, and acts as nucleation sites where C-S-H may form. This is contrary to the other batches, where it is assumed that the $CaCO_3$ is not finely divided in the mix which does not facilitate for large amounts of formation of C-S-H as good as the SL-70 batches.

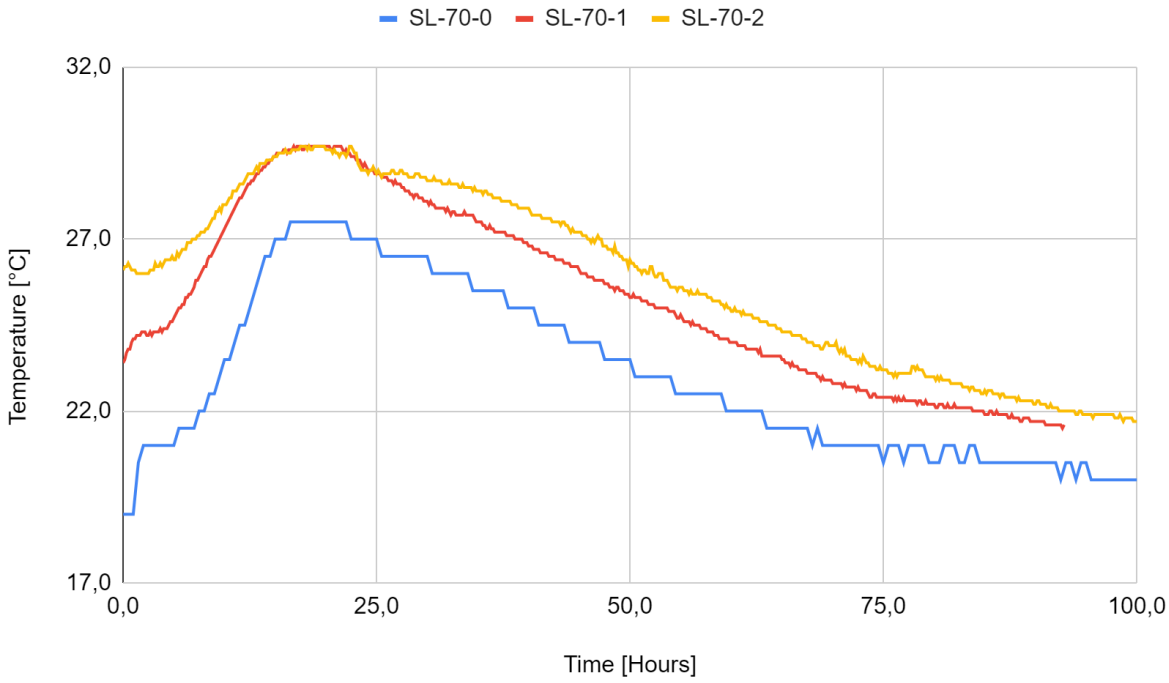

Figure 4.7: Temperature development for SL-70-0, SL-70-1 and SL-70-2

The previous research presented in section 2.4.1.4 did not observe the increased temperature and the earlier max temperature according to table 4.4. This is assumed to be due to more CO_2 added to the concrete mix and more CO_2 reacting with the cement. The heat development due to the reaction between C_3S, C_2S and CO_2 is approximately three times higher than normal hydration, ref 2.3.2. It is therefore observed a correlation between increased amount of CO_2 and higher temperatures.

4.2 Effect on hardened properties

4.2.1 Compressive strength

As described in section 3.4 there were conducted three different methods of curing: in water, in air and in a CO_2 rich environment. The compressive strength tests were done after 1, 3, 7 and 28 days. All results regarding the compressive strength are presented in Appendix X. This section will discuss the specimen cured in water followed by the specimen cured in air and a CO_2 environment.

4.2.1.1 Water cured specimens

The following figures present the compressive strength of the concrete cubes that were cured in water. The y-axis shows the compressive strength in MPa, the x-axis illustrates the days after casting. Above each column the change in percentage in relation to the batch without any injection of CO_2 is presented.

Figure 4.8 presents the compressive strength of the batches without any slag in the binder (BA-0). A decrease in compressive strength is registered after 1 day for both of the batches with CO_2 injected. The decrease was as much as 10,46 % for BA-0-1-W (1 wt% CO_2) and 15,25 % for BA-0-2-W (2 wt% CO_2). Furthermore the BA-0-1-W has an increase of 3,90 % after 3 days, 1,34 % after 7 days and a small decrease of 0,28 % after 28 days. BA-0-2-W on the other hand have a decrease of 0,60%, 3,97 % and 1,75 % after 3, 7 and 28 days respectively.

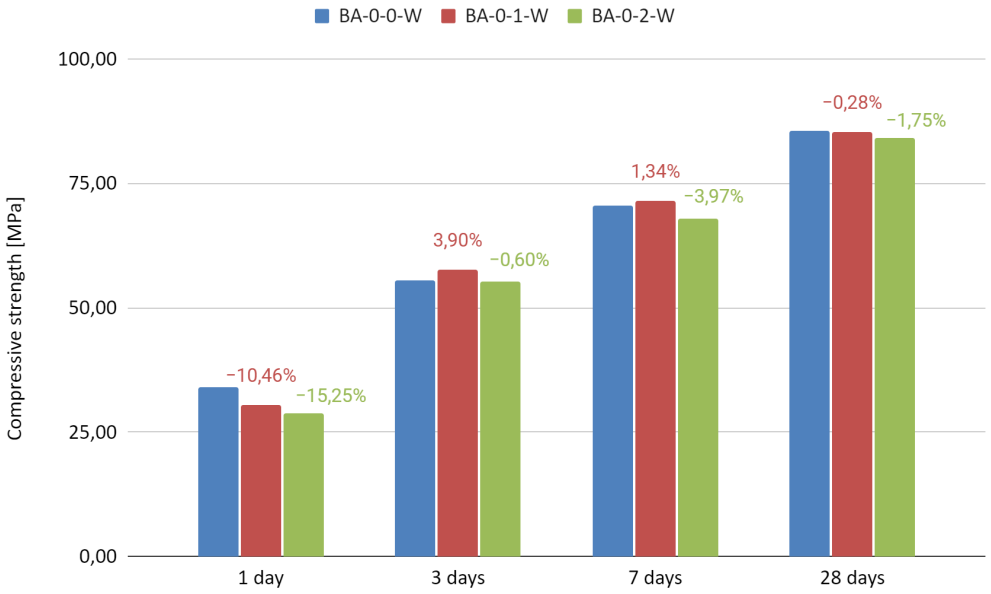

Figure 4.8: Compressive strength of BA-0 batches cured in water

The increased temperatures due to the injection of CO_2 should increase the early strength development in the concrete, but figure 4.8 above shows the contrary. The 1 day compressive strength is reduced and it is assumed that the early hydration products are coating the silicates and retarding dissolution or change in the dissolution mechanism. Once the initial product coating has been overcome the hydration accelerates due to increased product surface area providing nucleation sites. It is therefore assumed that the formation of $CaCO_3$ due to carbonation is more evenly dispersed in BA-0-1-W, which results in higher compressive strength at day 3 and 7. The formation of $CaCO_3$ in BA-0-2-W has clustered and therefore reduces the number of nucleation sites to facilitate the formation of C-S-H. According to equation 2.10 og 2.11, too large dosage of CO_2 may also produce silicate hydrate (S-H) instead of C-S-H, which may result in lower amount of C-S-H and lower compressive strength. The injection of CO_2 does seem to have marginal effects on the compressive strength of concrete with Anlegg cement, except for the earliest compressive strength which is significantly reduced.

Figure 4.9 below presents the compressive strength of the batches containing 20 % slag in the binder, and 0, 1 or 2 wt% CO_2 injected during mixing. SL-20-1-W have a decrease of 9,54 %, 1,95 %, 6,43 % and 7,06 % after 1, 3, 7 and 28 days respectively. SL-20-2-W have an increase of 3,08 % after 1 day, but a decrease of 1,38 %, 4,45% and 6,18 % after 3, 7 and 28 days respectively.

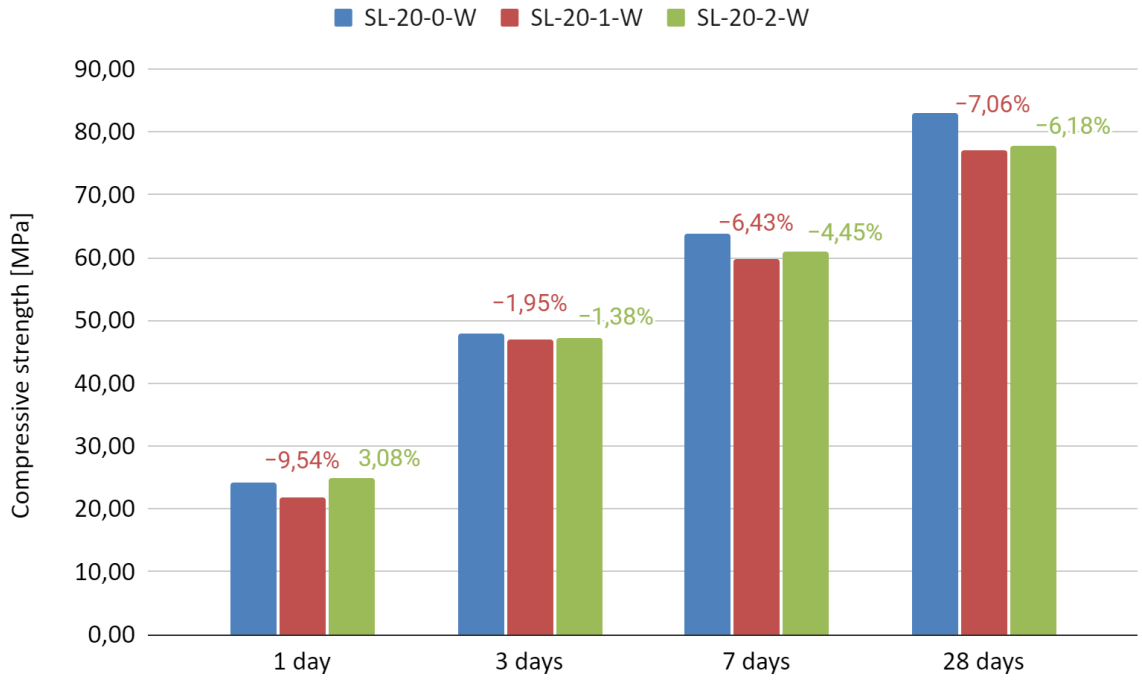

Figure 4.9: Compressive strength of SL-20 batches cured in water

The reduction in compressive strength after 1 day in SL-20-1-W may be due to the coating of initial hydration or carbonation products. The increase of SL-20-2-W may be that the coating is more rapidly dissolved and the higher temperature increases the early strength. The reduction after 3, 7, and 28 days is assumed to be because the amount of injected CO_2 is too large and the $CaCO_3$ that is formed clustered and reduced the nucleation sites for the C-S-H to form. Both of these factors reduce the formation of C-S-H, and therefore reduce the compressive strength. In section 2.3.3, it was explained that the slag is less reactive than cement, and the cement particles will disperse in the mix and react with more CO_2 than the slag. In this blend with 20 % slag in the binder it seems that this had no effect on the carbonation, and there were not formed more carbonated products as stated in section 2.3.3. This means that injection of CO_2 in a 20/80 blended slag cement does not have any positive contribution on the compressive strength, but rather a negative effect.

Figure 4.10 presents the compressive strength of concrete with 30 % slag in binder and 0, 1 or 2 wt% CO_2 injected during mixing. SL-30-1-W had an increase of 4,74 %, 3,57 %, 7,18 %, and 8,27 % after 1, 3, 7, and 28 days respectively. SL-30-2-W had a decrease of 9,54 % and 4,00 % after 1 and 3 days, but an increase of 3,48 % and 8,99% after 7 and 28 days.

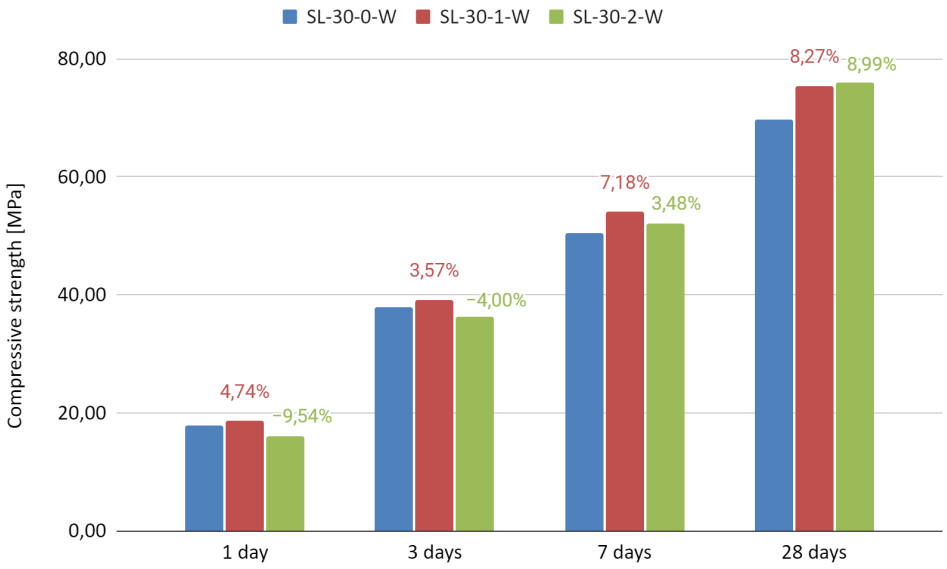

Figure 4.10: Compressive strength of SL-30 batches cured in water

The increase in early strength of SL-30-1-W is assumed to be due to the higher temperature development which increases the early strength development. The reduction in compressive strength of SL-30-2-W is assumed to be because of the initial coating of the hydration products which needs to be overcome to facilitate further nucleation sites to form C-S-H in the concrete. The increase of SL-30-1-W may illustrate what has been stated in section 2.3.3. The cement particles are dispersed in the mix, resulting in more cement particles exposed to carbonation. The slag allows the vigorous carbonation of cement to take place with fewer competitive sites. Then there is more $CaCO_3$ forming which increases the nucleation sites which facilitates more formation of C-S-H. The decrease after 3 days for SL-30-2-W may be due to several reasons. The clustering of $CaCO_3$ particles and formation of silicate hydrate instead of C-S-H may be some of the reasons. Also the carbonation products, as $CaCO_3$, may be coating the silicates. When the coating has been overcome the hydration may accelerate due to increased product surface area providing nucleation sites, as seen after the 1 day test. It seems that 2 wt% CO_2 may be a slower hydration than 1 wt%, but increasing after 3 days. The 30/70 blended slag cement has a positive improvement regarding the compressive strength, except for 1 and 3 days for the SL-30-2-W batch.

Figure 4.11 presents the compressive strength of the concrete with 70 % slag in binder and 0, 1 or 2 wt% CO_2 injected during mixing. SL-70-1-W had an increase of 8,23%, 25,33%, 26,57% and 22,65% after 1, 3, 7 and 28 days respectively. SL-70-2-W had a small decrease of 1,27% after 1 day, but an increase of 1,28%, 24,27% and 20,67% after 3, 7 and 28 days respectively.

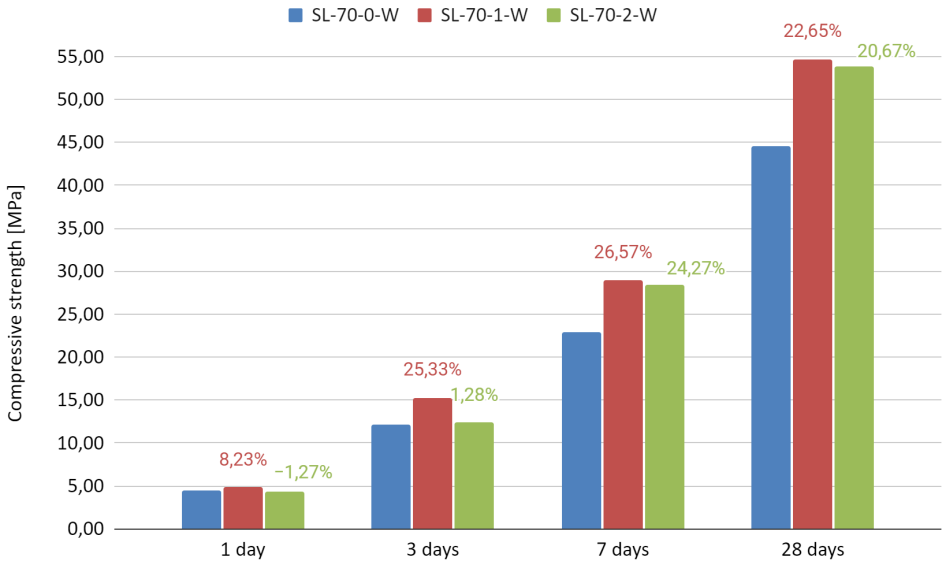

Figure 4.11: Compressive strength of SL-70 batches cured in water

The increase in compressive strength after 1 day for SL-70-1-W is due to several reasons, many discussed above. The higher temperatures increases the strength development, also the reaction between cement and CO_2 forms both $CaCO_3$ and C-S-H which may increase the strength. The reduction of SL-70-1-W is assumed to be because of the coating of the initial hydration products, explained above. The increase in compressive strength in SL-70-1-W and SL-70-2-W after 3, 7 and 28 days underlines what is assumed in the discussion of SL-30-1-W. Cement particles disperse in the mix reacting with more CO_2 due to fewer competitive sites. As mentioned above, this means more $CaCO_3$ which leads to more nucleation sites to facilitate more C-S-H. It seems therefore that an increased amount of slag in the binder is a positive effect when injecting CO_2 to the concrete. The negative effect of increasing slag in binder, is the slow hydration process which slows down the strength development.

In sum, blended slag cement with higher percentage of slag disperses the cement particles which facilitates for more cement particles to react with CO_2 and therefore forming more $CaCO_3$.

Previous research presented in section 2.4.2.1 had varying results regarding an increase in compressive strength. Kjos [27] observed a similar pattern as the BA-0 batches, meaning a decrease after 1 day and no significant differences at 28 days. Monkman, MacDonald and Hooton [28] observed a 14 % strength benefit at every age for batch 805, according to table 2.6. There may be several reasons for the difference, such as dosage duration, when CO_2 is added etc.

4.2.1.2 Air and CO_2 cured specimens

As a part of the experimental program, two other methods for curing were used: air curing and CO_2 curing. The curing procedure started after 1 day in the mold, and therefore the curing methods will be compared at day 3, 7 and 28. The curing methods will be compared to the concrete batches that were water cured to check if it is the CO_2 injected during mixing or in curing which has had the greatest effect. The main reason was to inspect if the concrete would have increased properties when exposed to CO_2 with atmospheric pressure. All results are presented in the appendix B.

Figure 4.12 below presents the compressive strength of each batch 3 days after casting. The y-axis is the compressive strength and the x-axis is the different concrete batches. The red columns are the specimens cured in the CO2 environment, where the percentage above the columns are the change relative to the specimen cured in water curing. As explained, the specimen was 1 day in the mold, then cured for two days in separate environments. Every batch, except BA-0-2-C and SL-30-1-C, had an increase in compressive strength after 3 days. The greatest effect was shown in the SL-70-1-C and SL-70-2-C batches, which had an increase of 15,52% and 30,86 % respectively. The compressive strength of the specimens cured in the CO2 environment is higher than the specimen cured in air.

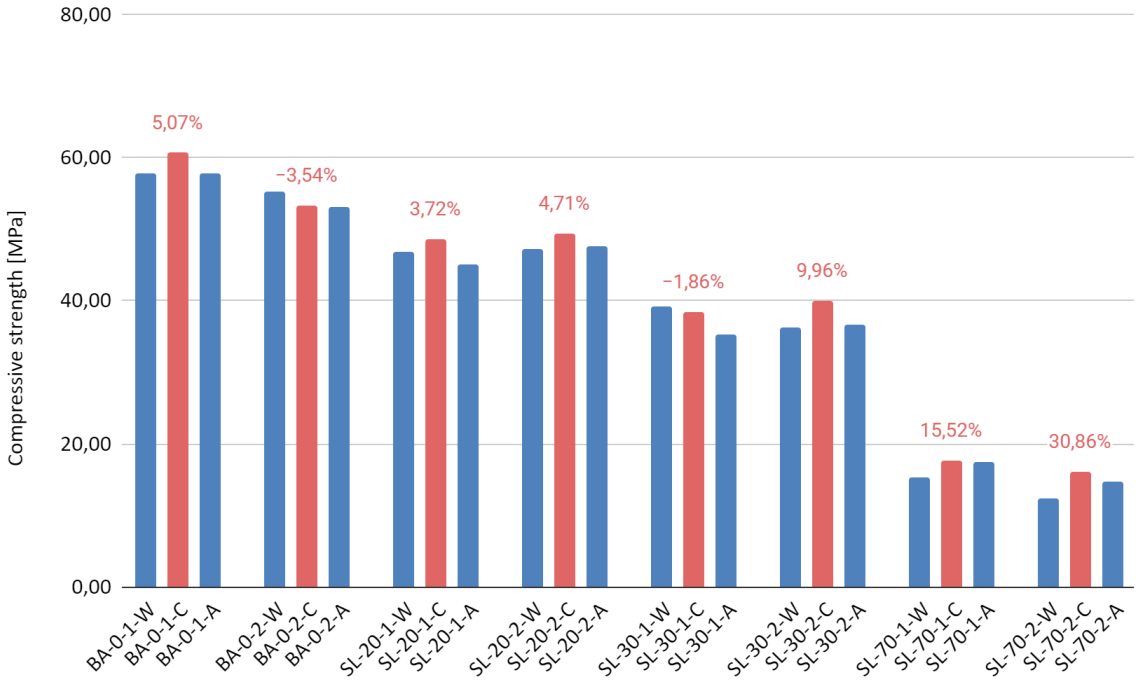

Figure 4.12: Compressive strength after 3 days - cured in W, A & C

Based on figure 4.12 it seems that the curing in the CO2 environment has a positive effect on the early compressive strength. This is assumed to be due to the reaction between C_3S, C_2S and CO_2 on the surface of the concrete, which forms C-S-H and $CaCO_3$. As explained earlier, this facilitates sites to form C-S-H which improves the compressive strength. Also an increase in hydration may be the reason for the increase in strength. The reaction between cement and CO_2 is exothermic and increases the temperature in the environment, which may increase the hydration. The temperature development described in 4.1.4 only measures the concrete straight after casting and not during the carbonation in the CO_2 box. An increase in temperature will accelerate the hydration, meaning an increase in the compressive strength.

The depth of the CO_2 intrusion is unknown and the concentration of CO_2 in the box is unknown. Therefore the batches that had an decrease might be due to leakage or due to low intrusion of the gas in the concrete. It was observed that when the specimens were taken out after 2 days, they were warm. This indicates that it has been a reaction, due to the exothermic reaction explained in equation 2.8 and 2.9.

After the curing in separate environments for two days, the specimens are moved to water curing until 28 days after casting. Figure 4.13 presents the results after 28 days of curing. Mostly reductions in compressive strength are observed, except an increase of 2,44% and 0,79% in BA-0-2-C and SL-20-2-C respectively. Reduction in the specimen cured in air is also registered, and this is as expected, due to the two days not cured in water. It is assumed that the reduction is due to a reduction in the temperatur, which means a slower hydration.

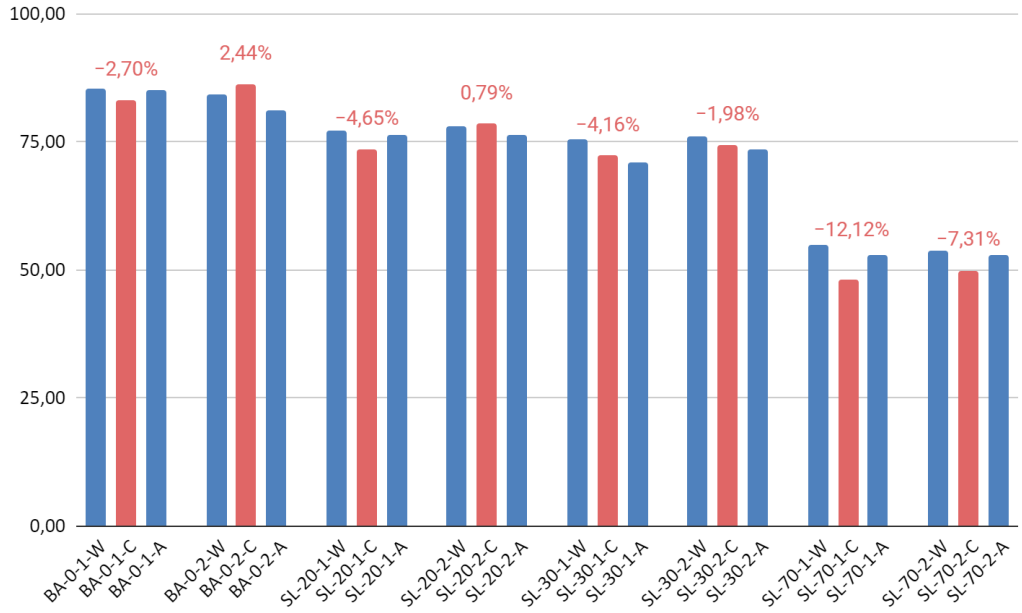

Figure 4.13: Compressive strength after 28 days - cured in W, A & C

The hydration is accelerated in the CO_2 chamber, which looks like retarding the hydration later on. Therefore, compressive strength of concrete cured in air and in the CO_2 environment shows no improvement compared to the specimen cured in water. The strength development actually decreased due to the curing methods. The $CaCO_3$ formed in the CO_2 environment may provide nucleation sites for the C-S-H to form, but this is only on the outer surface of the concrete. Therefore there is no increase in compressive strength later on in the curing period. It is assumed that the CO_2 intrusion was not sufficient and this indicates that CO_2 curing in a pressure vessel may improve the properties of the concrete.

4.2.2 Modulus of elasticity

Table 4.5 presents the results from the measurements of modulus of elasticity. One cylinder was tested for each curing method at each concrete batch. The tests were performed 28 days after casting.

The method of measuring the modulus of elasticity is described in section 3.5.2.2 and needs to be conducted accordingly. Several of the cylinders tested, did not result in a successful test. This is why there are such large deviations, and some results are not present. Based on the fact that several tests were not successful and some tests showed a clearly wrong result, it was decided to not analyze or draw any conclusion based on this.

There are mainly four sources of error that may affect the results. Firstly, the cylinders need to be cut to make a smooth surface for the compressive test machine. It was observed that the cuts were presumably not satisfactory. Secondly, the inputs in the compressive strength machine were not correctly programmed. This was discovered approximately half way through the experimental program and corrected later on. Thirdly, human failure may also play a role. The strain gauges need to be attached very carefully and in a correct manner. Lastly, the equipment failure is also a source of error and is often difficult to discover, and may have a large part of the failed tests. The strain gauges are sensitive equipment and do not handle much interference and hard handling.

Concrete batch	Modulus of elasticity [GPa]	Concrete batch	Modulus of elasticity [GPa]
BA-0-0-W	58,4	SL-30-0-W	12,8
BA-0-1-W	-	SL-30-1-W	-
BA-0-1-C	12,4	SL-30-1-C	-
BA-0-1-A	17,8	SL-30-1-A	-
BA-0-2-W	28,8	SL-30-2-W	36,0
BA-0-2-C	30,3	SL-30-2-C	33,6
BA-0-2-A	29,6	SL-30-2-A	31,1
SL-20-0-W	34,7	SL-70-0-W	12,2
SL-20-1-W	20,4	SL-70-1-W	22,5
SL-20-1-C	24,3	SL-70-1-C	68,7
SL-20-1-A	20,9	SL-70-1-A	23,6
SL-20-2-W	28,7	SL-70-2-W	51,5
SL-20-2-C	33,2	SL-70-2-C	33,2
SL-20-2-A	28,3	SL-70-2-A	36,1

Table 4.5: Modulus of elasticity of the experimental program

Kjos [27] observed an increase in modulus of elasticity in the batches with 0,36 wt% and 1,08 wt% CO_2, but a reduction with 0,72 wt% CO_2. Kjos also concludes that more research is needed to draw any conclusions.

4.2.3 Splitting tensile strength

The splitting tensile strength is presented in table 4.6. One measurement of each curing method of each concrete batch was conducted after 28 days.

Concrete batch	**Splitting tensile strength [MPa]**	**Concrete batch**	**Splitting tensile strength [MPa]**
BA-0-0-W	3,93	SL-30-0-W	3,28
BA-0-1-W	3,50	SL-30-1-W	3,82
BA-0-1-C	3,85	SL-30-1-C	2,85
BA-0-1-A	4,17	SL-30-1-A	4,11
BA-0-2-W	4,41	SL-30-2-W	3,89
BA-0-2-C	3,38	SL-30-2-C	4,01
BA-0-2-A	3,89	SL-30-2-A	4,10
SL-20-0-W	3,50	SL-70-0-W	2,70
SL-20-1-W	3,39	SL-70-1-W	3,23
SL-20-1-C	3,93	SL-70-1-C	3,73
SL-20-1-A	3,75	SL-70-1-A	3,67
SL-20-2-W	3,92	SL-70-2-W	3,54
SL-20-2-C	3,15	SL-70-2-C	3,64
SL-20-2-A	3,91	SL-70-2-A	3,89

Table 4.6: Splitting tensile strength of the experimental program

There are several sources of error in this experimental test, and is why there are some deviations in the measurements. The device in which the cylinder is located (figure 3.23) is skewed, and the compression machine is difficult to get completely level. The cylinder will

therefore not be subjected to a perpendicular force, and may result in the wrong direction of the stress. There are also some deviations in the appearance of the different cylinders, such as surface bubbles. These errors combined with the fact that only one test was performed for each concrete batch, makes it difficult to conclude based on the results given in table 4.6. Yet, it seems that there may be a correlation between increased splitting tensile strength and increasing addition of CO_2. All the specimens tested had a splitting tensile strength of 3,92% to 7,76% of the compressive strength, which is almost according to section 2.4.2.3.

The splitting tensile strength increases for every curing method of SL-20 batches, except the SL-20-1-W and SL-20-2-C. As discussed in section 4.2.1, SL-20 batches did not have a positive effect regarding the compressive strength. Therefore the increase in splitting tensile strength is suspicious.

Figure 4.14 below presents the splitting tensile strength of the SL-70 batches. The left y-axis is the splitting tensile strength in MPa, the right y-axis is the compressive strength in MPa, and the x-axis is the different concrete batches. The blue columns illustrate the splitting tensile strength and the red circles illustrate the compressive strength. The figure illustrates an increase in the splitting tensile strength relative to the SL-70-0-W, which is correct according to the theory in section 2.4.2.3. According to theory the SL-70-1-C should be decreasing, as the compressive strength is decreasing.

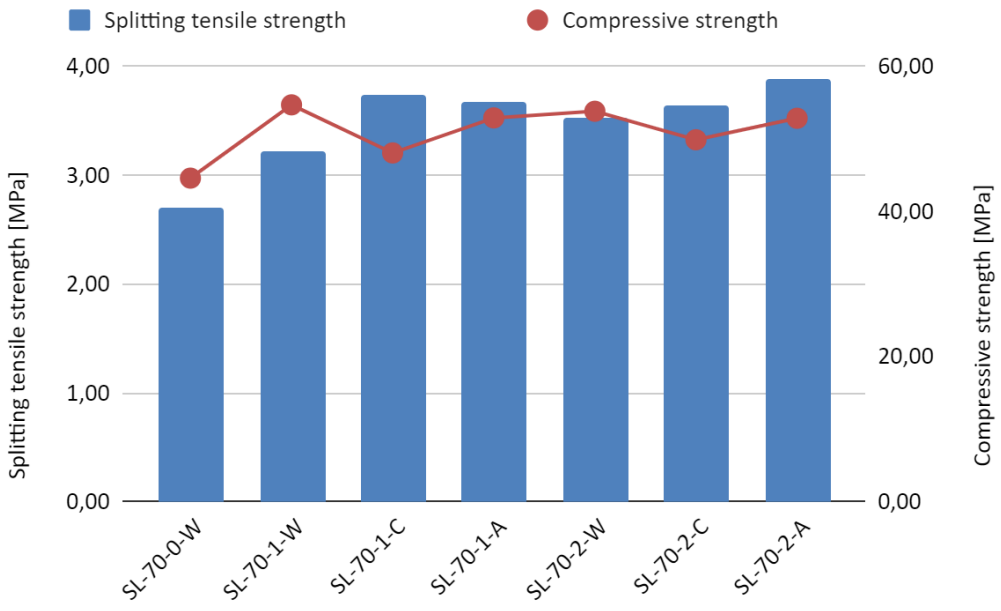

Figure 4.14: Splitting tensile strength of SL-70 batches

According to table 4.6, several inconsistencies are shown such as increase in splitting tensile strength in BA-0 and SL-20. An increase in SL-30 and SL-70 was expected. Due to the sources of errors and the results it is difficult to conclude if it is a correlation between splitting tensile strength and increasing amount of CO_2 injected to the concrete.

Kjos [27] observed a relation regarding the increased amount of CO_2 and the increase in splitting tensile strength, except the batch with 0,72 wt% CO_2. Every result regarding the tensile splitting test was in 5,48 % - 5,82 % of the compressive strength and is regarded as acceptable.

4.3 Effect on the chemical compositions

4.3.1 pH-measurements

Figure 4.15 presents the pH values measured from the experimental program. One measurement of each curing method from each batch was conducted. The test was performed after 28 days.

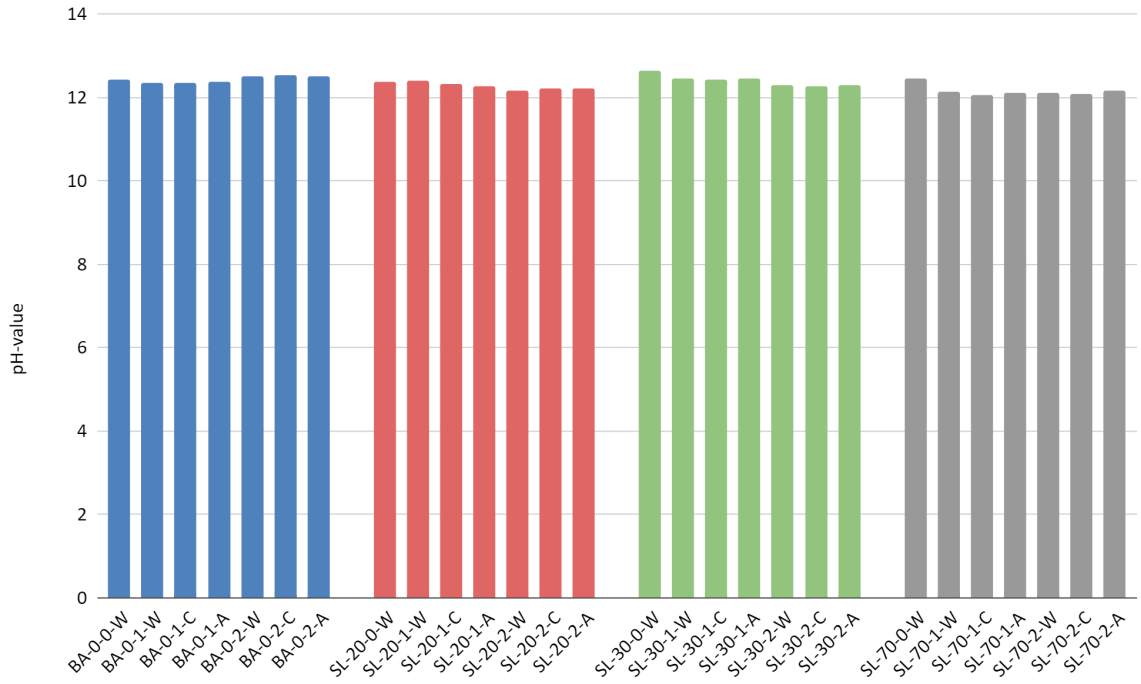

Figure 4. 15: pH - values for the experimental program

The pH-measurements vary from 12,06 and 12,63, which is normal values for concrete. This means that the CO_2 has reacted with C_3S and C_2S and therefore it is not more CO_2 to carbonate the concrete at a later stage and reduce the pH-value. The results are according to section 2.4.2.4. It is concluded that the carbonation treatment does not increase the risk of ferrous reinforcement depassivation due to reduced pore solution alkalinity.

4.3.2 Thermogravimetric Analysis

Thermogravimetric Analysis was performed 28 days after casting. The amount of data from the TGA is enormous and therefore only the most important parameters are presented in this section. An example of the data is presented in the appendix. One sample of crushed concrete was collected from each curing method of each batch with the exception of the specimens cured in CO_2, of which two samples were collected.

The TGA is done according to the method explained in section 3.5.3. Mass loss are measured as the temperature increases, and the most interesting temperature intervals are:

- 180-400 °C → Dehydration of C-S-H
- 400-600 °C → Dehydration of $Ca(OH)_2$
- 600-900 °C → Decarbonization of $CaCO_3$

The specimen cured in water will be presented first, followed by the specimen cured in CO_2.

4.3.2.1 Water cured specimens

Table 4.7 presents the mass loss% in the most important temperature intervals for each concrete batch. According to equation 3.9 in section 3.5.3.2, the CO_2 uptake of the concrete is calculated and also presented in table 4.7. The CO_2 uptake is shown in terms of binder wt%.

Concrete batch	Mass loss% 180-400 °C	Mass loss% 400-600 °C	Mass loss% 600-900 °C	CO_2 uptake
BA-0-0-W	2,98%	2,89%	2,89%	-
BA-0-1-W	3,11%	2,77%	3,49%	0,60%
BA-0-2-W	3,79%	3,05%	3,74%	0,85%
SL-20-0-W	3,84%	3,09%	4,15%	-
SL-20-1-W	3,85%	2,93%	3,01%	0%
SL-20-2-W	3,56%	2,41%	3,70%	0%
SL-30-0-W	3,68%	2,97%	2,49%	-
SL-30-1-W	3,23%	2,21%	2,66%	0,17%
SL-30-2-W	2,30%	1,38%	2,01%	0%
SL-70-0-W	2,68%	1,60%	1,63%	-
SL-70-1-W	3,02%	1,53%	2,14%	0,51%
SL-70-2-W	3,50%	1,62%	2,40%	0,77%

Table 4.7: Mass loss% for concrete batches cured in water

BA-0 batches show a correlation with the increased amount of CO_2 and the mass loss. BA-0-2-W had the largest total mass loss of 10,58% in relation to the BA-0-0-W with a total mass loss of 8,76%. Both the batches with CO_2 added had a larger mass loss in the 180-400 °C and 600-900 °C interval. BA-0-1-W had a decrease in the 400-600 °C interval, but BA-0-2-W had an increased mass loss in the same interval. The increased mass loss in 600-900 °C implies that $CaCO_3$ is formed as a result of the carbonation of the concrete. C-S-H dehydrates at 180-400 °C and the BA-0 batches with CO_2 had a larger mass loss in this interval. This is assumed to be due to the nucleation sites that $CaCO_3$ have, which increases the formation of C-S-H. Also according to equation 2.8 and 2.9 will C-S-H be formed as a result of the early age carbonation. C-H dehydrates in the 400-600 °C interval,

and therefore it seems that a larger dosage of CO_2 will increase the amount of C-H in the concrete, making the concrete more resistant to weather carbonation. Amount of CO_2 uptake increases as the amount of CO_2 injected into the concrete increases. The CO_2 uptake was 0,60% and 0,85% for BA-0-1-W and BA-0-2-W respectively. The increased mass loss in the 600-900 °C interval is due to decarbonization of $CaCO_3$ which is formed as cement reacts with CO_2. Based on table 4.7 it is concluded that the BA-0 batches will chemically bind CO_2 when injected during mixing.

Figure 4.16 illustrates the mass loss in percentage as a function of temperature of the SL-20 concrete batches. The y-axis is the mass loss% and the x-axis is the temperature in °C. Figure 4.17 presents the mass loss% in the three main temperature intervals. The y-axis indicates the mass loss in percentage, the x-axis presents the temperature intervals in °C, and the percentage above each column is the mass loss relative to the SL-20-0-W batch.

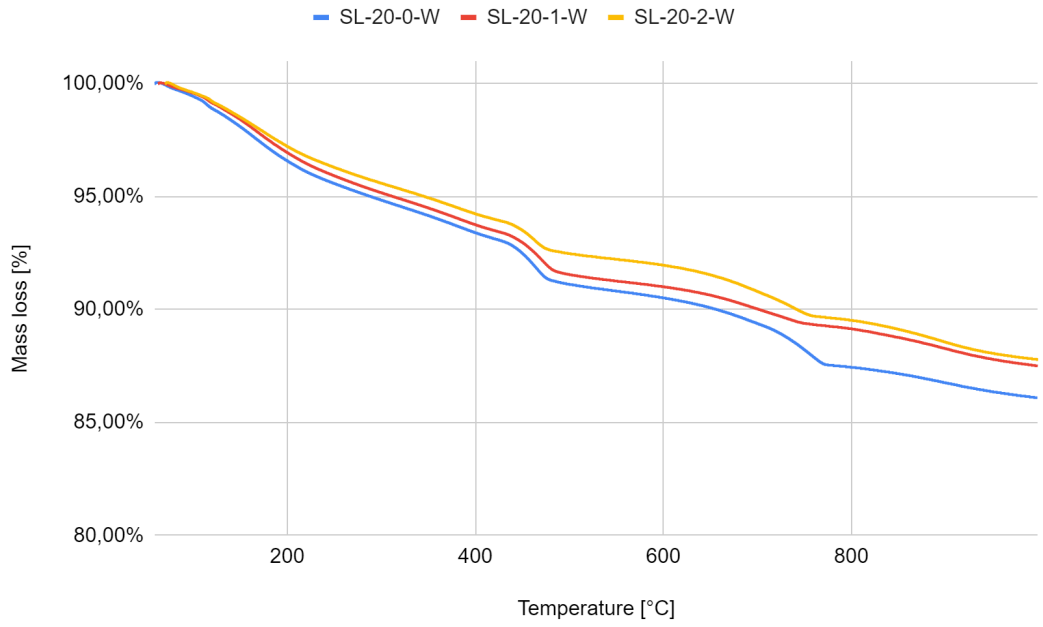

Figure 4.16: TGA of SL-20 concrete batches

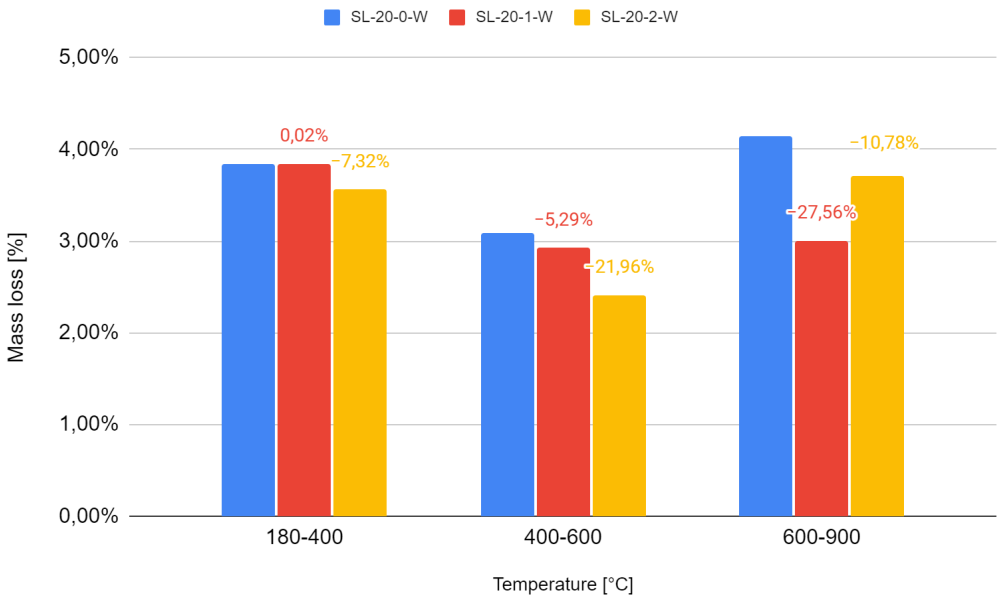

Figure 4.17: Mass loss% in important temperature intervals, SL-20

The total mass loss of SL-20-0-W was 11,09%, which was larger than both SL-20-1-W (9,78%) and SL-20-2-W (9,68%). The mass loss of SL-20-0-W was in fact the largest mass loss of every batch in table 4.7. A reaction between cement and CO_2 was observed when mixing, because of the loss in slump and the increased temperature development, ref section 4.1.1 and 4.1.4. The large total mass loss of SL-20-0-W is suspicious and there may be an error in the execution of the TGA.

The reduction in compressive strength also showed that the injection of CO_2 is not favorable regarding SL-20 batches. According to eq. 2.10 and 2.11 in section 2.3.2 a large dosage of CO_2 forms silicate hydrate (S-H) and $CaCO_3$ instead of C-S-H and $CaCO_3$. The injection of CO_2 might therefore be hindering the formation of C-S-H resulting in less mass loss in the interval 180-400 °C. $CaCO_3$ that is formed due to the carbonation might also be clustered and will not have the effect of acting as a growth site for formation of C-S-H. According to 2.4.3.2, C-S-H might also dehydrate up to a 1000 °C. The reduced formation of C-S-H in the batches with CO_2 and the clustering of $CaCO_3$ might be the reason for the low mass loss at both 180-400 °C and 600-900 °C. Another negative effect of the injection of CO_2 is the increased mass loss in the 400-600 °C interval, which implies a reduction in C-H. This reduces the ability to resist the weathering carbonation. It is not possible to calculate the CO_2 uptake in these concrete batches as the amount of $CaCO_3$ in the batches with CO_2 is lower

than the mass loss of SL-20-0-W in the 600-900 °C interval. It is therefore concluded that the 20/80 blended slag cement did not show a CO_2 uptake, and based on earlier sections it seems that the addition of CO_2 only has a negative effect on the properties of the concrete.

SL-30 batches show improvements regarding the injection of CO_2 in concrete with slag. According to table 4.7 above the total mass loss of SL-30-0-W was 9,14%, SL-30-1-W had a total mass loss of 8,09% and SL-30-2-W had a total mass loss of 5,68%. SL-30-2-W had the lowest mass loss of every batch in table 4.7, and there may be an error in the execution of the TGA. SL-30-1-W has a decrease of C-S-H (180-400 °C) and C-H (400-600 °C), but an increase of $CaCO_3$ (600-900 °C). The CO_2 uptake is calculated to be 0,17%, and is not a lot compared to BA-0 batches. This indicates that the slag cement is not as efficient as mentioned in section 2.3.3. SL-30-2-W has a decrease of C-S-H and C-H. The mass loss in the 600-900 °C interval is not large enough to examine if any of the CO_2 is chemically bound. This might be that there are only small amounts of $CaCO_3$ formed or that the dosage of CO_2 was too large. Based on section 4.2.1.1 it seems that there is in fact a reaction between CO_2 and the 30/70 blended slag cement, and it will increase some of the properties of the concrete. Only a CO_2 uptake was observed in the SL-30-1-W batch.

Figure 4.18 illustrates the mass loss in percentage as a function of temperature of the SL-70 concrete batches. The y-axis is the mass loss% and the x-axis is the temperature in °C. Figure 4.19 presents the mass loss in the three main temperature intervals. The y-axis presents the mass loss in percentage, the x-axis presents the temperature intervals in °C, and the percentage above each column is the mass loss relative to the SL-70-0-W.

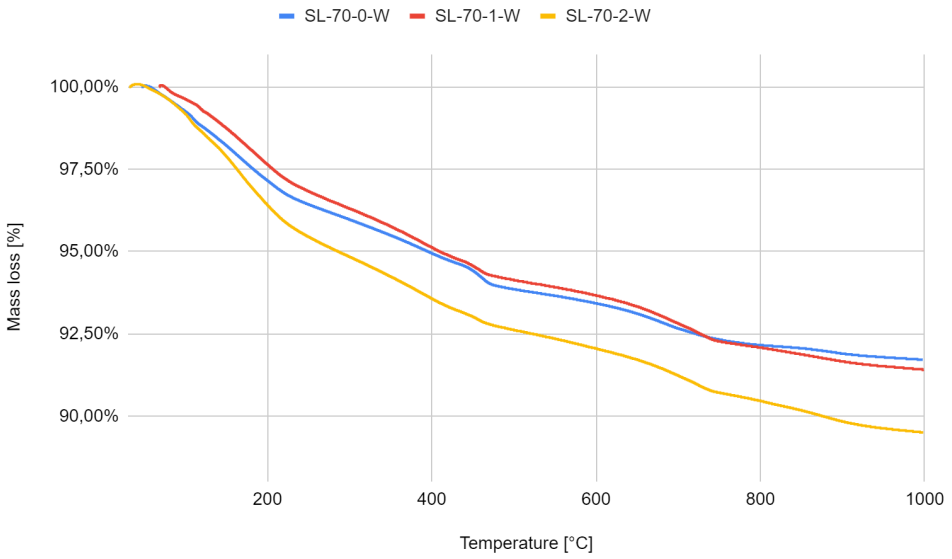

Figure 4.18: TGA of SL-70 concrete batches

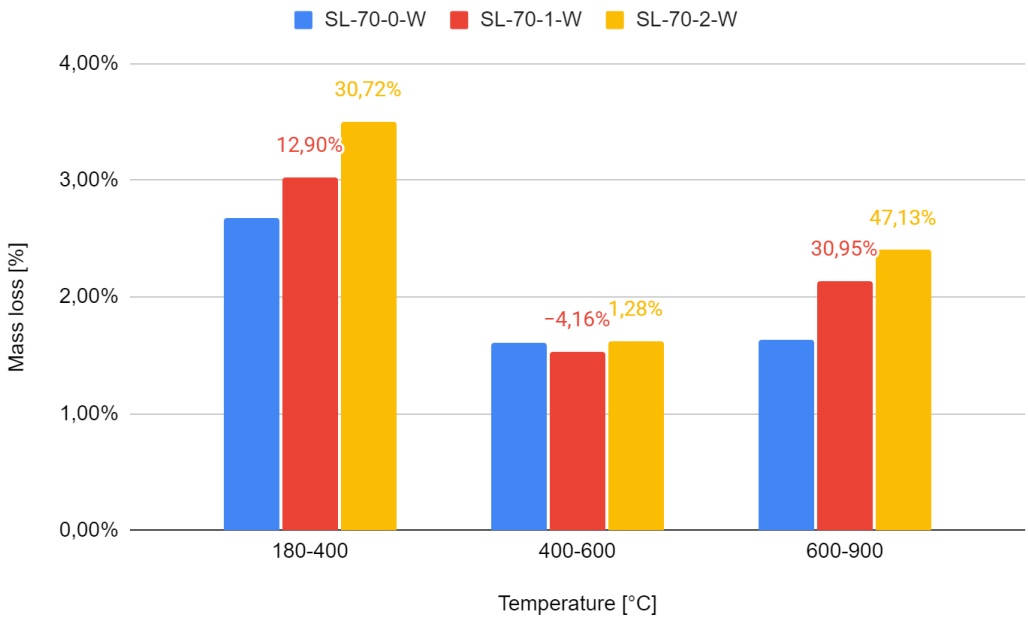

Figure 4.19: Mass loss% in important temperature intervals, SL-70

SL-70-0-W had a total mass loss of 5,91%, SL-70-1-W had a total mass loss of 6,70% and SL-70-2-W had a total mass loss of 7,52%. Both of the batches with CO_2 added during mixing had an increased mass loss in the 180-400 °C and 600-900 °C. SL-70-1-W had a decrease in the 400-600 °C interval, and SL-70-2-W had an increase in the same interval. According to section 2.3.2 will the reaction between cement and CO_2 form C-S-H and $CaCO_3$. The increase in the 180-400 °C and 600-900 °C indicates that this is the case for

these batches. The $CaCO_3$ is known to act as a nucleation site in which C-S-H will grow. Increased amounts of C-S-H is known to increase several of the mechanical properties, ref 4.2.1.1. The CO_2 uptake for SL-70-1-W and SL-70-2-W is 0,51% and 0,77% respectively. The CO_2 uptake of SL-70 batches is only about 10-15 % less of what the BA-0 batches will bind. Even with only 30 % cement in the binder, the SL-70 batches are very capable of binding CO_2 relative to BA-0. The slag allowed the vigorous carbonation of cement to take place with fewer competitive sites (Figure 2.3b section 2.3.3). The improvements in mechanical properties and ability to bind CO_2 are desired properties and might be a way of reducing the greenhouse emissions from the concrete industry.

Kjos [27] observed increased mass loss% in the 600-900 °C and 400-600 °C intervals. It is concluded that the loss in the 600-900 °C interval is due to the decarbonization of $CaCO_3$. Kjos also observed a CO_2 uptake of 0,39%, 0,66%, and 0,79% in the 0,36 wt%, 0,72 wt% and 1,08 wt% respectively.

4.3.2.2 CO_2 cured specimens

From the specimens cured in CO_2 (C) two samples were collected. One sample was taken from the center of the cube (inner = I) and one from the outer layer of the cube (outer = O). This was done to observe if there is an increase in carbonation products or C-S-H due to the CO_2 curing. Table 4.8 below presents the mass loss% in the most important temperature intervals in SL-20 and SL-70 batches. SL-20 and SL-70 batches will be presented and discussed in this section. All remaining results will be presented in the appendix C.

Table 4.8 presents SL-20 and SL-70 specimens cured in CO_2 environment and the mass loss% in the three main temperature intervals. The CO_2 uptake is shown in terms of binder wt%, and is calculated based on the difference in mass loss% in CO minus mass loss% in CI.

Concrete batch	Mass loss% 180-400 °C	Mass loss% 400-600 °C	Mass loss% 600-900 °C	CO_2 uptake
SL-20-1-CI	3,44%	2,54%	2,87%	-
SL-20-1-CO	3,68%	2,72%	3,01%	0,14%
SL-20-2-CI	2,91%	1,99%	2,81%	-
SL-20-2-CO	3,94%	2,66%	3,81%	1,00%
SL-70-1-CI	1,12%	0,71%	1,14%	-
SL-70-1-CO	2,71%	1,50%	2,99%	1,85%
SL-70-2-CI	2,47%	1,32%	1,77%	-
SL-70-2-CO	2,92%	1,43%	2,04%	0,27%

Table 4.8: Mass loss% for SL-20 and SL-70 batches cured in CO_2

Table 4.8 clearly presents the effects of curing concrete in a CO_2 environment. Every temperature interval shows an increase in mass loss at the samples collected from the outer surface of the specimens. There is an increased amount of C-S-H, C-H and $CaCO_3$ in the outer layer of the concrete, which indicates that CO_2 is bound in the concrete. SL-20-1-CO had a CO_2 uptake of 0,14 %, whereas SL-20-2-CO had a 1,0 % uptake. SL-70-1-CO had an CO_2 uptake of 1,85 %, and SL-70-2-CO had an 0,27% uptake. The large deviations in CO_2 uptake is believed to be because of two reasons. First, the concentration of CO_2 in the curing process is unknown and might vary from test to test. The second reason is that the batches with lower uptake might be saturated with CO_2 at the outer layer and therefore there is not much cement to react with.

As described in section 4.2.1.2, it is difficult to assume how deep the intrusion of CO_2 is when there is no pressure. The table 4.8 proves that there is a reaction, but it does not show how deep into the specimen it is. Therefore, the effect of curing concrete specimens in a CO_2 rich environment without pressure is not preferred in relation to cure in water. Yet, it still will chemically bind CO_2, which is preferable in the fight against greenhouse gas emissions.

4.4 Source of Errors in the Experimental Program

In the following section, the sources of error, that could influence the results, are summarized:

1. Weighing of the material during proportioning
    a. May result in wrong proportioning and affect both fresh properties and hardened properties.
2. Surface damages on the concrete cubes and cylinders, due to low workability
    a. May affect the compressive strength, modulus of elasticity, and splitting tensile strength. Overall, this was not of great concern because the specimens were thoroughly checked.
3. Modulus of elasticity
    a. To get a successful test smooth surfaces is of great importance. This was not the case in several of the tests. The saw was the main problem.
    b. Human error in which the equipment needs to be used carefully and input in the program needs to be regularly checked.
    c. Equipment error in which the strain gauges need to be attached carefully and in the correct manner.
4. Splitting tensile strength
    a. Equipment errors in which both the machine and stand where the concrete was inserted were skewed.
5. TGA
    a. Collecting samples used in TGA may result in irregularities. The concrete sample is crushed, and therefore small aggregate particles may be taken into the test and may affect the results.
6. pH
    a. Same as above problem as TGA may occur; aggregates may affect the test.

5 Conclusion

Several effects of injecting CO_2 during mixing of concrete with different content of slag have been observed and quantified in accordance with the experimental program. The following conclusions are summarized, based on both the literature and the results;

1. Effect on fresh properties

It has been shown that the slump of the concrete is greatly reduced as CO_2 is injected into the concrete during mixing. There were not observed a large increase in the air content in any of the concrete batches, and the small increase was within the normal values. The small increase in air content was assumed to be due to the loss in workability. Fresh density was reduced, and the reduction was because of the loss in workability. Both the air content and fresh density of the concrete showed an improvement as the workability improved. Workability was improved by adding more superplasticizer during mixing. Concrete batches with addition of CO_2 showed an increase in initial temperature and a higher maximum temperature. This was assumed to be because of the exothermic reaction between C_3S, C_2S and CO_2.
It was observed that the same effects on the fresh properties are present in all the concrete batches, regardless of the amount of slag in the binder.

2. Effect on hardened properties

The specimens with CO_2 added during mixing were cured in 3 different environments; water, air and CO_2.
The compressive strength of BA-0-W cured in water showed a considerable decrease in compressive strength after 1 day. After 3, 7 and 28 days only a small and insignificant deviation was observed in compressive strength. SL-20-W batches had only negative effects of the injection of CO_2, as the compressive strength was reduced after 1, 3, 7 and 28 days. SL-30-W batches showed some improvements in relation to the SL-20-W batches. The compressive strength of SL-30-1-W had higher compressive strength at each test day. SL-30-2-W had a decrease at day 1 and 3, but increased at day 7 and 28. SL-70-W batches had the greatest effect of injecting CO_2 during mixing. Only SL-70-2-W had a small and insignificant decrease after 1 day. Both SL-70-1-W and SL-70-2-W had a significant increase in compressive strength. **It is observed that the increase of slag content in the binder has a better reaction when injecting CO_2 during mixing, resulting in improvement of the compressive strength.**

With regards to the specimen cured in a CO_2 environment showed an increase in compressive strength after 3 days, except BA-0-2-C and SL-30-1-C. Both SL 70-1-C and SL-70-2-C showed the largest increase of 16 % and 31 % respectively, relative to the specimen cured in water. **The compressive strength improvements did not occur at the 7 and 28 days, and it is concluded that the intrusion of the CO_2 gas was not deep enough to improve any mechanical properties.**

Modulus of elasticity measurements did not go according to the experimental plan because of several sources of errors. No conclusion can be drawn based on the observed results given in section 4.2.2.

Splitting tensile strength showed a minor correlation with the increased amount of CO_2 added to the concrete. Despite some of the sources of errors described above, a smaller correlation between the addition of CO_2 and increased splitting tensile strength may thus be observed.

3. Effect on the chemical composition

The pH-values are observed to be between 12,1 and 12,6 and it is concluded that the CO_2 fully reacts with the cement and will not result in later carbonation of the concrete.

The chemical composition varies widely in every concrete batch. BA-0-W and SL-70-W batches had an increase in C-S-H, whereas SL-20-W and SL-30-W batches had a decrease. BA-0-W batches showed an increase in CO_2 uptake, with BA-0-2-W had an uptake of 0,85% in terms of binder wt%. Even with only 30% cement in the binder, SL-70-1-W and SL-70-2-W were capable of chemically binding 0,51% and 0,77% CO_2 respectively. **It seems that the slag allowed the vigorous carbonation of cement to take place with fewer competitive sites, which may have increased several of the mechanical properties.**

It is also observed that the concrete cured in CO_2 had a larger content of $CaCO_3$ and C-S-H in the outer layer of the specimens. CO_2 uptake was observed. **It is assumed that there is a low intrusion of CO_2 due to only atmospheric pressure in the curing process which does not improve any mechanical properties.**

Replacing cement with slag and injecting CO_2 during mixing might be one of the methods to reduce the greenhouse gas emissions from the concrete industry.

6 Future work

The following items are my suggestions that can be proposed for future work within the field of injecting CO_2 during mixing with or without different amount of slag;

- Conduct compressive strength after a longer time period, such as 56, 84, 112 days or more. The intent is to observe the strength development over a longer time period and observe if the compressive strength development continues further.
- Subject blended slag cement in a CO_2 curing pressure tank to observe if the benefits increase.
- Perform the experimental program and try to optimize the amount of CO_2 added to the concrete.
- Measure the temperature development immediately after addition of the CO_2, with shorter time intervals.
- Test modulus of elasticity and splitting tensile strength with more specimens to determine the effect of adding CO_2.
- Perform TGA at several different time periods to examine development of C-S-H and $CaCO_3$ earlier in the hydration period.
- Examine the effect of injecting CO_2 during mixing with more slag in the binder or other pozzolanas. Also a combination of several pozzolanas.
- Examine if the injecting of CO_2 is optimized by using carbonated water.

Bibliography

[1] R. Benestad and J. Mamen, “Klimaendringer”, 7. may 2021, [Internet], Available: https://snl.no/klimaendringer. [Found 15. may 2021]

[2] United Nations Climate Change, “The Paris Agreement”, [Internet], Available: https://unfccc.int/process-and-meetings/the-paris-agreement/the-paris-agreement [Found 15. may 2021]

[3] Regjeringen, “Norge forsterker klimamålet for 2030 til minst 50 prosent og opp mot 55 prosent”, 7. februaruy 2020, [Internet], Available: https://www.regjeringen.no/no/aktuelt/norge-forsterker-klimamalet-for-2030-til-minst-50-prosent-og-opp-mot-55-prosent/id2689679/ [Found 15. may 2021].

[4] K. Bramslev and A. K. Kvellheim, “Betong er en del av klimaløsningen”, 14. april 2020, [Internet], Available: https://www.sintef.no/siste-nytt/2020/-betong-er-en-del-av-klimalosningen/ [Found 15. may 2021].

[5] Norcem, “Sementproduksjon og CO2”, [Internet], Available: https://www.norcem.no/no/sementproduksjon-co2 [Found 15. may 2021].

[6] B. Pedersen, “1.1 Bakgrunn og historiske tilbakeblikk” in *Sementer med flygeaske og slagg: Lab- og felterfaringer*, 2015, p. 6-8.

[7] IEA, “About CCUS”, [Internet], Available: https://www.iea.org/reports/about-ccus [Found 15. may 2021].

[8] Norcem, “Norcem og karbonfangst”, [Internet], Available: https://www.norcem.no/no/CCS [Found 15. may 2021].

[9] M. Maage, “Chapter 1 - Practice” in *TKT 4215 Concrete Technology 1*, 2010, p. 1-3 - 1-4.

[10] K. N. Kjellsen, “Chapter 5 - Cement” in *TKT 4215 Concrete Technology 1*, 2015, p. 5-3 - 5-6.

[11] E. J. Sellevold, “Chapter 6 - Hydration” in *TKT 4215 Concrete Technology 1*, 2014, p. 6-3 - 6-8.

[12] B. Pedersen, “3.2.2 Slagg” in *Sementer med flygeaske og slagg: Lab- og felterfaringer*, 2015, p. 28.

[13] B. Pedersen, “3.4.2 Slagg” in *Sementer med flygeaske og slagg: Lab- og felterfaringer*, 2015, p. 34-36.

[14] S. Monkman, “Use of GGBF slag in concrete” in *Maximizing carbon uptake and performance gain in slag-containing concrete through early carbonation*, Doctoral dissertation, 2008, p. 38-29.

[15] S. Monkman, “Types of Concrete Carbonation”, *Technical Note from Carbon Cure*, p. 1-4.

[16] C. J. Goodbrake, J. F. Young and R. L. Berger, “Reaction og Beta-Dicalcium Silicate and Tricalcium Silicate with Carbon Dioxide and Water Vapor” *Journal of the American Ceramic Society*, vol. 62, 1979, p. 168-171.

[17] M. Thomas, “Impact of CO_2 Utilization in Fresh Concrete on Corrosion of Steel Reinforcement”, *Technical Note from Carbon Cure*, 2019, p. 2.

[18] S. Monkman and Y. Shao, “Assessing the carbonation Behavior of Cementitious Materials”, *Journal of materials in civil engineering*, 2006.

[19] J. Kwasny, M. Basheer og M. I. Russel, “CO2 Sequestration in Cement-Based Materials During Mixing Process Using Carbonated Water and Gaseous CO2” in *International Conference on the Durability of Concrete Structures*, Purdue University, 2014.

[20] S. Kashef-Haghighi and S. Ghoshal, “CO2 Sequestration in Concrete through Accelerated Carbonation Curing in a Flow-through Reactor” *Industrial & Engineering Chemistry Research*, vol. 49, 2010, pp. 1143-1149.

[21] S. Monkman and Y. Shao, “Carbonation-curing of slag-cement concrete for binding CO_2 and improving performance”, in *Journal of Materials in Civil Engineering*, 2010.

[22] J. Silvestre, N. Silvestre and J. de Brito, “Review on concrete nanotechnology”, in *European Journal of Environmental and Civil Engineering*, vol 20, 2015, p. 469-470.

[23] S. Monkman, P. A. Kenward, G. Dipple, M. MacDonald and M. Raudsepp, “Activation of cement hydration with carbon dioxide”, in *Journal of Sustainable Cement-Based Materials*, vol. 7, 2018, p. 160-181.

[24] T. Sato and F. Diallo, “Seeding Effect of Nano-CaCO3 on the Hydration of Tricalcium Silicate” *Jornal of the Transportation Research Board*, vol. 2141, 2010, pp. 61-67.

[25] L. Poudyal, K. Adhikari and M. Won, “Mechanical and Durability Properties of Portland Limestone Cement (PLC) Incorporated with Nano Calcium Carbonate ($CaCO_3$)”, in *Materials*, 2021, p. 9.

[26] Z. Ge, K. Wang, R. Sun, D. Huang and Y. Hu, “Properties of self-consolidating concrete containing nano-CaCO3” *Journal of Sustainable Cement-Based Materials*, vol. 3, 2014, pp. 191-200.

[27] A.T. Kjos, “The Effect of Adding CO2 in Fresh Concrete”, Master thesis, University of Stavanger, 2020, p. 51-78.

[28] S. Monkman, M. MacDonald and R. Hooton, “Using Carbon Dioxide as a Beneficial Admixture in Ready-Mix Concrete,» in *International Concrete Sustainability Conference*, 2015.

[29] X. Liu, L. Chen, A. Liu and X. Wang, “Effect of Nano-CaCO3 on Properties of Cement Paste” in *International Conference on Future Energy, Environment, and Materials*, 2012.

[30] S. Smeplass, “Chapter 12 - Strength of Concrete” in *TKT 4215 Concrete Technology 1*, 2012, p. 12-19.

[31] M. Maage, “8.5 Betongens stivhet - elastisitetsmodul” in *Betong - regelverk, teknologi og utførelse*, Byggnæringens Forlag, p. 200-201, 2015.

[32] M. Maage, “8.4 Strekkfasthet, bøyestrekkfasthet og skjærfasthet” in *Betong - regelverk, teknologi og utførelse*, Byggnæringens Forlag, p. 198-199,2015.

[33] S. Monkman and M. Thomas, “CarbonCure Durability Assessment Report”, *Technical Note from Carbon Cure*.

[34] J. A. Grubb, H. S. Limaye and A. M. Kakade, “Testing pH of Concrete”, *Need for a standard procedure*, p. 78-83, 2007.

[35] Vidya og S. Rao, “THERMOGRAVIMETRIC ANALYSIS OF CONCRETE”, *International Journal of Modern Trends in Engineering and Research*, 2019.

List of Tables

List of Figures

Appendix

Appendix A - p. 106

- Proportioning of the concrete batches
- Temperature development

Appendix B - p. 114

- Compressive strength
- Splitting tensile strength

Appendix C - p. 127

- pH-measurements
- TGA

Appendix D - p. 131

- Norcem Anleggsement CEM I 52,5 N, Product Data
- Ground Granulated Blast Furnace Slag, Physical and Chemical Properties
- Superplasticizer Product Data

Appendix A

Mix design - Experimental program part one

	Reference	**20 % slag**	**30 % slag**	**70 % slag**
Material	**Amount**			
Cement - CEM I 52,5 N [kg]	31,0	25,0	21,0	9,0
Slag [kg]	0	6,0	9,0	21,0
Aggregate - 0/8 mm [kg]	56,2	56,2	56,2	56,2
Aggregate - 8/16 mm [kg]	56,5	56,5	56,5	56,5
Water [kg]	12,0	12,0	12,0	12,0
Superplasticizer - Dynamon SX-N [g]	261	194,5	143,0	138,0
W/C	**Matrix volume [l/m³]**		**Mix volume [l]**	
0,40	340		65	

Mix design - Experimental program part two with 1 wt% CO_2

	Reference	**20 % slag**	**30 % slag**	**70 % slag**
Material	**Amount**			
Cement - CEM I 52,5 N [kg]	36,9	29,5	25,8	11,1
Slag [kg]	0	7,4	11,1	25,8
Aggregate - 0/8 mm [kg]	69,2	69,2	69,2	69,2
Aggregate - 8/16 mm [kg]	69,5	69,5	69,5	69,5
Water [kg]	14,8	14,8	14,8	14,8
Superplasticizer - Dynamon SX-N [g]	367	259,3	193,0	505,0
CO_2 gas [g]	369	369	369	369
W/C	**Matrix volume [l/m³]**		**Mix volume [l]**	
0,40	340		80	

Mix design - Experimental program part two with 2 wt% CO_2

	Reference	**20 % slag**	**30 % slag**	**70 % slag**
Material	**Amount**			
Cement - CEM I 52,5 N [kg]	36,9	29,5	25,8	11,1
Slag [kg]	0	7,4	11,1	25,8
Aggregate - 0/8 mm [kg]	69,2	69,2	69,2	69,2
Aggregate - 8/16 mm [kg]	69,5	69,5	69,5	69,5
Water [kg]	14,8	14,8	14,8	14,8
Superplasticizer - Dynamon SX-N [g]	601,5	894,5	825,5	602,0
CO_2 gas [g]	738	738	738	738
W/C	**Matrix volume [l/m³]**		**Mix volume [l]**	
0,40	340		80	

Temperature development

The temperatures are given every 30 minutes, because of the large amount of data.

	BA-0-0	BA-0-1	BA-0-2	SL-20-0	SL-20-1	SL-20-2	SL-30-0	SL-30-1	SL-30-2	SL-70-0	SL-70-1	SL-70-2
Time [Hours]	**Temperature [°C]**											
0,0	19	28	30,1	17,0	26	30,8	19,0	25,3	25,9	19,0	23,4	26,1
0,5	19,2	28	30	17,0	26	31,1	19,0	25,2	26	19,0	23,8	26,3
1,0	19,4	27,5	30	17,0	26,5	31,2	20,5	25,2	26	19,0	24,1	26,1
1,5	19,6	28	30,1	18,5	26,5	31,1	21,0	25,3	26,1	20,5	24,2	26
2,0	19,8	28	30,2	18,5	26,5	31,2	21,0	25,4	26	21,0	24,3	26
2,5	20	28,5	30,4	19,0	26,5	31,6	21,0	25,6	26	21,0	24,2	26
3,0	20,3	29,5	31,1	19,0	27	32,1	21,0	25,9	26	21,0	24,3	26,1
3,5	20,6	30	32	19,5	28	32,9	21,0	26,6	26,2	21,0	24,3	26,2
4,0	21	31,5	33,4	20,0	28,5	34	21,5	27,4	26,4	21,0	24,4	26,3
4,5	21,5	33,5	35,2	20,0	30	35,2	21,5	28,4	26,7	21,0	24,5	26,4
5,0	22,2	35,5	37	20,0	31	36,3	22,0	29,4	27,1	21,0	24,7	26,4
5,5	23,1	37,5	38,8	20,5	32,5	37,5	22,0	30,5	27,8	21,5	25	26,5
6,0	24,1	39,5	40,6	20,5	33,5	38,8	22,5	31,6	28,5	21,5	25,1	26,7
6,5	25,2	42	42,6	20,5	35	40,2	23,0	32,7	29,3	21,5	25,4	26,9
7,0	26,7	44,5	44,5	21,0	36	41,4	24,0	33,8	30	21,5	25,6	27
7,5	28,3	47	46,3	21,0	37,5	42,6	24,5	35	30,8	22,0	25,9	27,1
8,0	30,2	48,5	47,6	21,0	39	43,6	25,5	36,1	31,4	22,0	26,2	27,2
8,5	32,1	49,5	48,8	21,5	40,5	44,4	26,5	37,4	32,2	22,5	26,5	27,4
9,0	34,1	50,5	49,6	22,0	42	45	27,5	38,5	32,9	22,5	26,7	27,6
9,5	36,2	51	50,2	23,0	43	45,4	28,5	39,5	33,8	23,0	27	27,9
10,0	38,6	51,5	50,6	23,5	44	45,8	29,5	40,2	34,5	23,5	27,3	28
10,5	40,9	52	50,9	24,5	44,5	46,1	30,5	40,9	35,1	23,5	27,6	28,2

11,0	42,9	52	51	25,5	45	46,3	32,0	41,4	35,9	24,0	27,9	28,4
11,5	44,5	52	51,1	26,5	45	46,3	33,0	41,7	36,5	24,5	28,2	28,6
12,0	45,7	52	51,1	27,5	45,5	46,4	34,5	42	37	24,5	28,4	28,7
12,5	46,5	51,5	51	29,0	45,5	46,4	35,5	42,2	37,4	25,0	28,6	28,9
13,0	47,1	51,5	50,7	30,5	46	46,4	37,0	42,3	37,7	25,5	28,8	29
13,5	47,4	51	50,5	31,5	46	46,3	38,0	42,4	38	26,0	29	29,2
14,0	47,7	51	50,2	33,0	46	46,2	38,5	42,5	38,2	26,5	29,1	29,2
14,5	47,9	50,5	49,8	34,5	45,5	46	39,0	42,5	38,4	26,5	29,3	29,3
15,0	48	50	49,4	36,0	45,5	45,9		42,6	38,4	27,0	29,4	29,4
15,5	47,9	50	49	37,5	45,5	45,7		42,5	38,5	27,0	29,5	29,5
16,0	47,8	49,5	48,6	39,0	45	45,5		42,5	38,5	27,0	29,6	29,6
16,5	47,7	49	48,2	40,0	45	45,3		42,4	38,5	27,5	29,6	29,5
17,0	47,5	48,5	47,7	41,0	45	45,1		42,3	38,5	27,5	29,6	29,6
17,5	47,2	48	47,3	41,0	44,5	44,7		42,1	38,5	27,5	29,7	29,7
18,0	46,9	47,5	46,9	41,5	44,5	44,5		41,9	38,5	27,5	29,7	29,7
18,5	46,7	47	46,5	41,5	44	44,2		41,8	38,4	27,5	29,7	29,6
19,0	46,3	46,5	45,9	42,0	43,5	43,8		41,5	38,4	27,5	29,7	29,7
19,5	45,9	46	45,5	42,0	43,5	43,5		41,4	38,3	27,5	29,7	29,7
20,0	45,5	45,5	45,1	42,0	43	43,3		41,1	38,2	27,5	29,7	29,6
20,5	45,1	45	44,6	42,0	42,5	42,9		40,8	38,1	27,5	29,6	29,6
21,0	44,6	44,5	44,1	42,0	42,5	42,6		40,6	38	27,5	29,7	29,5
21,5	44,4	44	43,7	41,5	42,5	42,2		40,3	37,8	27,5	29,7	29,5
22,0	43,9	43,5	43,2	41,5	42	41,9		40	37,6	27,5	29,6	29,4
22,5	43,1	43	42,7	41,5	41,5	41,6		39,8	37,4	27,0	29,4	29,7
23,0	42,6	42,5	42,4	41,0	41	41,1		39,5	37,2	27,0	29,3	29,5
23,5	42,2	42	42	41,0	40,5	40,6		39,2	37	27,0	29,2	29
24,0	41,8	42	41,5	40,5	40	40,2		39	36,7	27,0	29,1	29
24,5	41,4	41,5	41,1	40,5	39,5	39,8		38,7	36,3	27,0	29	29
25,0	41	41	40,6	40,0	39	39,4		38,4	36	27,0	28,9	28,9
25,5	40,8	40	40,2	40,0	38,5	38,9		38,1	35,5	26,5	28,8	28,8

26,0	40,4	39,5	39,8	39,5	38	38,5		37,7	35,2	26,5	28,8	28,9
26,5	40,1	39	39,3	39,5	37,5	38,1		37,4	34,9	26,5	28,7	29
27,0	39,6	38,5	38,9	39,0	37,5	37,8		37	34,5	26,5	28,6	28,9
27,5	39,1	38	38,5	38,5	37	37,4		36,7	34,2	26,5	28,5	29
28,0	38,9	37,5	38	38,5	36,5	37,1		36,4	33,9	26,5	28,4	28,9
28,5	38,5	37	37,5	38,0	36	36,6		36	33,5	26,5	28,3	28,8
29,0	38,1	37	37,2	37,5	35,5	36,2		35,8	33,1	26,5	28,3	28,9
29,5	37,8	36,5	37	37,0	35,5	35,9		35,6	32,7	26,5	28,2	28,8
30,0	37,4	36	36,7	36,5	35	35,5		35,2	32,5	26,5	28,1	28,7
30,5	37	35,5	36,3	36,5	34,5	35,3		35	32,2	26,0	28	28,7
31,0	36,7	35	35,9	36,0	34,5	34,9		34,7	31,9	26,0	27,9	28,7
31,5	36,4	35	35,4	35,5	34	34,6		34,4	31,7	26,0	27,9	28,6
32,0	36	34,5	35,1	35,5	34	34,3		34,1	31,5	26,0	27,9	28,6
32,5	35,8	34	34,9	35,0	33,5	34		33,9	31,2	26,0	27,8	28,6
33,0	35,4	33,5	34,5	34,5	33,5	33,8		33,6	31	26,0	27,7	28,6
33,5	35,2	33,5	34,3	34,5	33	33,5		33,3	30,8	26,0	27,7	28,6
34,0	34,9	33	33,9	34,0	32,5	33,1		33	30,6	26,0	27,7	28,5
34,5	34,5	32,5	33,6	34,0	32,5	33		32,7	30,4	25,5	27,7	28,4
35,0	34,2	32,5	33,3	33,0	32	32,8		32,4	30,2	25,5	27,5	28,4
35,5	33,9	32	33,1	33,0	32	32,6		32,1	30,1	25,5	27,4	28,3
36,0	33,7	32	32,9	32,5	31,5	32,2		31,9	29,8	25,5	27,3	28,3
36,5	33,3	31,5	32,5	32,5	31,5	32		31,6	29,6	25,5	27,3	28,2
37,0	33	31	32,2	32,0	31	31,7		31,4	29,4	25,5	27,2	28,2
37,5	32,7	31	32	31,5	31	31,6		31,1	29,2	25,5	27,2	28,1
38,0	32,4	30,5	31,8	31,5	30,5	31,3		30,9	29,1	25,0	27,1	28,1
38,5	32,2	30	31,5	31,0	30,5	31,1		30,7	28,9	25,0	27,1	28
39,0	32	30	31,2	30,5	30	30,9		30,4	28,6	25,0	27	27,9
39,5	31,7	29,5	31	30,5	30	30,7		30,2	28,4	25,0	26,9	27,9
40,0	31,5	29,5	30,8	30,0	29,5	30,4		29,9	28,3	25,0	26,8	27,9
40,5	31,2	29,5	30,5	30,0	29,5	30,3		29,7	28	25,0	26,7	27,7

41,0	31	29	30,4	29,5	29	30		29,4	27,9	24,5	26,7	27,7
41,5	30,7	28,5	30,1	29,5	29	29,8		29,3	27,7	24,5	26,6	27,6
42,0	30,5	28,5	29,9	29,0	29	29,7		29,2	27,5	24,5	26,5	27,6
42,5	30,4	28	29,6	28,5	28,5	29,5		28,9	27,4	24,5	26,5	27,5
43,0	30,1	28	29,4	28,5	28,5	29,3		28,8	27,2	24,5	26,4	27,5
43,5	29,7	27,5	29,2	28,0	28	29,1		28,6	27,1	24,5	26,3	27,5
44,0	29,6	27,5	29	28,0	28	28,9		28,4	26,9	24,0	26,3	27,3
44,5	29,4	27	28,8	27,5	28	28,8		28,2	26,7	24,0	26,2	27,2
45,0	29,2	27	28,6	27,5	27,5	28,6		28,1	26,6	24,0	26,1	27,2
45,5	28,9	27	28,5	27,0	27,5	28,4		28	26,3	24,0	26	27,1
46,0	28,9	26,5	28,3	27,0	27	28,3		27,8	26,3	24,0	25,9	27
46,5	28,6	26	28	26,5	27	28,1		27,6	26,1	24,0	25,8	26,9
47,0	28,4	26	27,9	26,5	27	27,8		27,5	26	24,0	25,8	27
47,5	28,3	26	27,7	26,0	26,5	27,7		27,3	25,8	23,5	25,7	26,8
48,0	28	25,5	27,6	26,0	26,5	27,6		27,2	25,7	23,5	25,6	26,7
48,5	27,7	25,5	27,3	26,0	26,5	27,5		27,1	25,5	23,5	25,5	26,8
49,0	27,6	25,5	27,2	25,5	26,5	27,3		26,9	25,4	23,5	25,5	26,5
49,5	27,3	25	27,1	25,5	26	27,2		26,8	25,3	23,5	25,4	26,4
50,0	27,1	25	26,9	25,0	26	27,1		26,7	25,2	23,5	25,3	26,4
50,5	27	25	26,6	25,0	26	27		26,6	25	23,0	25,3	26,2
51,0	27	24,5	26,3	25,0	25,5	26,8		26,5	25	23,0	25,3	26,1
51,5	26,6	24,5	26,2	25,0	25,5	26,7		26,4	24,9	23,0	25,2	26,1
52,0	26,7	24,5	26	24,5	25,5	26,6		26,3	24,7	23,0	25,1	26,2
52,5	26,4	24	25,9	24,5	25,5	26,4		26,2	24,6	23,0	25	25,9
53,0	26,2	24	25,8	24,5	25,5	26,3		26,1	24,5	23,0	25	26
53,5	26	24	25,8	24,0	25	26,2		26	24,4	23,0	25	25,8
54,0	25,9	24	25,6	24,0	25	26		26	24,4	23,0	24,9	25,6
54,5	25,8	23,5	25,5	24,0	25	26		26	24,4	22,5	24,8	25,6
55,0	25,6	23,5	25,4	24,0	25	25,9		25,8	24,3	22,5	24,8	25,6
55,5	25,5	23,5	25,3	23,5	24,5	25,7		25,6	24,2	22,5	24,6	25,5

56,0	25,6	23,5	25,3	23,5	24,5	25,6		25,5	24	22,5	24,5	25,5
56,5	25,4	23	25,1	23,5	24,5	25,4		25,4	24	22,5	24,5	25,4
57,0	25,3	23	25	23,5	24,5	25,3		25,3	24	22,5	24,4	25,4
57,5	25,2	23	25,1	23,5	24	25,2		25,2	23,9	22,5	24,4	25,4
58,0	25	23	25,1	23,0	24	25,1		25	23,9	22,5	24,3	25,3
58,5	24,9	22,5	24,9	23,0	24	25		25	23,8	22,5	24,2	25,2
59,0	24,7	22,5	24,7	23,0	24	24,9		24,9	23,8	22,5	24,1	25,1
59,5	24,6	22,5	24,6	23,0	24	24,8		24,8	23,7	22,0	24,1	25,1
60,0	24,5	22	24,5	23,0	23,5	24,7		24,7	23,6	22,0	24	24,9
60,5	24,4	22	24,4	23,0	23,5	24,6		24,6	23,5	22,0	24	24,9
61,0	24,4	22	24,4	22,5	23,5	24,5		24,5	23,5	22,0	23,9	24,8
61,5	24,2	22	24,2	22,5	23,5	24,5		24,4	23,4	22,0	23,8	24,8
62,0	24,2	22	24,1	22,5	23,5	24,3		24,4	23,3	22,0	23,8	24,8
62,5	24,1	21,5	24,1	22,5	23,5	24,2		24,3	23,2	22,0	23,8	24,7
63,0	24	21,5	23,9	22,5	23	24,1		24,2	23,2	22,0	23,6	24,6
63,5	23,9	21,5	23,9	22,0	23	24,1		24,2	23,1	21,5	23,6	24,6
64,0	23,7	21,5	23,8	22,0	23	24		24,1	23	21,5	23,6	24,5
64,5	23,6	21,5	23,7	22,0	23	23,9		24	23	21,5	23,6	24,4
65,0	23,6	21	23,7	22,0	23	23,8		23,9	22,9	21,5	23,5	24,3
65,5	23,5	21	23,6	21,5	22,5	23,9		23,9	22,9	21,5	23,4	24,3
66,0	23,4	21	23,5	21,5	22,5	23,7		23,7	22,8	21,5	23,4	24,2
66,5	23,3	21	23,5	21,5	22,5	23,6		23,6	22,7	21,5	23,3	24,2
67,0	23,2	21	23,4	21,5	22,5	23,5		23,4	22,6	21,5	23,2	24,1
67,5	23,1	21	23,3	21,5	22	23,5		23,4	22,6	21,5	23,1	24
68,0	23	20,5	23,3	21,0	22	23,4		23,4	22,5	21,0	23,1	24
68,5	23,2	20,5	23,1	21,0	22	23,2		23,3	22,5	21,5	23	23,9
69,0	23,1	20,5	22,9	21,0	22	23,2		23,3	22,4	21,0	23	23,8
69,5	22,9	20,5	23,2	21,0	22	23,1		23,2	22,4	21,0	22,9	24

Appendix B

Compressive strength

The concrete batch codes used in the appendix deviates from the codes used in the thesis:

- The first two letters indicates what is in the binder:
  BA=100 % cement
  SL=slag in binder
- The first numbers indicates how much slag is in the binder:
  This varies from BA-01 = 0 % slag, and up to SL-20, SL-30 and SL-70 which is 20%, 30% or 70% slag
- The next number indicates how much CO_2 that is added, measured in wt% of the binder. This varies from 0, 1 and 2 wt% CO_2
- The next part is the number of days after casting, and which specimen number.
  3B = 3 days after casting and second specimen. There are 3 specimen at each testing day (A, B or C)
- The last part of the code is how the specimen is cured.
  V = Water cured
  CO2 = CO2 environment
  L = Air cured
  If no prefix is shown it is cured in water.

An example: SL-70-1-7C-CO2
Concrete with 70% slag in binder and 1 wt % CO_2 added during mixing. The test is performed after 7 days, and it is the third specimen. The specimen has been cured in a CO_2 environment.

Date	Concrete batch	Compressive strength [MPa]	Average	Standard deviation
07.04.2021	BA-01-0-1A	32,57		
07.04.2021	BA-01-0-1B	33,81		
07.04.2021	BA-01-0-1C	35,82	34,07	1,64
09.04.2021	BA-01-0-3A	56,10		
09.04.2021	BA-01-0-3B	55,88		
09.04.2021	BA-01-0-3C	54,85	55,61	0,67
13.04.2021	BA-01-0-7A	68,85		
13.04.2021	BA-01-0-7B	70,62		
13.04.2021	BA-01-0-7C	72,34	70,60	1,75
04.05.2021	BA-01-0-28A	85,76		
04.05.2021	BA-01-0-28B	85,09		
04.05.2021	BA-01-0-28C	86,14	85,66	0,53
26.02.2021	BA-01-1-1A	30,31		
26.02.2021	BA-01-1-1B	30,33		
26.02.2021	BA-01-1-1C	30,87	30,50	0,32
28.02.2021	BA-01-1-3A-CO2	62,10		
28.02.2021	BA-01-1-3B-CO2	60,98		
28.02.2021	BA-01-1-3C-CO2	59,04	60,71	1,55
28.02.2021	BA-01-1-3A-L	59,58		
28.02.2021	BA-01-1-3B-L	56,14		
28.02.2021	BA-01-1-3C-L	57,82	57,85	1,72
28.02.2021	BA-01-1-3A-V	57,69		
28.02.2021	BA-01-1-3B-V	58,81		
28.02.2021	BA-01-1-3C-V	56,83	57,78	0,99
04.03.2021	BA-01-1-7A-CO2	72,86		
04.03.2021	BA-01-1-7B-CO2	72,76		

04.03.2021	BA-01-1-7C-CO2	68,47	71,36	2,51
04.03.2021	BA-01-1-7A-L	71,80		
04.03.2021	BA-01-1-7B-L	69,06		
04.03.2021	BA-01-1-7C-L	69,15	70,00	1,56
04.03.2021	BA-01-1-7A-V	71,76		
04.03.2021	BA-01-1-7B-V	71,60		
04.03.2021	BA-01-1-7C-V	71,28	71,55	0,24
25.03.2021	BA-01-1-28A-V	85,11		
25.03.2021	BA-01-1-28B-V	85,11		
25.03.2021	BA-01-1-28C-V	86,06	85,43	0,55
25.03.2021	BA-01-1-28A-L	85,28		
25.03.2021	BA-01-1-28B-L	84,78		
25.03.2021	BA-01-1-28C-L	85,20	85,09	0,27
25.03.2021	BA-01-1-28A-C	82,45		
25.03.2021	BA-01-1-28B-C	84,99		
25.03.2021	BA-01-1-28C-C	81,91	83,12	1,64
16.03.2021	BA-01-2-1A	30,19		
16.03.2021	BA-01-2-1B	27,88		
16.03.2021	BA-01-2-1C	28,54	28,87	1,19
18.03.2021	BA-01-2-3A-C	53,76		
18.03.2021	BA-01-2-3B-C	50,50		
18.03.2021	BA-01-2-3C-C	55,70	53,32	2,63
18.03.2021	BA-01-2-3A-L	54,75		
18.03.2021	BA-01-2-3B-L	52,42		
18.03.2021	BA-01-2-3C-L	52,39	53,19	1,35
18.03.2021	BA-01-2-3A-V	55,21		
18.03.2021	BA-01-2-3B-V	53,76		
18.03.2021	BA-01-2-3C-V	56,86	55,28	1,55
22.03.2021	BA-01-2-7A-C	67,30		

22.03.2021	BA-01-2-7B-C	65,54		
22.03.2021	BA-01-2-7C-C	64,81	65,88	1,28
22.03.2021	BA-01-2-7A-L	64,68		
22.03.2021	BA-01-2-7B-L	70,01		
22.03.2021	BA-01-2-7C-L	70,25	68,31	3,15
22.03.2021	BA-01-2-7A-V	62,83		
22.03.2021	BA-01-2-7B-V	71,10		
22.03.2021	BA-01-2-7C-V	69,48	67,80	4,38
12.04.2021	BA-01-2-28A-V	82,63		
12.04.2021	BA-01-2-28B-V	84,45		
12.04.2021	BA-01-2-28C-V	85,40	84,16	1,41
12.04.2021	BA-01-2-28A-L	79,86		
12.04.2021	BA-01-2-28B-L	83,69		
12.04.2021	BA-01-2-28C-L	79,77	81,11	2,24
12.04.2021	BA-01-2-28A-C	86,18		
12.04.2021	BA-01-2-28B-C	84,94		
12.04.2021	BA-01-2-28C-C	87,53	86,22	1,30
09.02.2021	SL-20-0-1A	24,09		
09.02.2021	SL-20-0-1B	24,52		
09.02.2021	SL-20-0-1C	24,10	24,24	0,25
11.02.2021	SL-20-0-3A	47,76		
11.02.2021	SL-20-0-3B	47,47		
11.02.2021	SL-20-0-3C	48,28	47,84	0,41
15.02.2021	SL-20-0-7A	63,50		
15.02.2021	SL-20-0-7B	64,02		
15.02.2021	SL-20-0-7C	64,01	63,84	0,30
08.03.2021	SL-20-0-28A	84,20		
08.03.2021	SL-20-0-28B	82,74		

08.03.2021	SL-20-0-28C	82,23	83,06	1,02
26.02.2021	SL-20-1-1A	21,48		
26.02.2021	SL-20-1-1B	22,39		
26.02.2021	SL-20-1-1C	21,90	21,92	0,46
28.02.2021	SL-20-1-3A-CO2	48,97		
28.02.2021	SL-20-1-3B-CO2	49,05		
28.02.2021	SL-20-1-3C-CO2	47,93	48,65	0,62
28.02.2021	SL-20-1-3A-L	45,16		
28.02.2021	SL-20-1-3B-L	45,36		
28.02.2021	SL-20-1-3C-L	44,79	45,10	0,29
28.02.2021	SL-20-1-3A-V	47,46		
28.02.2021	SL-20-1-3B-V	47,02		
28.02.2021	SL-20-1-3C-V	46,23	46,90	0,62
04.03.2021	SL-20-1-7A-CO2	57,83		
04.03.2021	SL-20-1-7B-CO2	56,03		
04.03.2021	SL-20-1-7C-CO2	52,40	55,42	2,77
04.03.2021	SL-20-1-7A-L	55,92		
04.03.2021	SL-20-1-7B-L	55,73		
04.03.2021	SL-20-1-7C-L	57,00	56,22	0,69
04.03.2021	SL-20-1-7A-V	60,04		
04.03.2021	SL-20-1-7B-V	60,01		
04.03.2021	SL-20-1-7C-V	59,16	59,74	0,50
25.03.2021	SL-20-1-28A-V	78,46		
25.03.2021	SL-20-1-28B-V	74,39		
25.03.2021	SL-20-1-28C-V	78,73	77,19	2,43
25.03.2021	SL-20-1-28A-L	75,56		
25.03.2021	SL-20-1-28B-L	76,79		
25.03.2021	SL-20-1-28C-L	76,24	76,20	0,62
25.03.2021	SL-20-1-28A-C	75,23		

25.03.2021	SL-20-1-28B-C	72,17		
25.03.2021	SL-20-1-28C-C	73,42	73,61	1,54
19.03.2021	SL-20-2-1A	25,57		
19.03.2021	SL-20-2-1B	23,52		
19.03.2021	SL-20-2-1C	25,86	24,98	1,28
21.03.2021	SL-20-2-3A-C	48,76		
21.03.2021	SL-20-2-3B-C	49,81		
21.03.2021	SL-20-2-3C-C	49,62	49,40	0,56
21.03.2021	SL-20-2-3A-L	47,13		
21.03.2021	SL-20-2-3B-L	47,19		
21.03.2021	SL-20-2-3C-L	48,34	47,55	0,68
21.03.2021	SL-20-2-3A-V	48,39		
21.03.2021	SL-20-2-3B-V	45,90		
21.03.2021	SL-20-2-3C-V	47,24	47,18	1,25
25.03.2021	SL-20-2-7A-V	60,95		
25.03.2021	SL-20-2-7B-V	60,63		
25.03.2021	SL-20-2-7C-V	61,43	61,00	0,40
25.03.2021	SL-20-2-7A-L	56,98		
25.03.2021	SL-20-2-7B-L	57,50		
25.03.2021	SL-20-2-7C-L	59,00	57,83	1,05
25.03.2021	SL-20-2-7A-C	60,76		
25.03.2021	SL-20-2-7B-C	59,11		
25.03.2021	SL-20-2-7C-C	60,76	60,21	0,95
15.04.2021	SL-20-2-28A-V	79,77		
15.04.2021	SL-20-2-28B-V	75,97		
15.04.2021	SL-20-2-28C-V	78,03	77,92	1,90
15.04.2021	SL-20-2-28A-L	74,33		
15.04.2021	SL-20-2-28B-L	77,95		
15.04.2021	SL-20-2-28C-L	76,60	76,29	1,83

15.04.2021	SL-20-2-28A-C	77,42		
15.04.2021	SL-20-2-28B-C	79,48		
15.04.2021	SL-20-2-28C-C	78,72	78,54	1,04
20.02.2021	SL-30-0-1A	17,63		
20.02.2021	SL-30-0-1B	17,77		
20.02.2021	SL-30-0-1C	17,97	17,79	0,17
22.02.2021	SL-30-0-3A	38,34		
22.02.2021	SL-30-0-3B	38,64		
22.02.2021	SL-30-0-3C	36,61	37,86	1,10
26.02.2021	SL-30-0-7A	50,17		
26.02.2021	SL-30-0-7B	49,71		
26.02.2021	SL-30-0-7C	51,35	50,41	0,85
19.03.2021	SL-30-0-28A	71,70		
19.03.2021	SL-30-0-28B	70,24		
19.03.2021	SL-30-0-28C	66,96	69,63	2,43
10.03.2021	SL-30-1-1A	18,35		
10.03.2021	SL-30-1-1B	18,61		
10.03.2021	SL-30-1-1C	18,94	18,63	0,30
12.03.2021	SL-30-1-3A-L	36,62		
12.03.2021	SL-30-1-3B-L	34,58		
12.03.2021	SL-30-1-3C-L	34,85	35,35	1,11
12.03.2021	SL-30-1-3A-C	38,73		
12.03.2021	SL-30-1-3B-C	38,57		
12.03.2021	SL-30-1-3C-C	38,16	38,49	0,29
12.03.2021	SL-30-1-3A-V	38,88		
12.03.2021	SL-30-1-3B-V	39,54		
12.03.2021	SL-30-1-3C-V	39,23	39,22	0,33

16.03.2021	SL-30-1-7A-V	54,82		
16.03.2021	SL-30-1-7B-V	54,17		
16.03.2021	SL-30-1-7C-V	53,10	54,03	0,87
16.03.2021	SL-30-1-7A-L	51,62		
16.03.2021	SL-30-1-7B-L	50,39		
16.03.2021	SL-30-1-7C-L	49,23	50,41	1,20
16.03.2021	SL-30-1-7A-C	52,92		
16.03.2021	SL-30-1-7B-C	53,34		
16.03.2021	SL-30-1-7C-C	51,87	52,71	0,76
06.04.2021	SL-30-1-28A-V	76,72		
06.04.2021	SL-30-1-28B-V	74,73		
06.04.2021	SL-30-1-28C-V	74,73	75,39	1,15
06.04.2021	SL-30-1-28A-C	72,76		
06.04.2021	SL-30-1-28B-C	72,73		
06.04.2021	SL-30-1-28C-C	71,29	72,26	0,84
06.04.2021	SL-30-1-28A-L	71,97		
06.04.2021	SL-30-1-28B-L	69,44		
06.04.2021	SL-30-1-28A-L	71,82	71,08	1,42
24.03.2021	SL-30-2-1A	16,18		
24.03.2021	SL-30-2-1B	16,16		
24.03.2021	SL-30-2-1C	15,94	16,09	0,13
26.03.2021	SL-30-2-3A-L	36,09		
26.03.2021	SL-30-2-3B-L	37,32		
26.03.2021	SL-30-2-3C-L	36,63	36,68	0,62
26.03.2021	SL-30-2-3A-V	36,06		
26.03.2021	SL-30-2-3B-V	35,73		
26.03.2021	SL-30-2-3C-V	37,26	36,35	0,81
26.03.2021	SL-30-2-3A-C	40,22		
26.03.2021	SL-30-2-3B-C	39,65		

26.03.2021	SL-30-2-3C-C	40,04	39,97	0,29
30.03.2021	SL-30-2-7A-V	51,70		
30.03.2021	SL-30-2-7B-V	53,00		
30.03.2021	SL-30-2-7C-V	51,80	52,17	0,72
30.03.2021	SL-30-2-7A-L	52,88		
30.03.2021	SL-30-2-7B-L	52,05		
30.03.2021	SL-30-2-7C-L	52,13	52,35	0,46
30.03.2021	SL-30-2-7A-C	53,17		
30.03.2021	SL-30-2-7B-C	51,90		
30.03.2021	SL-30-2-7C-C	51,60	52,22	0,83
20.04.2021	SL-30-2-28A-V	75,59		
20.04.2021	SL-30-2-28B-V	74,41		
20.04.2021	SL-30-2-28C-V	77,68	75,89	1,66
20.04.2021	SL-30-2-28A-C	73,42		
20.04.2021	SL-30-2-28B-C	74,87		
20.04.2021	SL-30-2-28C-C	74,88	74,39	0,84
20.04.2021	SL-30-2-28A-L	75,46		
20.04.2021	SL-30-2-28B-L	71,55		
20.04.2021	SL-30-2-28C-L	73,81	73,61	1,96
20.02.2021	SL-70-0-1A	4,53		
20.02.2021	SL-70-0-1B	4,08		
20.02.2021	SL-70-0-1C	4,75	4,45	0,34
22.02.2021	SL-70-0-3A	12,52		
22.02.2021	SL-70-0-3B	12,09		
22.02.2021	SL-70-0-3C	11,99	12,20	0,28
26.02.2021	SL-70-0-7A	23,27		
26.02.2021	SL-70-0-7B	22,44		
26.02.2021	SL-70-0-7C	22,86	22,86	0,42

19.03.2021	SL-70-0-28A	44,32		
19.03.2021	SL-70-0-28B	44,70		
19.03.2021	SL-70-0-28C	44,82	44,61	0,26
19.03.2021	SL-70-1-1A	4,83		
19.03.2021	SL-70-1-1B	5,00		
19.03.2021	SL-70-1-1C	4,63	4,82	0,19
21.03.2021	SL-70-1-3A-C	18,03		
21.03.2021	SL-70-1-3B-C	18,39		
21.03.2021	SL-70-1-3C-C	16,57	17,66	0,96
21.03.2021	SL-70-1-3A-L	18,45		
21.03.2021	SL-70-1-3B-L	16,89		
21.03.2021	SL-70-1-3C-L	17,17	17,50	0,83
21.03.2021	SL-70-1-3A-V	14,88		
21.03.2021	SL-70-1-3B-V	15,79		
21.03.2021	SL-70-1-3C-V	15,20	15,29	0,46
25.03.2021	SL-70-1-7A-V	28,18		
25.03.2021	SL-70-1-7B-V	29,59		
25.03.2021	SL-70-1-7C-V	29,02	28,93	0,71
25.03.2021	SL-70-1-7A-L	27,37		
25.03.2021	SL-70-1-7B-L	26,80		
25.03.2021	SL-70-1-7C-L	27,72	27,30	0,46
25.03.2021	SL-70-1-7A-C	27,74		
25.03.2021	SL-70-1-7B-C	27,88		
25.03.2021	SL-70-1-7C-C	29,00	28,21	0,69
15.04.2021	SL-70-1-28A-L	53,21		
15.04.2021	SL-70-1-28B-L	52,11		
15.04.2021	SL-70-1-28C-L	53,43	52,92	0,71
15.04.2021	SL-70-1-28A-V	54,69		
15.04.2021	SL-70-1-28B-V	55,33		

15.04.2021	SL-70-1-28C-V	54,13	54,72	0,60
15.04.2021	SL-70-1-28A-C	51,22		
15.04.2021	SL-70-1-28B-C	46,10		
15.04.2021	SL-70-1-28C-C	46,94	48,09	2,75
07.04.2021	SL-70-2-1A	4,65		
07.04.2021	SL-70-2-1B	4,37		
07.04.2021	SL-70-2-1C	4,17	4,40	0,24
09.04.2021	SL-70-2-3A-V	12,14		
09.04.2021	SL-70-2-3B-V	12,20		
09.04.2021	SL-70-2-3C-V	12,73	12,36	0,32
09.04.2021	SL-70-2-3A-L	14,17		
09.04.2021	SL-70-2-3B-L	14,94		
09.04.2021	SL-70-2-3C-L	14,92	14,68	0,44
09.04.2021	SL-70-2-3A-C	16,52		
09.04.2021	SL-70-2-3B-C	16,13		
09.04.2021	SL-70-2-3C-C	15,86	16,17	0,33
13.04.2021	SL-70-2-7A-V	27,78		
13.04.2021	SL-70-2-7B-V	29,17		
13.04.2021	SL-70-2-7C-V	28,26	28,40	0,71
13.04.2021	SL-70-2-7A-C	28,52		
13.04.2021	SL-70-2-7B-C	27,68		
13.04.2021	SL-70-2-7C-C	28,41	28,20	0,46
13.04.2021	SL-70-2-7A-L	28,20		
13.04.2021	SL-70-2-7B-L	28,27		
13.04.2021	SL-70-2-7C-L	30,23	28,90	1,15
04.05.2021	SL-70-2-28A-V	55,00		
04.05.2021	SL-70-2-28B-V	53,56		
04.05.2021	SL-70-2-28C-V	52,94	53,83	1,06
04.05.2021	SL-70-2-28A-L	55,40		

04.05.2021	SL-70-2-28B-L	52,82		
04.05.2021	SL-70-2-28C-L	50,37	52,86	2,52
04.05.2021	SL-70-2-28A-C	50,83		
04.05.2021	SL-70-2-28B-C	49,80		
04.05.2021	SL-70-2-28C-C	49,07	49,90	0,88

Splitting tensile strength

Concrete batch	Max force at fracture [kN]	Length of specimen [mm]	Diameter of specimen [mm]	Splitting tensile strength [MPa]
BA-0-0-W	260,21	281,0	150,0	3,93
BA-0-1-W	231,51	281,0	150,0	3,50
BA-0-1-C	254,50	281,0	150,0	3,85
BA-0-1-A	276,24	281,0	150,0	4,17
BA-0-2-W	291,89	281,0	150,0	4,41
BA-0-2-C	223,76	281,0	150,0	3,38
BA-0-2-A	257,18	281,0	150,0	3,89
SL-20-0-W	231,85	281,0	150,0	3,50
SL-20-1-W	224,50	281,0	150,0	3,39
SL-20-1-C	259,80	281,0	150,0	3,93
SL-20-1-A	248,32	281,0	150,0	3,75
SL-20-2-W	259,70	281,0	150,0	3,92
SL-20-2-C	208,78	281,0	150,0	3,15

SL-20-2-A	258,52	281,0	150,0	3,91
SL-30-0-W	217,23	281,0	150,0	3,28
SL-30-1-W	252,52	281,0	150,0	3,82
SL-30-1-C	188,80	281,0	150,0	2,85
SL-30-1-A	271,99	281,0	150,0	4,11
SL-30-2-W	257,34	281,0	150,0	3,89
SL-30-2-C	265,12	281,0	150,0	4,01
SL-30-2-A	271,45	281,0	150,0	4,10
SL-70-0-W	178,68	281,0	150,0	2,70
SL-70-1-W	213,53	281,0	150,0	3,23
SL-70-1-C	246,99	281,0	150,0	3,73
SL-70-1-A	243,17	281,0	150,0	3,67
SL-70-2-W	233,94	281,0	150,0	3,54
SL-70-2-C	240,94	281,0	150,0	3,64
SL-70-2-A	257,14	281,0	150,0	3,89

Appendix C

pH-measurements

Concrete batch	pH - measurement	Concrete batch	pH - measurement
BA-0-0-W	12,42	SL-30-0-W	12,63
BA-0-1-W	12,36	SL-30-1-W	12,45
BA-0-1-C	12,36	SL-30-1-C	12,43
BA-0-1-A	12,37	SL-30-1-A	12,45
BA-0-2-W	12,52	SL-30-2-W	12,29
BA-0-2-C	12,53	SL-30-2-C	12,27
BA-0-2-A	12,52	SL-30-2-A	12,29
SL-20-0-W	12,38	SL-70-0-W	12,46
SL-20-1-W	12,4	SL-70-1-W	12,15
SL-20-1-C	12,32	SL-70-1-C	12,06
SL-20-1-A	12,28	SL-70-1-A	12,1
SL-20-2-W	12,17	SL-70-2-W	12,12
SL-20-2-C	12,22	SL-70-2-C	12,08
SL-20-2-A	12,22	SL-70-2-A	12,16

TGA

Because of the enormous data of TGA, only an example is given below:

Index	Ts	t	HF	Weight	Tr
[#]	[°C]	[s]	[mW]	[mg]	[°C]
0	70,1	0	−0,71	43,05	50
1	70,04	1	−0,67	43,05	50,5
2	69,97	2	−0,52	43,05	51
3	69,92	3	−0,27	43,05	51,5
4	69,92	4	0,05	43,05	52
5	69,94	5	0,32	43,05	52,5
6	70	6	0,56	43,05	53
7	70,08	7	0,81	43,05	53,5
8	70,18	8	1,05	43,05	54
9	70,35	9	1,28	43,05	54,5
10	70,54	10	1,47	43,05	55
11	70,77	11	1,65	43,06	55,5
12	71,03	12	1,65	43,06	56
13	71,32	13	1,57	43,06	56,5
14	71,66	14	1,37	43,07	57
15	72,02	15	1,08	43,07	57,5
16	72,42	16	0,58	43,07	58
17	72,83	17	−0,04	43,07	58,5
18	73,28	18	−0,78	43,07	59
19	73,72	19	−1,62	43,07	59,5
20	74,18	20	−2,52	43,06	60
21	74,65	21	−3,38	43,06	60,5
22	75,11	22	−4,23	43,06	61
23	75,59	23	−5,09	43,06	61,5
24	76,05	24	−5,93	43,05	62
25	76,51	25	−6,73	43,05	62,5
26	76,98	26	−7,44	43,04	63
27	77,45	27	−8,12	43,04	63,5

28	77,91	28	−8,71	43,04	64
29	78,37	29	−9,27	43,03	64,5
30	78,82	30	−9,79	43,03	65
31	79,28	31	−10,26	43,02	65,5

Mass loss in the most important temperature intervals for every TGA performed.

Concrete batch	**Mass loss 600-900 °C**	**Mass loss 400-600 °C**	**Mass loss 180-400 °C**	**Total mass loss**
BA-0-0-W	2,89%	2,89%	2,98%	8,76%
BA-0-1-W	3,49%	2,77%	3,11%	9,37%
BA-0-1-CI	3,29%	3,26%	3,55%	10,09%
BA-0-1-CO	3,38%	3,27%	3,51%	10,16%
BA-0-1-A	3,06%	3,04%	3,34%	9,44%
BA-0-2-W	3,74%	3,05%	3,79%	10,58%
BA-0-2-CI	3,65%	3,16%	3,78%	10,59%
BA-0-2-CO	3,16%	1,96%	2,41%	7,52%
BA-0-2-A	4,75%	3,13%	3,78%	11,66%
SL-20-0-W	4,15%	3,09%	3,84%	11,09%
SL-20-1-W	3,01%	2,93%	3,85%	9,78%
SL-20-1-CI	2,87%	2,54%	3,44%	8,85%
SL-20-1-CO	3,01%	2,72%	3,68%	9,41%
SL-20-1-A	2,35%	2,34%	3,02%	7,71%
SL-20-2-W	3,70%	2,41%	3,56%	9,68%

SL-20-2-CI	2,81%	1,99%	2,91%	7,72%
SL-20-2-CO	3,81%	2,66%	3,94%	10,42%
SL-20-2-A	3,48%	2,33%	3,46%	9,28%
SL-30-0-W	2,49%	2,97%	3,68%	9,14%
SL-30-1-W	2,66%	2,21%	3,23%	8,09%
SL-30-1-CI	2,95%	2,56%	3,80%	9,31%
SL-30-1-CO	3,61%	2,26%	3,33%	9,20%
SL-30-1-A	2,59%	2,32%	3,36%	8,27%
SL-30-2-W	2,01%	1,38%	2,30%	5,68%
SL-30-2-CI	2,30%	1,65%	2,73%	6,68%
SL-30-2-CO	2,81%	1,97%	3,21%	7,98%
SL-30-2-A	2,40%	1,66%	2,85%	6,91%
SL-70-0-W	1,63%	1,60%	2,68%	5,91%
SL-70-1-W	2,14%	1,53%	3,02%	6,70%
SL-70-1-CI	1,14%	0,71%	1,12%	2,97%
SL-70-1-CO	2,99%	1,50%	2,71%	7,19%
SL-70-1-A	2,19%	1,66%	3,38%	7,23%
SL-70-2-W	2,40%	1,62%	3,50%	7,52%
SL-70-2-CI	1,77%	1,32%	2,47%	5,55%
SL-70-2-CO	2,04%	1,43%	2,92%	6,38%
SL-70-2-A	2,21%	1,59%	3,21%	7,02%

Appendix D

Norcem Anleggsement product data

PRODUKTDATABLAD

ANLEGGSEMENT

CEM I 52,5 N

Sist revidert desember 2018

Sementen tilfredsstiller kravene i NS-EN 197-1:2011 til Portlandsement CEM I 52,5 N.

Egenskap		Deklarerte data	Krav ifølge NS-EN 197-1:2011
Finhet (Blaine m^2/kg)		415	
Spesifikk vekt (kg/dm^3)		3,14	
Volumbestandighet (mm)		1	10
Begynnende størkning (min)		120	45
Trykkfasthet (MPa)	1 døgn	21	
	2 døgn	33	20
	7 døgn	49	
	28 døgn	63	52,5
Sulfat (% SO_3)		4,0	4,0
Klorid (% Cl^-)		0,07	0,10
Vannløselig krom (ppm Cr^{6+})		2	2[1]
Alkalier (% Na_2O_{ekv})		0,6	
Klinker (%)		96	95-100
Sekundære bestanddeler (%)		4	0-5

1. I henhold til EU forordning REACH Vedlegg XVII punkt 47 krom VI-forbindelser.

NORCEM
HEIDELBERGCEMENT Group

Norcem AS, Postboks 142, Lilleaker, 0216 Oslo
Tlf. 22 87 84 00 firmapost@norcem.no www.norcem.no

Ground Granulated Blast Furnace Slag product data

MEROX
- Ett företag i SSAB-koncernen -

Safety Data Sheet
according to Regulation (EC) No 1907/2006

SECTION 1: IDENTIFICATION OF THE SUBSTANCE/MIXTURE AND OF THE COMPANY

1.1 Product identifier

Trade name:	MERIT 5000
Substance name:	Ground granulated blast furnace slag
Chemical / technical product name:	Ground granulated blast furnace slag
EC No:	266-002-0
CAS No:	65996-69-2
Reach Registration No:	01-2119487456-25

1.2 Uses

Relevant identified uses of the substance or mixture:	Used e.g. in the manufacturing of concrete, part of self-levelling compound increasing bearing capacity in soils, and as a cohesive in asphalt.
Uses advised against:	The product should only be used according the relevant identified uses specified above. If the product is used for any other purposes, it is recommended to contact Merox.

1.3 Details of the supplier of the safety data sheet

Supplier:	SSAB MEROX AB
Address:	613 80 OXELÖSUND
Telephone No:	46(0)155 - 25 44 00
Telefax No:	+46(0)155 - 25 52 21
E-mail:	msds@merox.se

1.4 Emergency telephone number

Emergencies (24 hours):	112 (the European emergency number)
Health advice and information (24 hours):	+44 (0) 845 4647 (UK only)

SECTION 2: HAZARDS IDENTIFICATION

2.1 Classification of the substance

2.1.1 CLASSIFICATION ACCORDING TO CLP [REGULATION (EC) NO 1272/2008]

Classification:	The product is not classified as a dangerous substance under the current legislation for classification and labelling of dangerous chemical substances and mixtures.

2.1.2 CLASSIFICATION ACCORDING TO DSD (COUNCIL DIRECTIVE 67/548/EEC)

Classification:	The product is not classified as a dangerous substance under the current legislation for classification and labelling of dangerous chemical substances and mixtures.

2.2 Label elements

Substance name:	Ground granulated blast furnace slag
CAS No:	65996-69-2

SECTION 9: PHYSICAL AND CHEMICAL PROPERTIES

9.1 Information on basic physical and chemical properties

Property	Value		Method / Remarks
Physical state:	Solid - amorphous powder		-
Granulometry:	D10 D50 D90	~ 2.4 µm ~ 12 µm ~ 45 µm	< 0.1 % (w/w) of total in grain size fraction 1 - 4 µm. Laser Malvern Mastersizer 2000
Colour as supplied:	White		-
Odour:	None		-
Odour threshold:	Not applicable		-
pH:	11,2		DIN 38414-S4 (10:1 liquid/solid ratio)
Melting point / freezing point:	1200 - 1350 °C		-
Initial boiling point and boiling range:	Not applicable		Melting point >300 °C
Flash point:	Not applicable		Inorganic substance
Evaporation rate:	Not applicable		-
Flammability (solid, gas):	Non flammable		-
Upper/lower flammability or explosive limits:	Non explosive		-
Vapour pressure:	Not applicable		Melting point >300 °C
Vapour density:	Not applicable		Melting point >300 °C
Density:	2920 kg/m^3		-
Bulk density:	Ca 600 - 1400 kg/m^3		-
Solubility in water:	Substance	Konc (mg/l)	DIN 38414-S4 (10:1 liquid/solid

	As Cd Co Cr (total) Cu Fe Hg Mn Mo Ni Pb Se V Zn	< 0,002 < 0,0005 < 0,005 0,03 < 0,005 < 0,01 < 0,0002 < 0,001 0,4 < 0,01 0,004 0,001 < 0,002 0,02	ratio). Values are given for the liquid phase. The metals are not present as free ions, but occur in different minerals in the slags.
Solubility in organic solvents:	Insoluble in organic solvents		-
Partition coefficient: n-octanol/water:	Not applicable		Inorganic substance
Auto-ignition temperature:	Not applicable		-
Decomposition temperature:	Not applicable		-
Viscosity:	Solid		-
Explosive properties:	Non explosive		-
Oxidising properties:	No oxidising properties		-
9.2 Other safety information			
Property	**Value**		**Method / Remarks**
Solubility in fat:	Insoluble in fat		-
Conductivity:	Not applicable		-
Dissociation constant in water (pKa):	Not applicable		-
Glass content:	99 %		-
Specific surface:	4600-5400 cm^2/g (Blaine)		-

Superplasticizer product data

MAPEI

Dynamon SX-N

Superplastiserende tilsetningsstoff

BESKRIVELSE
Dynamon SX-N er et svært effektivt superplastiserende tilsetningsstoff basert på modifiserte akrylpolymerer. Produktet tilhører **Dynamon-systemet** basert på den Mapei-utviklede DPP-teknologien (DPP = Designed Performance Polymers), der tilsetningsstoffenes egenskaper skreddersys til ulike betongformål. **Dynamon-systemet** er utviklet på basis av Mapeis egen sammenstilling og produksjon av monomerer.

BRUKSOMRÅDER
Dynamon SX-N er et tilnærmet allround-produkt som er anvendelig i all betong for å øke støpeligheten og/eller redusere tilsatt vannmengde.

Noen spesielle bruksområder er:

- Vanntett betong med krav til høy eller svært høy fasthet og med strenge krav til bestandighet i aggressive miljøer.
- Betong med særlige krav til høy støpelighet; i konsistensklasser S4 og S5 etter NS-EN 206.
- Selvkomprimerende betong med ønske om lengre åpentid. Om nødvendig kan SKB stabiliseres med en viskositetsøker - **Viscofluid** eller **Viscostar**.
- Til produksjon av frostbestandig betong - da i kombinasjon med luftinnførende tilsetningsstoffer - **Mapeair**. Valg av type luftinnførende stoff gjøres ut fra egenskapene til de andre delmaterialer som er tilgjengelige.
- Til golvstøp for å oppnå en smidig betong med bedret støpelighet. Store doseringer og lave temperaturer kan retardere betongen noe.

EGENSKAPER
Dynamon SX-N er en vannløsning av aktive akrylpolymerer som effektivt dispergerer (løser opp) sementklaser.

Denne effekten kan prinsipielt utnyttes på tre måter:

1. For å redusere mengden tilsatt vann, men samtidig beholde betongens støpelighet. Lavere v/c-forhold gir høyere fasthet, tetthet og bestandighet i betongen.
2. For å forbedre støpeligheten sammenlignet med betonger med samme v/c-forhold. Fastheten forblir dermed den samme, men muliggjør forenklet utstøping.
3. For å redusere både vann og sementmengde uten å forandre betongens mekaniske styrke. Gjennom denne metoden kan en blant annet redusere kostnadene (mindre sement), redusere betongens svinnpotensial (mindre vann) og redusere faren for temperaturgradienter på grunn av lavere hydratasjonsvarme.
Spesielt er denne siste effekten viktig ved betonger med større sementmengder.

Dynamon SX-N

KOMPATIBILITET MED ANDRE PRODUKTER

Dynamon SX-N lar seg kombinere med andre Mapei tilsetningsstoffer, som f.eks størkningsakselererende stoffer som **Mapefast** og størkningsretarderende stoffer som **Mapetard**.
Produktet lar seg også kombinere med luftinnførende tilsetningsstoffer, **Mapeair**, for produksjon av frostbestandig betong.

Valg av type luftinnførende stoff gjøres ut fra egenskapene til de andre delmaterialer som er tilgjengelige.

DOSERING

Dynamon SX-N tilsettes for å oppnå ønsket resultat (styrke, bestandighet, støpelighet, sementreduksjon) ved å variere doseringen mellom 0,4 og 2,0 % av sement + flyveaske + mikrosilika. Ved økt dosering økes også betongens åpentid, dvs. tiden betongen lar seg bearbeide. Større doseringsmengder og lave betongtemperaturer gir en retardert betong. Vi anbefaler alltid prøvestøper med aktuelle parametere.

Til forskjell fra konvensjonelle melaminеller naftalenbaserte superplastiserende tilsetningsstoffer, utvikler **Dynamon SX-N** maksimal effekt uavhengig av tilsettingstidspunkt, men tilsetningstidspunktet kan påvirke nødvendig blandetid.

Dersom **Dynamon SX-N** tilsettes etter at minst 80 % av blandevannet er inne vil blandetiden generelt være kortest. Det er likevel viktig med utprøvinger tilpasset eget blandeutstyr.

Dynamon SX-N kan også tilsettes direkte i automikser på bygg- eller anleggsplass. Betongen bør da blandes med maksimal hastighet på trommelen i ett minutt pr. m³ betong i lasset, men minimum 5 minutter.

EMBALLASJE

Dynamon SX-N leveres i 25 liters kanner, 200 liters fat, 1000 liter IBC-tanker og i tank.

LAGRING

Produktet må oppbevares ved temperaturer mellom +8°C og +35°C. I lukket emballasje bevarer produktet sine egenskaper i minst 12 måneder. Hvis produktet utsettes for direkte sollys, kan det føre til variasjoner i fargetonen uten at dette påvirker egenskapene til produktet.

SIKKERHETSINSTRUKSJONER FOR KLARGJØRING OG BRUK

For instruksjon vedrørende sikker håndtering av våre produkter, vennligst se siste utgave av sikkerhetsdatablad på vår nettside www.mapei.no

PRODUKT FOR PROFESJONELL BRUK.

MERK

De tekniske anbefalinger og detaljer som fremkommer i denne produktbeskrivelse representerer vår nåværende kunnskap og erfaring om produktene. All overstående informasjon må likevel betraktes som retningsgivende og gjenstand for vurdering. Enhver som benytter produktet må på forhånd forsikre seg om at produktet er egnet for tilsiktet anvendelse. Brukeren står selv ansvarlig dersom produktet blir benyttet til andre formål enn anbefalt eller ved feilaktig utførelse.

Vennligst referer til siste oppdaterte versjon av teknisk datablad som finnes tilgjengelig på vår webside www.mapei.no

JURIDISK MERKNAD

Innholdet i dette tekniske databladet kan kopieres til andre prosjektrelaterte dokumenter, men det endelige dokumentet må ikke suppleres eller erstatte betingelsene i det tekniske datablad, som er gjeldende, når MAPEI-produktet benyttes. Det seneste oppdaterte datablad er tilgjengelig på vår hjemmeside www.mapei.no
ENHVER ENDRING AV ORDLYDEN ELLER BETINGELSER, SOM ER GITT ELLER AVLEDET FRA DETTE TEKNISKE DATABLADET, MEDFØRER AT MAPEI SITT ANSVAR OPPHØRER.

Alle relevante referanser for produktet er tilgjengelige på forespørsel og fra www.mapei.no

Dynamon SX-N

TEKNISKE DATA (typiske verdier)	
PRODUKTBESKRIVELSE	
Form:	væske
Farge:	gulbrun
Viskositet:	lettflytende; < 30 mPa·s
Tørrstoffinnhold (%):	18,5 ± 1,0
Densitet (g/cm³):	1,06 ± 0,02
pH:	6,5 ± 1
Kloridinnhold (%):	< 0,05
Alkaliinnhold (Na_2O-ekvivalenter) (%):	< 2,0

6392-07-2017(NO)

MAPEI
BUILDING THE FUTURE